Large-area forest productivity estimation using bitemporal data from airborne laser scanning and digital aerial photogrammetry

Bonitering i skogbruksplantakster ved bruk av bitemporale data fra flybåren laserskanning og digital fotogrammetri basert på flybilder

Lennart Noordermeer

Large-area forest productivity estimation using bitemporal data from airborne laser scanning and digital aerial photogrammetry
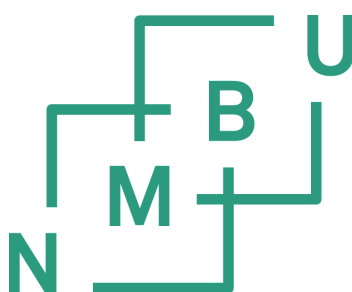
Bonitering i skogbruksplantakster ved bruk av bitemporale data fra flybåren laserskanning og digital fotogrammetri basert på flybilder

Philosophiae Doctor (PhD) Thesis

Lennart Noordermeer

Norwegian University of Life Sciences
Faculty of Environmental Sciences and Natural Resource Management

Ås (2020)

PhD Supervisors

Prof. Ole Martin Bollandsås

Faculty of Environmental Sciences and Natural Resource Management

Norwegian University of Life Sciences

P.O. Box 5003, NO – 1432 Ås, Norway

Prof. Erik Næsset

Faculty of Environmental Sciences and Natural Resource Management

Norwegian University of Life Sciences

P.O. Box 5003, NO – 1432 Ås, Norway

Prof. Terje Gobakken

Faculty of Environmental Sciences and Natural Resource Management

Norwegian University of Life Sciences

P.O. Box 5003, NO – 1432 Ås, Norway

Evaluation committee

Dr. Lars Torsten Waser

Swiss Federal Institute for Forest, Snow and Landscape Research WSL

Zürcherstrasse 11, CH-8903 Birmensdorf, Switzerland

Prof. Veli-Matti Maltamo

School of Forest Sciences

University of Eastern Finland

Yliopistokatu 7, Joensuu Campus, P.O.Box 111, FI-80101 Joensuu, Finland

Prof. Tron Haakon Eid

Faculty of Environmental Sciences and Natural Resource Management

Norwegian University of Life Sciences

P.O. Box 5003, NO – 1432 Ås, Norway

Preface

I am actually quite surprised that I ended up doing this PhD, and that I even enjoyed it. I have had more of an interest in practical work, sustained by stacking timber in Tasmania, measuring plots in the Netherlands and harvesting timber in Østerdalen. Sometimes my back still hurts from those endeavors, giving me all the more reason to appreciate the opportunity to work in research. After my Masters, there was a brief moment in which I was unsure whether to apply for this PhD or to continue in the commercial sector. But I quickly made up my mind. Apart from the cool topic, I knew that Skogrover would provide a pretty sweet work environment. Therefore, I would first and foremost like to thank my colleagues for this. My team of supervisors, Ole Martin, Terje and Erik- your support has made this project doable and enjoyable. Thank you Skogrovers: Hans Ole, Victor, Marie-Claude, Roar, las Ana's, Ida, Eirik, Ben, Arvid, Jaime and Tyrone, even though you were working at Nibio, for good Ping-Pong matches and a great time in and outside the office. My gratitude also extends to the Norwegian University of Life Sciences, Norwegian Forestry Development Fund, Viken Skog SA, Norwegian Forest Owners' Trust Fund and Research Council of Norway for funding my work. Finally, I would like to thank my family for being there and supporting me. If only Opa Gewoon could have seen this. Asun- thank you for loving me for who I am, and for putting up with me throughout the years.

Lennart Noordermeer

Ås, March 27, 2020

Contents

Abstract

Site index (SI) indicates the magnitude of timber production that can be realized at a given site and is a crucial variable in forest planning. In Norwegian forest management inventories, SI is commonly quantified with large uncertainty by means of aerial image interpretation, field assessment and information from previous inventories. Airborne laser scanning (ALS) and digital aerial photogrammetry (DAP) have revolutionized the field of forest inventory in recent decades, however operational practices for SI estimation have remained unchanged since the 1970s. The main objective of this thesis was to develop practical methods of SI estimation using bitemporal tree height data derived from ALS and DAP.

The first study presented two practical methods of SI estimation; (i) the direct method, in which models are applied for direct prediction of SI from bitemporal ALS metrics, and (ii) the indirect method in which the SI is derived indirectly from estimates of canopy height development over time. Both methods provided reliable SI estimates, however the direct method was most accurate. Operational application of the methods requires undisturbed forest growth. Hence, the second study assessed the use of bitemporal ALS data for classification of various types of changes in forest structure, and showed that such changes can be classified with high accuracy at plot level. In the third study, a practical method for predicting and mapping SI in repeated ALS-based forest inventories was demonstrated. The method included a forest disturbance classification, and the direct method was then applied to forest areas classified as undisturbed. The last study compared the economic utility of six methods of ALS- and DAP-based SI estimation and conventional practices in a cost-plus-loss analysis, by which the economic losses due to sub-optimal treatment decisions were added to the inventory costs. The study showed that SI can be estimated from bitemporal combinations of ALS and DAP data with unprecedented accuracy and at a lower cost than conventional methods.

This thesis shows that bitemporal ALS and DAP data are highly suitable for the estimation of SI. The methods presented here can be used to predict, estimate and map SI at sub-stand level automatically over large areas of forest. They are practically applicable and cost-efficient, and can be adopted to replace conventional practices of SI estimation in repeated forest management inventories.

Sammendrag

Bonitet er et uttrykk for potensialet for virkesproduksjon på et gitt areal, og er en svært viktig variabel innen skogbruksplanlegging. I skogbruksplantakster i Norge bestemmes ofte boniteten med stor usikkerhet ved manuell tolkning av flybilder, støttet med feltbefaringer og informasjon fra tidligere takster. Bruk av tredimensjonale data fra flybåren laserskanning (ALS) og digital fotogrammetri basert på flybilder (DAP) har revolusjonert skoginventering de siste tiårene, men operative metoder for bonitering har holdt seg uendret siden 1970-tallet. Hovedmålet med denne avhandlingen var å utvikle praktiske metoder for bonitering ved bruk av bitemporale data fra ALS og DAP. Fire studier ble utført for å nå dette målet.

Den første studien presenterte to praktiske metoder for bonitering; (i) den direkte metoden, der en modell blir tilpasset for direkte prediksjon av bonitet på grunnlag av bitemporale ALS variabler, og (ii) den indirekte metoden der boniteten blir avledet indirekte fra den estimerte overhøydeutviklingen over tid. Begge metodene ga pålitelige estimater, men den direkte metoden var mer presis. Operativt bruk av metodene krever at skogsområder klassifiseres etter om det har forekommet vesentlige skogsforstyrrelser. Følgelig testet den andre studien bruk av bitemporale ALS data for klassifisering av endringer i skogstruktur, og viste at slike endringer kan klassifiseres med høy nøyaktighet på prøveflatenivå. Den tredje studien demonstrerte en praktisk metode for kartlegging av bonitet i repeterte ALS-baserte skogbruksplantakster. Skogsforstyrrelser ble først klassifisert, og den direkte metoden ble deretter brukt på skogsområder klassifisert som uforstyrret. Den siste studien sammenlignet ulike metoder for ALS- og DAP-basert bonitering med dagens praksis i en nytte-kostnadsanalyse, der nåverditap som følge av suboptimale behandlingsbeslutninger ble lagt til takstkostnadene. Direkte metoder basert på bitemporale kombinasjoner av ALS og DAP data var mest nøyaktige og ga de laveste totale kostnader.

Denne avhandlingen viser at bitemporale data fra ALS og DAP er svært godt egnet for bonitering i repeterte skogbruksplantakster. Metodene som presenteres her kan brukes til å predikere, estimere og kartlegge bonitet automatisk, med høy detaljeringsgrad og over store skogsarealer. De er praktisk anvendelige og kostnadseffektive, og kan erstatte dagens praksis for bonitering.

List of papers

I Noordermeer, L., Bollandsås, O. M., Gobakken, T., & Næsset, E. (2018). Direct and indirect site index determination for Norway spruce and Scots pine using bitemporal airborne laser scanner data. *Forest ecology and management*, 428, 104-114.

II Noordermeer, L., Økseter, R., Ørka, H. O., Gobakken, T., Næsset, E., & Bollandsås, O. M. (2019). Classifications of forest change by using bitemporal airborne laser scanner data. *Remote Sensing*, 11(18), 2145.

III Noordermeer, L., Gobakken, T., Næsset, E., & Bollandsås, O. M. (2020). Predicting and mapping site index in operational forest inventories using bitemporal airborne laser scanner data. *Forest ecology and management*, 457, 117768.

IV Noordermeer, L., Gobakken, T., Næsset, E., & Bollandsås, O. M. (Under review). Economic utility of 3D remote sensing data for estimation of site index in forest management inventories: A comparison of airborne laser scanning, digital aerial photogrammetry and conventional practices.

1. Introduction

Accurate information on the state of forests is crucial for sustainable forest management. In Norway as well as many other countries, forest management inventories are implemented periodically, typically every 10-15 years, with the aim of providing data for tactical and strategic planning of individual forest properties. Since the 1950s, it has been common practice to collect information for each individual treatment unit (stand) within a property, whereby initially all stands were visited in the field (Næsset, 2014). During the 1970s and into the 1990s, geographical information systems and stereo photogrammetry were increasingly used, reducing the need for field visits substantially (Eid, 1996). Tree species, development stage and forest productivity were interpreted from aerial images, and analogue stereo plotters were used for stand delineation, measurement of stand height and crown closure, which in turn could be used to predict timber volume.

Airborne laser scanning (ALS) was introduced around the year 2000, which has since revolutionized the field of forest inventory. In forest management inventories today, most stand attributes relevant for forest planning are derived from remotely sensed data. Some are commonly estimated from ALS data, attributes such as timber volume, basal area, dominant height, mean tree height and number of stems. Other stand attributes can effectively be interpreted from aerial images, such as the dominant tree species and forest development stage. One crucial attribute however, one which has long remained challenging to estimate from remotely sensed data, is a forests' capacity to produce timber.

1.1   Forest productivity

Forest productivity reflects the growth rate of a forest and the magnitude of timber production that can be realized at a given site, and provides crucial information for forest management planning. It summarizes a range of environmental and climatic factors that influence forest growth: growing degree days, temperature, precipitation, geographic location and elevation (Messaoud and Chen, 2011), light, water and site nutrition (Boisvenue and Running, 2006) radiation, wind speed and foliar nutrients (Watt et al., 2010) and topography and geology (Socha, 2008). In addition, management-related factors are known to influence forest productivity, such

as the choice of tree species, regeneration method, provenance, planting density and thinning regime (Skovsgaard and Vanclay, 2008).

The assessment of forest productivity has been a fundamental task for as long as production forests have been managed. Already towards the end of the 18th century, Paulsen (1795) and Hartig (1795) pioneered the assessment of forest productivity by developing indices based on altitude and soil type. Around the same time, de Laillevaut et al. (1803) was the first to advocate the use of stand height at a given index age for assessing forest productivity (Batho and García, 2006). This age-height approach, however, received numerous bouts of criticism (Hartig, 1892; Monserud, 1981; Weise, 1880), and several alternative approaches have been proposed. In Finland, for example, forest productivity is classified indirectly on the basis of understory vegetation (Cajander, 1909). Huang and Titus (1993) proposed an index of forest productivity based on the relationship between tree height and diameter at breast height (DBH). Berrill and O'Hara (2014) estimated forest productivity by indexing the basal area and volume increment of the dominant species. Despite the above-mentioned criticism and alternative approaches, however, stand height at an index age has become the most widely accepted measure of forest productivity worldwide (Stearns-Smith, 2002), known as the site index.

1.2   Site index

Site index (SI) is defined as the average height attained by dominant trees (Hdom) at a given index age (Spurr et al. (1973), Fig. 1). Hdom is typically defined as the mean height of the 100 largest trees per ha according to DBH (Hamilton, 1985), although alternative definitions of Hdom have been proposed; for example the mean height of a fixed percentage of largest or tallest trees, or the height of the tallest tree (Kramer, 1959), or the mean height of the 10 largest trees per 0.1 ha according to DBH (Matérn, 1976). Stand age is commonly defined as the mean age at breast height weighted by basal area (Sharma et al., 2011). The choice of breast height as the reference for age determination is not only considered practical for the collection of core samples, but it also avoids unwanted effects of variations in height development in the very beginning of the stand development (Husch, 1956).
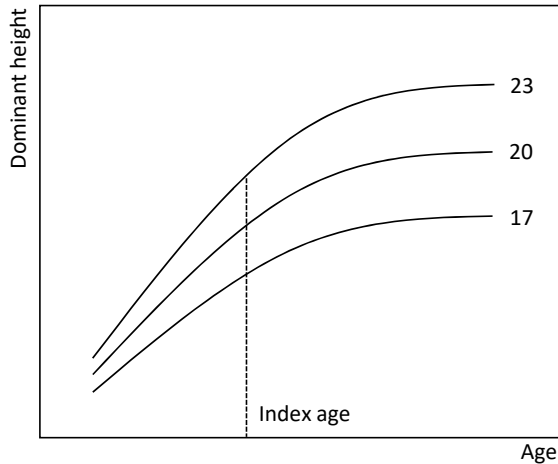
Fig. 1. The site index concept: each curve represents the development of dominant height over
age and represents a site index, expressed as the dominant height at a given index age.

Originally, the main argument for assessing forest productivity on the basis of
age-height relationships is that tree height increment is highly correlated with
volume increment (Heyer, 1883). Another argument is that Hdom increment, as
opposed to volume increment, is largely independent of stem density and thus
thinning regime (Skovsgaard and Vanclay, 2008). SI is traditionally derived from
the age and height of site trees using empirical SI models which relate Hdom,
age and forest productivity (Tveite, 1976, 1977). SI models can be used both for
predicting Hdom development and for assessing forest productivity (Sharma et al.,
2011). Although SI models are continuous functions, and there is no conceptual
limit to the number of SI curves, a standardized set of indices is commonly used.
In Norway, where the index age is 40, discrete indices typically range from 6 m to
26 m which are considered to cover the realistic range of age-height relationships
in productive forest.

1.3   Age-height approach

The traditional way of determining the SI in the field is by collecting core samples
from dominant trees to determine the age at breast height, and then measuring the
height of the same trees (Carmean, 1975; Hagglund et al., 1981). The SI can then
be predicted using empirical models with age and Hdom as predictors. Because
the obtained SI is based on the age at breast height and the corresponding tree
height, it will have been influenced by all variations in growing conditions from the

moment the site tree or trees reached breast height until the time of measurement. The effect of such variations will however be distributed over the entire observation period (age at breast height), and such effects will therefore be dampened as site trees grow older.

1.4   Height-differential approach

As an alternative to the age-height approach, the height-differential approach is based on periodic height growth over a shorter time span than the age at breast height. Such an approach has been shown to be particularly useful in regeneration forests (Wakeley, 1954), in cases where the age is unknown or uncertain (Arias-Rodil et al., 2015) and in cases where Hdom growth has been restricted (Skovsgaard and Vanclay, 2008). Height-differential methods of SI estimation offer several advantages over the age-height approach. First, they are age-independent, meaning that expensive and error-prone core samples are not required. Second, they are applicable to data obtained from permanent sample plots, on which coring is typically avoided. Third, periodic changes in growing conditions can be captured, providing more timely information on recent growing conditions. It must be noted however, that height-differential methods are more sensitive to random variations in growing conditions, which in some cases may be a disadvantage. For example, the effect of exceptionally unfavorable weather conditions that persisted over a number of growing seasons will be much greater on height-differential SI estimates than age-height SI estimates.

1.5   Operational practices

Site index is one of the most fundamental variables in forest management planning. In commercial forestry, SI determines the optimal silvicultural treatment, timing of the final harvest, the sustainable yield, and forms the basis for property taxation and yield forecasts. Reliable SI estimates are therefore crucial for efficient and sustainable forest management. In operational forest management inventories however, SI is ranked among the most error-prone variables (Eid, 1992), and incorrect SI estimates can potentially lead to negative economic consequences for forest owners due to incorrect treatment decisions (Eid et al., 2000). Errors in SI may, for example, lead to sub-optimal timing of final harvest and choice of regeneration method, potentially leading to considerable financial losses. Despite its implications for forest planning however, methods of SI estimation have changed little since the 1970s.

In forest management inventories, SI is commonly estimated with substantial error by aerial image interpretation. The interpreters typically look for indications of growing conditions such as forest structure, tree species composition and topography, and the assessment may be supported by field assessments and information from previous inventories. Studies have documented that errors of around 20% may be expected for conventional methods of SI estimation (Eid, 1992) and that the SI is commonly incorrectly determined for more than 50% of a given inventory area (Gisnås, 1982; Næsset, 1994). The main challenge is that SI is difficult to assess subjectively from aerial image, and even when measured in the field, errors in age (Niklasson, 2002; Villalba and Veblen, 1997) and height (Vasilescu, 2013) of site trees make it difficult to obtain reliable SI estimates. Even the selection of site trees is a subjective task to some extent, which is particularly challenging in uneven-aged stands.

1.6 Airborne laser scanning

In many countries around the world, airborne laser scanning (ALS) has increasingly been used for forest inventory over the past two decades (Maltamo et al., 2014). ALS systems provide detailed and precise three-dimensional (3D) information on the structure of forest canopy and the height of the terrain (Fig. 2), and offer the ability to estimate a range of biophysical forest characteristics with great detail and accuracy (Næsset, 2002; White et al., 2013a). Its widespread use has largely been motivated by the ability to provide continuous and detailed forest canopy information over large areas and at a low cost.
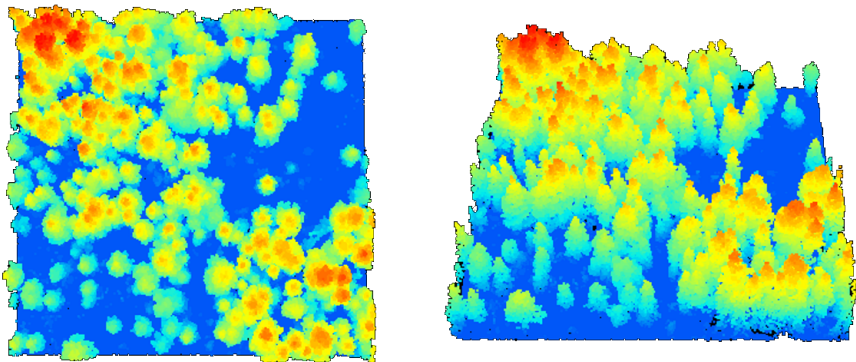

Fig. 2. Example of an airborne laser scanning point cloud seen from above (left) and from a top side view (right). Colors indicate the height of laser echoes, ranging from low values (blue) to high values (red).

ALS systems were initially developed for topographic purposes; primarily to generate digital terrain models (Bufton et al., 1991). Just a few years after the first commercial ALS systems were introduced, a number of studies were conducted with the aim of estimating forest attributes such as tree height, volume, tree number, and diameter distribution (Magnussen and Boudewyn, 1998; Næsset, 1997a,b; Nilsson, 1996). A great potential was demonstrated for its use in forest inventory, and Næsset (2002) proposed the area-based approach, which is now the most common ALS-based forest inventory method (White et al., 2013a). The area-based approach comprises two stages Næsset (2002). In the first stage, models are developed which relate plot level forest attributes as response variables to ALS metrics which describe the height and density of the canopy as predictors. The ALS metrics used for model calibration are computed from ALS data that are clipped from within the spatial extent of the sample plots. In the second stage, the models are used to predict the desired forest attributes over a grid tessellating a given area of interest, allowing for wall-to-wall mapping of the attributes. The grid cells are of the same size as the sample plots, and ALS data are clipped from within each cell and used to compute the same ALS metrics used in the model calibration. Maps can then be constructed from the model predictions, providing a spatially explicit and continuous overview over the forest attributes within the area of interest.

Besides the construction of forest maps, model predictions of forest attributes can be used to estimate population means and totals, whereby in general, design-based and model-based inference are the most common approaches (McRoberts et al., 2010). Design-based inferential methods are based on probability samples of either field plots alone (Tomppo et al., 2010) or both field plots and remotely sensed data (Andersen et al., 2009). Model-based inferential methods are based on models that link field plot data, regardless of the sampling design, to either wall-to-wall (McRoberts et al., 2013) or a probability sample of remotely sensed data (Gobakken et al., 2012). In stand level forest inventories based on ALS, model predictions within stands are typically aggregated to estimate stand level means and totals according to a model-based framework (Woods et al., 2011). Whichever inferential method is used, an accuracy assessment is a crucial component of ALS maps and related spatial products, and justifies inference from the sample to the target population. Thereby, the main goal of the assessment is to provide information on the quality of predictions, estimates and maps, based on a comparison with ground truth data (McRoberts et al., 2010).

1.7   Digital aerial photogrammetry

In recent years, digital aerial photogrammetry (DAP) has emerged as an alternative to ALS, providing the means to generate spatially continuous 3D point cloud data from aerial images (Fig. 3). By stereo-matching points on overlapping aerial images and determining the parallax, i.e., the apparent positional change of stationary objects due to a change in viewing position (Lillesand et al., 2015), canopy height information can be generated automatically over large areas (Rahlf et al., 2017; White et al., 2013b). The use of DAP as a substitute for ALS in an area-based inventory approach has shown potential in numerous studies (Bohlin et al., 2012; Hawryło et al., 2017; Pitt et al., 2014; Rahlf et al., 2017; Straub et al., 2013; Noordermeer et al., 2019).
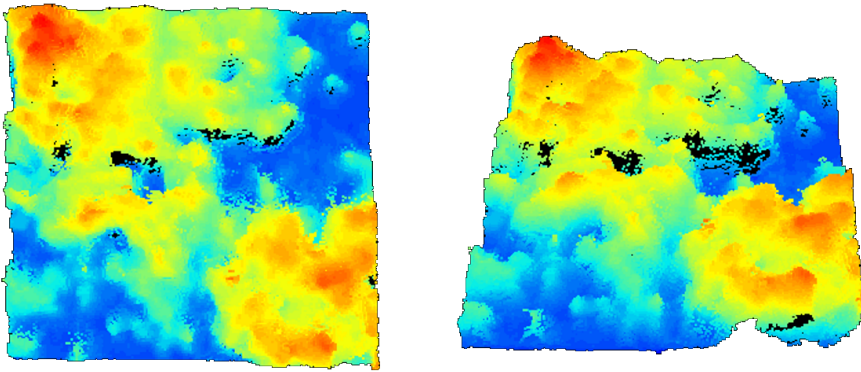
Fig. 3. Example of a digital aerial photogrammetry (DAP) point cloud seen from above (left) and from a top side view (right). Colors indicate point heights ranging from low values (blue) to high values (red). As opposed to airborne laser scanning data (Fig. 2), DAP data mainly characterize the outer envelope of the canopy; gaps within the canopy are less well defined, and sub-canopy vegetation and terrain surface are poorly characterized.

In DAP point cloud data, the individual points represent the 3D placement of pixels matched on two or more aerial images. For a pixel to be matched, it must appear in at least two overlapping images, so the technology only works for objects visible on the images. In forest areas, DAP data are therefore mainly restricted to the structure of the upper canopy, whereas ALS data also provide sub-canopy information on the height of understory vegetation and the terrain due to the laser pulses penetrating the canopy (White et al., 2018).

A main advantage of DAP data is that they are generally cheaper than ALS data (White et al., 2013b). Image acquisition campaigns are usually carried out at higher altitudes than ALS campaigns, and therefore cover larger areas in shorter time, which is one of the reasons for DAP data being cheaper than ALS data. The use of DAP data for forest inventory applications is however dependent on a previous ALS dataset providing information on the height of the terrain. Thus, DAP may be considered particularly useful as a low-cost means to update existing ALS inventories (Ali-Sisto and Packalen, 2016; Goodbody et al., 2019), for example by taking advantage of aerial imagery acquired as part of orthophoto campaigns (Ginzler and Hobi, 2015).

1.8 Bitemporal tree height data

While ALS data have found widespread application in forest inventory (Maltamo et al., 2014), recent years have witnessed a new development; ALS-based forest inventories implemented 10-15 years ago, are now entering into the second inventory cycle. As a result, the availability of bitemporal ALS data is increasing, opening for a range of new applications within forest inventory. In addition, DAP data can now be used as an alternative data source for updating forest inventories, in cases where previously acquired ALS data can provide a digital terrain model. Such bitemporal combinations of ALS and subsequent DAP data have been shown to provide useful information for forest growth monitoring (Goodbody et al., 2019; Tompalski et al., 2018).

The increasing availability of bitemporal 3D data has triggered great interest in their application in forest inventory. Multi-temporal canopy information can be useful for forest change monitoring, for example for estimating forest height growth (Hyyppä et al., 2003; Næsset and Gobakken, 2005; Yu et al., 2006) and changes in aboveground biomass (Skowronski et al., 2014; Zhao et al., 2018). In addition, multi-temporal 3D data have emerged as a promising tool for estimating SI, because SI is directly related to the accumulated canopy height increment over time (Miller and Beers, 1982; Tveite, 1977). Indeed, several studies have shown how multi-temporal 3D data can be used for SI estimation. For example, Véga and St-Onge (2009) generated canopy height sequences from historical aerial photographs and a single ALS dataset, and derived the SI at plot level by matching the canopy height increments with SI curves. Other studies obtained good results by deriving the SI from bitemporal ALS data at the level of individual trees (Hollaus et al., 2015; Solberg et al., 2019). The results of the mentioned studies showed that

multi-temporal tree height data derived from ALS and DAP data can be useful for estimating SI. However, more research was needed in developing methods of SI estimation using bitemporal 3D data, particularly practical methods that can efficiently be applied in repeated area-based inventories.

2. Research objectives

The main objective of this thesis was to develop practical methods of SI estimation using bitemporal tree height data derived from ALS and DAP. Four specific objectives were formulated to reach this objective, each of which was featured in a separate paper:

1. To assess and compare two different methods of SI estimation using bitemporal ALS-derived tree height data.

The first paper presented two practical methods of SI estimation, the (i) direct and (ii) indirect method. By direct SI estimation, field observations of SI are regressed against bitemporal ALS-derived canopy height metrics, and the regression models are applied for direct prediction of SI. By indirect SI estimation, the SI is derived from the estimated Hdom at the initial point in time, the estimated Hdom increment and the length of the observation period.

2. To assess the utility of bitemporal ALS data for forest change classification.

Undisturbed forest growth is a prerequisite for reliable SI estimation. The operational application of the abovementioned methods requires the identification of forest areas in which disturbances are likely to have occurred during the observation period, i.e., between measurement occasions. The suitability of spatial units (grid cells) for SI estimation must be classified based on whether such disturbances have occurred, to ensure that predictions of SI are limited to undisturbed forest. The second paper therefore assessed the use of bitemporal ALS data for classification of various forest changes.

3. To demonstrate a practical method for predicting and mapping SI over large areas in repeated ALS-based forest inventories.

Based on the conclusions drawn from the first two papers, the third paper demonstrated a complete method for predicting and mapping SI over large areas, which included discrimination between tree species and identification of forest areas that had been subject to forest disturbance. By using bitemporal datasets acquired as part of three repeated operational inventories conducted by a commercial forest owners' cooperative, the proof-of-concept could thus be validated in an operational context.

4. To assess the economic utility of remotely sensed 3D data for estimation of SI in forest management inventories.

The last paper compared seven inventory methods of SI estimation in a cost-plus-loss analysis, by which the expected economic losses due to sub-optimal treatment decisions were added to the inventory costs. The methods were: direct estimation using models dependent on (i) bitemporal ALS data and (ii) ALS and subsequent DAP data, indirect estimation from canopy height trajectories estimated from (iii) bitemporal ALS data and (iv) ALS and subsequent DAP data, direct estimation using the age from the stand register and single-date canopy height estimated from (v) ALS and (vi) DAP data, and manual interpretation from (vii) aerial imagery supported by field assessment and information from previous inventories.

3. Materials

3.1 Study areas

The data used in this thesis were collected in four repeated ALS-based forest inventories in: Krødsherad (50 km^2), Nordre land (490 km^2), Hole (45 km^2) and Tyristrand (60 km^2) (Fig. 4), hereafter referred to as districts A, B, C and D, respectively. The districts are located in the boreal zone in southeastern Norway. The majority of the forest land is privately owned, and forestry activities such as silvicultural operations, harvests and timber sales are mostly organized and implemented by forest owners' cooperatives. The forests are mostly coniferous, composed of Norway spruce (*Picea abies* (L.) Karst.) and Scots pine (*Pinus sylvestris* L.). Deciduous species are found mainly in younger stands, and include silver birch (*Betula pendula* Roth) and downy birch (*Betula pubescens* Ehrh.).
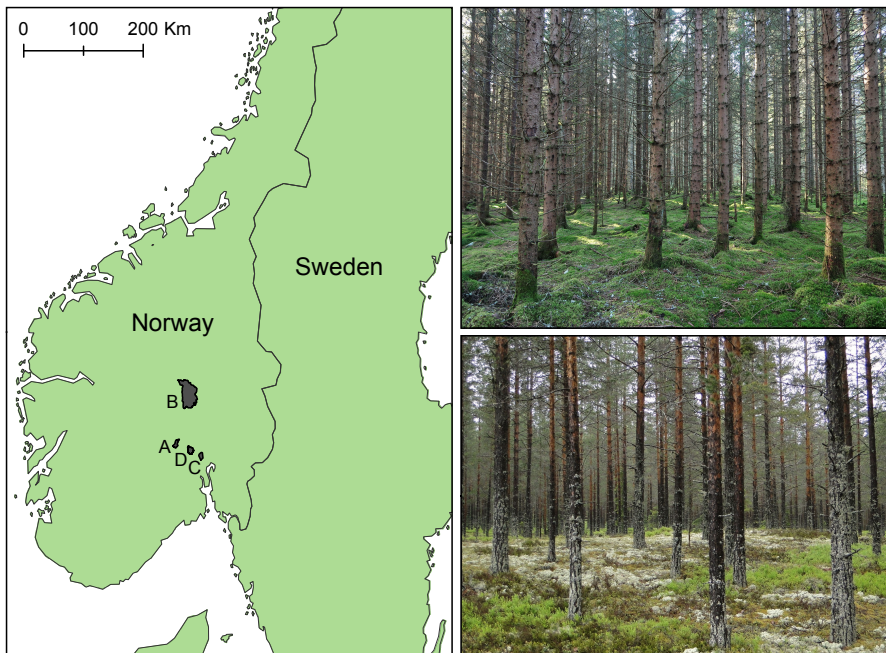

Fig. 4. Map of the locations of the four districts, in which Norway spruce
(top right) and Scots pine (bottom right) are the main tree species.

3.2 Forest inventory data

The bitemporal datasets used in this thesis were acquired by Viken Skog SA, one of the larger Norwegian forest owners' cooperatives, which implemented the inventories. Field plot data, aerial imagery and ALS data from two inventory cycles were used. An overview over the inventories used in each paper is given in Table 1. During the first inventory cycle in the early 2000s, the use of ALS was in its experimental phase, and the inventories provided a means to test its usefulness for forest inventory applications Næsset (2004a,b, 2007). In the years 2016-2017, the inventories were among the first ALS-based forest management inventories to be repeated, thus providing bitemporal field and remotely sensed data.

Table 1. Inventories used in the analyses.

	District			
	A	B	C	D
Paper I	•			
Paper II	•	•	•	•
Paper III		•	•	•
Paper IV	•			

During the first inventory cycle, locations of sample plots were determined by means of stratified systematic sampling designs, using separate regular grids for the individual strata. The designs ensured a wide variety of forest types in terms of species composition, development class and SI. A total of 621 circular sample plots were distributed throughout the districts, with areas of 233 m^2 in district A and 250 m^2 in the remaining districts.

In addition to the sample plots, a total of 137 validation plots were measured in districts A, B and C. In district A, square validation plots of 3700 m^2 were distributed over subjectively chosen stands with the aim of covering a wide variety of forest types. The validation plots were divided into 16 subplots of approximately 233 m^2. In districts B and C, circular validation plots of 1000 m^2 were distributed over mature forest stands, and divided into quadrants of 250 m^2. For details on the inventory designs see Næsset (2004a,b, 2007) and Noordermeer et al. (2020). An overview over the number of plots measured in the inventories is given in Table 2.

Table 2. Summary of plot surveys.

District	Name	First inventory cycle		Second inventory cycle	
		No. of sample plots	No. of validation plots	No. of sample plots	No. of validation plots
A	Krødsherad	116	57	131	49
B	Nordre Land	265	40	180	21
C	Hole	120	40	90	29
D	Tyristrand	120	0	108	0

During the first inventory cycle (T1), the field plots were measured during the summers of 2001, 2003-2004, 2005 and 2006 for districts A-D, respectively. All living trees with a DBH > 10 cm were callipered, and tree species were recorded. Approximately 10 sample trees were selected using a relascope and their heights were measured using a Vertex™ hypsometer. Plot locations were determined with global positioning system (GPS) and global navigation satellite system (GLONASS) measurements. The plots were revisited at T2, and in case no final harvest had taken place, re-measured using the same field protocol. In addition, two site trees were selected within the sample plots at T2, being the largest trees according to DBH of the dominant species. A total of 16 and 4 site trees were selected within validation plots in districts A and B/C, respectively. The heights of site trees were measured and the age at breast height was determined by coring.

3.3 Remotely sensed data

For all districts, aerial imagery and ALS data were acquired at two points in time. The aerial imagery was used for stand delineation and subjective interpretation of the dominant tree species, development class and SI. Hence, the photo-interpretation formed the basis for the stratification as well as providing stand level information in the inventories.

The ALS data covering the districts at T1 were acquired during the summers of 2001, 2003, 2004 and 2005 for districts A-D, respectively. Subsequent ALS datasets covering the districts were acquired in 2016 (T2). All ALS data were acquired under leaf-on conditions, the data acquisition parameters are shown in Table 3. The ALS data were processed by the vendors, including filtering and tiling, and echo heights were normalized by generating digital terrain models as triangular irregular networks from echoes classified as ground, and subtracting the height of the terrain from the echo heights.

Table 3. Specifications of the airborne laser scanning data used in this thesis.

District	First acquisition			Second acquisition		
	Instrument	Year	Echo density	Instrument	Year	Echo density
A	Optech ALTM 1210	2001	1 m^{-2}	Riegl LMS Q-1560	2016	12 m^{-2}
B	Optech ALTM 1233	2003	1 m^{-2}	Riegl LMS Q-1560	2016	4 m^{-2}
C	Optech ALTM 1233	2004	1 m^{-2}	Riegl LMS Q-1560	2016	10 m^{-2}
D	Optech ALTM 3100	2005	1 m^{-2}	Riegl LMS Q-1560	2016	8 m^{-2}

For the analysis of paper IV, aerial imagery was used to generate a DAP point cloud by image matching. The imagery was acquired in 2016 as part of a national orthophoto campaign, covering an area much larger than district A, with 75 flight lines and a total of 8500 images. The mean flying altitude was 5300 meters and the images were captured with approximately 20% side- and 80% forward overlap. The software SURE Aerial (Rothermel et al., 2012) was used to generate the point cloud, using the default settings. Normalization of the DAP point cloud was performed by using the ALS-derived terrain model generated for T2. The resulting DAP point cloud had a point density of 37 points/m^2.

4. Methods

4.1 Field data computation

Using the field datasets acquired at T2, the SI was predicted for individual site trees with empirical SI models (Sharma et al., 2011) using age and height as predictors. Heights had only been measured for site trees and sample trees, so the heights of all callipered trees were imputed using the skogR package (Ørka, 2020) in R. For all districts and for both points in time, the Hdom was computed as the mean height of those trees that corresponded to the 100 largest trees according to DBH. For the analyses of papers II and III, the number of stems (N) was computed from the calipered trees, scaled to per ha values. In addition, the aboveground biomass (AGB) was predicted for individual callipered trees using allometric models (Marklund, 1988), and plot level AGB was computed as the sum of AGB predictions scaled to per ha values. For the analysis of paper IV, the mean age of site trees was computed for validation plots, and the basal area (G) was computed as the area in m^2 per ha.

4.2 Point cloud metrics

The laser echoes, i.e., ALS points, that fell within the spatial extent of the plots were extracted from the bitemporal ALS datasets, and height distributions were created for the computation of point cloud metrics. All points with heights < 2 m above the ground were excluded for the computation of point cloud metrics, as they were not considered to belong to the canopy. For paper I, ALS metrics were computed separately for first and last laser echoes, however for the remaining papers, only first echoes were used because they were considered to be most sensitive to changes in canopy height. Canopy height metrics were computed as the mean height, maximum height, standard deviation and coefficient of variation, and the heights at the 10th, 20th, ..., 90th percentiles of height distributions. In paper II, the kurtosis and skewness of the height distributions were computed as well. The height range between the lowest canopy point and the 95th percentile was divided into 10 bins of equal height, and canopy density metrics were computed as the proportion of points above each fraction divided by the total number of points. Differential metrics were computed as the differences between metrics computed for T2 and the corresponding metrics computed for T1. For the analysis of paper

III, regular grids were generated by tessellating districts B, C and D into cells of 250 m^2, and point cloud metrics were computed for each grid cell. For paper IV, DAP points were extracted in addition to the ALS points, whereby only the mean point height and 90th percentile for the two points in time and the differences therein were used in the analysis, as they were considered to be most relevant for characterizing canopy height development.

4.3 Data analyses

The first objective of this thesis was to assess and compare two methods of SI estimation using bitemporal ALS-derived tree height data. Paper I presented the (i) direct and (ii) indirect methods. In the direct method, plot level values of SI, based on the age and height of site trees, were regressed against bitemporal ALS canopy height metrics. The regression models were then applied for direct prediction of SI. The indirect method corresponds to the height-differential approach described in section 1.4, where SI is derived from Hdom growth over a given time interval. For both points in time, Hdom was regressed against ALS canopy height metrics computed from the corresponding point cloud. The models were then applied to the validation plots to predict Hdom for individual subplots, and the Hdom was then estimated for each validation plot as the mean value of predictions made for subplots. Thus, Hdom was estimated at both points in time for each validation plot. The SI was then calculated from the initial Hdom, the Hdom increment and the length of the observation period (Fig. 5). For each validation plot, the age needed to reach the initial Hdom was calculated for all discrete values of SI ranging from 5 to 30. The Hdom was then projected to T2 using empirical SI models (Sharma et al., 2011), given each value of SI and the calculated age added to the length of the observation period. Finally, the SI was obtained by interpolating between the two SI curves which corresponded most closely to the actual Hdom at T2. Ground reference values of height-differential SI were computed in the same way, only using field-observed Hdom from the two points in time as opposed to laser-estimated Hdom.
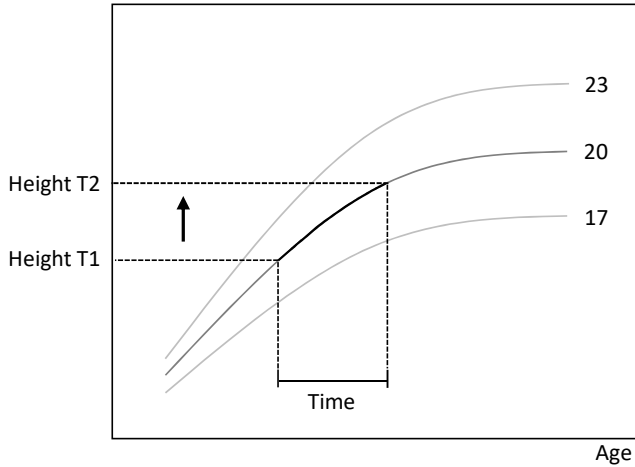
Fig. 5. Illustration of the indirect method, by which the SI is derived from the initial dominant height (Height T1), the estimated dominant height increment (Height T2 – Height T1) and the length of the observation period (Time).

In accordance with the second objective, the utility of bitemporal ALS data for forest change classification was assessed in paper II. Four sets of change categories were classified: (i) increasing and decreasing Hdom, (ii) increasing and decreasing AGB, (iii) undisturbed and disturbed forest, and (iv) forestry activities, namely untouched, partial harvest and clearcut. The k-nearest neighbor (kNN) method (Cover and Hart, 1967) was applied for the classification of the different changes based on bitemporal ALS data. The field-based change classes were assigned on the basis of changes in ground reference data on each plot. A decrease in Hdom or AGB was used as an indicator of forest disturbance. In the forestry activity classification, the untouched class comprised undisturbed forest, the partial harvest class comprised forest in which a temporary reduction in Hdom, AGB or N had taken place, and the clearcut class comprised the same reductions, and an additional rule that AGB had to be reduced by more than 90%.

Based on the conclusions of papers I and II, a large-area operational application of the direct method was demonstrated in paper III. Following an area-based inventory approach, forest areas were first classified as disturbed or undisturbed using the methods presented in paper II, whereby the classification was applied over a grid tessellating the inventory areas into 250 m^2 grid cells. The direct method was then applied to undisturbed grid cells, to avoid predictions of SI in

areas where silvicultural treatments, natural calamities or other events likely had disrupted forest growth during the observation period.

In paper IV, the economic values of seven inventory methods of SI estimation were compared by means of a cost-plus-loss analysis. Thus, both the accuracy and the economic values of the methods were assessed. Direct and indirect methods were applied using bitemporal combinations of ALS and DAP data, and SI was additionally estimated from single-date ALS and DAP data and registered stand age. The SI retrieved from the stand register represented the estimates obtained by conventional practices. The inventory costs were calculated for each inventory method, based on information obtained from the forest owners' cooperative that implemented the inventory and the vendor that supplied the remotely sensed data. Then, the economic losses due to sub-optimal treatment decisions were calculated using the forest scenario model GAYA (Hoen and Eid, 1990; Hoen and Gobakken, 1997), and added to the inventory cost. To calculate the losses, optimal treatment schedules were first generated for the validation plots using ground reference data assumed to be error-free, and their net present values (NPVs) were calculated. Then, sub-optimal treatment schedules and NPVs were generated using erroneous SI estimates obtained with the seven inventory methods. The losses were calculated as the difference between the NPV of the optimal treatment schedules and the NPVs of the sub-optimal treatment schedules generated using erroneous SI estimates. Finally, the total inventory costs were calculated for each inventory method as the mean NPV losses of each inventory method added to the inventory cost.

4.4   Validation

For the analyses of papers I and IV, SI was estimated for 42 validation plots with areas of ~ 3700 m^2. The models were first applied to each individual subplot to predict the SI, and validation plot level SI was subsequently estimated as the mean of SI predictions made for subplots within the validation plot. Field data on the age and height of site trees allowed for a comparison of the laser-estimated SI with ground reference values of SI. To evaluate the accuracy of the indirect method in paper I, ground reference values of height-differential SI, calculated from ground reference Hdom from the two points in time, were compared with the corresponding values of SI estimated from bitemporal ALS data.

Cross validation was used for the evaluation of the classification accuracies in paper II. Single plots were removed iteratively, and the kNN classifiers were fitted with data from the remaining plots. For each iteration, the out-of-sample plot was classified, and the procedure was repeated until each plot obtained a class label. The accuracies of the classifications were then assessed using the overall accuracy and kappa.

In paper III, cross validation was used to assess the accuracy of disturbance classifications and SI predictions at the level of the 250 m^2 sample plots. In addition, the models for predicting SI were applied to the circular validation plots of 1000 m^2 located in districts B and C. The validation plots were divided into four quadrants, and SI was estimated for each validation plot as the mean of predictions made for quadrants classified as undisturbed.

The accuracy of SI predictions in paper I was assessed by computing the mean differences (MD) and root mean square error (RMSE). The RMSE is a collective expression of the magnitude of the random and systematic deviations between the true and the estimated value. In paper III, the RMSE relative to the ground reference mean (RMSE%) was additionally computed, and in paper IV, the MD relative to the ground reference mean (MD%) was also used in the assessment.

5. Results and discussion

5.1 Methods of SI estimation

Overall, the direct method was slightly more accurate than the indirect method (Table 4), which may be expected because direct estimates only contain a single set of errors as opposed to errors occurring for both points in time (McRoberts et al., 2014). Systematic errors were, however, greater for estimates obtained by the direct method than those obtained by the indirect method. The direct method provided better accuracy in pine-dominated forest than in spruce-dominated forest, while the indirect method worked equally well in either species groups.

Table 4. Mean differences (MD) and root mean square errors (RMSE) between ground reference and laser-estimated H40 site index obtained for validation plots in district A.

Method	Dominant species	MD	RMSE
Direct	Spruce	-0.67	1.78
Direct	Pine	0.53	1.08
Indirect	Spruce	-0.13	1.82
Indirect	Pine	-0.04	1.82

There were strong correlations between ground reference values of SI and bitemporal ALS metrics, which is a logical result; larger values of ALS metrics that reflect initial canopy height and canopy height increment suggest a high SI. However, no previous study had modelled SI directly from bitemporal ALS data and applied the models in an area-based inventory approach. Although several studies had used bitemporal ALS data for predicting SI at the level of individual trees (Hollaus et al., 2015; Kvaalen et al., 2015; Solberg, 2010), such methods have less potential for use in repeated forest management inventories. Firstly because individual tree analyses require point densities $> 5\text{-}10$ m^{-2} (Yu et al., 2010), which is higher than what is commonly available from previous inventories carried out 10-15 years earlier. Secondly, the area-based method is the most common method for ALS-based forest inventory (White et al., 2013a), and the direct and indirect methods proposed in paper I can thus more easily be incorporated in operational forest management inventories.

Although less accurate, the indirect method provided a practical alternative because it is age-independent. In a previous study, Véga and St-Onge (2009) estimated SI indirectly from a time series of canopy height models constructed from historical DAP data and an ALS-derived digital terrain model. Using a similar approach, Persson and Fransson (2016) used two canopy height models constructed from bitemporal ALS data. The two studies differed from paper I, however, in that the temporal resolutions were 58 and 3 years, respectively, and because they used canopy height models as opposed to area-based estimates of Hdom. The temporal resolution of 15 years in paper I is a more likely scenario in repeated ALS-based forest inventories, and the results may therefore be more relevant from an operational perspective.

Two main advantages of indirect SI estimation are that no additional field work is required, as SI is estimated from Hdom at two points in time, and that the obtained SI estimates reflect recent growing conditions. However, being based on Hdom development over a much shorter window of time than the more common age-height approach, also makes the indirect method more sensitive to errors. Accurate and precise Hdom estimates are required at both points in time, as small deviations at either point in time will have great impact on the obtained SI estimates. Particularly systematic errors occuring at both points in time and in oppsite directions will have considerable negative impact on the accuracy of the obtained SI estimates. The direct method, on the other hand, has the advantage that it can easily be incorporated in repeated ALS-based forest inventories, in which models are already commonly applied for direct prediction of forest attributes. Another advantage of the direct approach is that field data from only a single point in time are needed.

5.2 Classifications of forest change

Paper II demonstrated that changes in ALS data are good indicators of various types of changes in forest structure. Cross validation of the kNN classifiers revealed high accuracies for all change classifications (0.88–0.96 overall accuracy, Fig. 6). Especially changes in Hdom and AGB were easily detected from bitemporal ALS data.
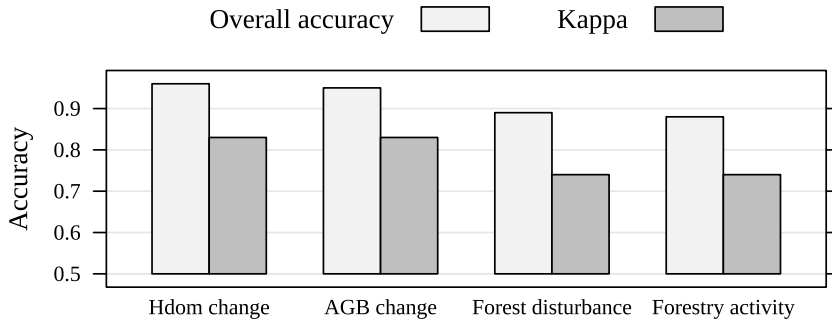
Fig. 6. Accuracies obtained for classifications of changes in dominant height (Hdom), aboveground biomass (AGB), forest disturbances and forestry activities.

The result that bitemporal ALS data are suitable for classification of changes in forest structure may be expected. The utility of single-date ALS data for the estimation of Hdom and AGB has long been recognized (Jochem et al., 2011; Kandare et al., 2017), because they provide accurate information on the height and density of the canopy. Therefore, bitemporal ALS data can be expected to be useful in identifying changes in such structural parameters. In a previous study, Næsset et al. (2013) classified the same forestry activity classes distinguished in paper II from bitemporal ALS data at plot level and obtained an overall accuracy of 0.94. However, only few other studies had assessed the use of bitemporal ALS data for forest change classification, which were limited to the detection of single harvested trees (Yu et al., 2004) and canopy gaps (Solberg, 2010; St-Onge and Vepakomma, 2004).

The obtained results were particularly relevant to this thesis because the classification of forest change is an essential task when estimating SI from bitemporal ALS data in an operational context. All such methods require spatial units to be classified based on whether any substantial forest disturbances have occurred during the observation period. Areas in which silvicultural treatments or natural calamities have disrupted forest growth, for example, will be unsuitable for SI estimation. Therefore, the results were encouraging in that bitemporal ALS data acquired as part of repeated ALS-based forest inventories proved to be highly useful in the classification of such changes in forest structure. The availability of bitemporal 3D data will increase as forest management inventories are continuously updated, allowing for the operational application of forest change classifications.

5.3 Predicting and mapping site index

A practical method for predicting and mapping SI was demonstrated in paper III, which can be applied in repeated area-based forest inventories in which bitemporal 3D data are available. The method has three major advantages over conventional practices in operational inventories. First, the estimation of SI is performed automatically, as opposed to manual photo interpretation, and is therefore more time-efficient. Second, the predictions are based on objective statistical relationships between ground reference values of SI and bitemporal ALS metrics, as opposed to subjective assessment. Third, maps of SI can be generated with a spatial resolution of sample plots, i.e., a much higher resolution than what is common in stand level inventories. Within-stand variations of SI can be considerable (Eid, 1992) and sub-stand level information on SI may improve the utility of the data for forest planning (Eid and Økseter, 1999).
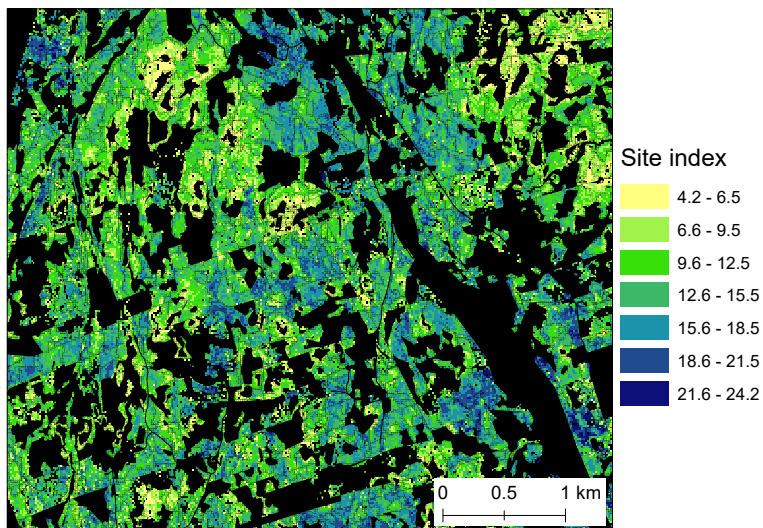
Fig. 7. Subset of the site index map constructed for district C. Areas
classified as unsuitable for site index prediction are shown in black.

The results confirmed the conclusions drawn from paper I in that bitemporal ALS data are a useful data source when estimating SI. Values of RMSE% obtained for sample plots and validation plots ranged from 10.81-20.03 (Table 5). After applying the models for predicting SI across the districts, cell level predictions covering 337, 24 and 70 km^2 were generated for districts B, C and D, respectively.

The SI predictions provided quasi-continuous SI maps covering stands of spruce and pine (Fig. 7).

Table 5. Accuracy assessment of site index predictions.

	Sample plots		Validation plots	
District	MD%	RMSE%	MD%	RMSE%
B	0.03	16.21	5.19	12.97
C	0.11	20.03	0.40	15.41
D	-0.21	10.81	-	-

Certain proportions of the forest areas were omitted from the maps because they were classified as disturbed. For those areas, predictions would have to be made during the next inventory cycle, and in the current inventory, SI estimation would have to rely on information obtained from the field, a previous inventory or aerial image interpretation. As an alternative, areas classified as disturbed may be in proximity to areas for which predictions of SI can be made, in which case values could also be imputed based on values of SI from neighboring grid cells.

Besides a classification of the suitability of forest areas for SI estimation, wall-to-wall information on the dominant tree species and development stage are required to ensure that the correct species-specific models are used for prediction, and that predictions for regeneration forest are avoided. The maps will be limited to forest stands which have passed the regeneration stage, because Norwegian SI functions do not apply to forests younger than 15 years at breast height (Sharma et al., 2011).The analysis of paper III relied on species and development stage data obtained from the stand register. As an alternative, however, tree species classification could be performed at grid cell level using remotely sensed data (Dalponte et al., 2012; Ørka et al., 2013). Similarly, the forest development stage can effectively be classified from ALS data (Valbuena et al., 2016; van Ewijk et al., 2011). Thus, essentially all the above-mentioned classifications could be performed on the basis of remotely sensed data, which could prove highly beneficial when combined with the methods proposed in this thesis. Particularly cell level information on the dominant tree species may improve the accuracy of SI predictions, because tree species are likely to vary within stands, at least to some extent.

5.4   Cost-plus-loss analysis

The economic utility of seven methods of SI estimation were compared in paper IV. The first part of the analysis comprised the accuracy assessment of the methods. The results confirmed the conclusions drawn in paper I and III in that direct methods of SI estimation provided reliable estimates (Table 6). One of the novel aspects of paper IV in relation to previous studies, was that the use of DAP was tested as an alternative data source at T2. The accuracies of SI estimates obtained from the bitemporal combination of ALS and subsequent DAP were almost identical to those obtained from bitemporal ALS data.

Table 6. Site index estimation errors.

Inventory method	RMSE (m)	MD (m)	RMSE%	MD%
Direct method, bitemporal ALS	1.49	0.02	9.79	0.13
Direct method, ALS and subsequent DAP	1.53	-0.11	10.04	-0.71
Indirect method, bitemporal ALS	2.46	1.54	16.11	10.12
Indirect method, ALS and subsequent DAP	2.66	1.10	17.49	7.21
Single-date ALS	2.11	0.65	13.91	4.29
Single-date DAP	2.11	0.51	13.88	3.36
Conventional practices	2.38	0.50	15.67	3.30

The use of single-date ALS and DAP data in combination with age obtained from the stand register provided a practical alternative to the use of bitemporal 3D data, and proved to be suitable for SI estimation when applied to even-aged stands of which the age is known with high certainty. In a previous study, Holopainen et al. (2010) investigated a similar approach by classifying five forest site types on the basis of single-date ALS data and stand register age, and obtained an overall accuracy of 70.9%. Packalén et al. (2011) obtained very accurate estimates of SI with a RMSE% of 3 in eucalyptus monocultures in Brazil. In the latter study however, the forest structure was considerably more homogenous than what is common in Norway, as the trees had been planted in rows with a fixed stem density, and the exact years of planting were known.

The second part of the study comprised the cost-plus-loss analysis. Also here, direct methods of SI estimation based on bitemporal 3D data gave the best results. The inventory costs were similar among inventory methods, partly because previously collected ALS data were assumed to be free of cost. However, economic losses due to the use of erroneous data in the planning process differed substantially (Table 7), and therefore the total inventory costs as well. The total cost obtained for direct estimation using ALS and subsequent DAP data was 29.80 € ha^{-1}, whereas the total cost of using conventional practices was 63.66 € ha^{-1}, indicating that the total cost can be reduced by more than 30 € ha^{-1} by taking advantage of bitemporal 3D data.

Table 7. Inventory costs, mean losses and total costs for the seven methods of SI estimation.

Inventory method	Inventory cost (€ ha^{-1})	Mean loss (€ ha^{-1})	Total cost (€ ha^{-1})
Direct method, bitemporal ALS	5.45	27.94	33.40
Direct method, ALS and subsequent DAP	4.56	25.30	29.80
Indirect method, bitemporal ALS	5.40	75.30	80.70
Indirect method, ALS and subsequent DAP	4.50	51.84	56.34
Single-date ALS	5.40	59.88	65.28
Single-date DAP	4.50	56.70	61.20
Conventional practices	5.46	58.20	63.66

6. Conclusions and perspectives

6.1 Conclusions

This thesis presents practical methods of SI estimation using bitemporal data obtained in repeated forest management inventories. The data used in this thesis proved to be highly suitable for SI estimation. The methods presented here can be used to predict, map and estimate SI at sub-stand level automatically over large areas of forest, and can be adopted to replace conventional practices of SI estimation in operational inventories.

Both the direct and indirect methods presented in paper I were accurate in estimating SI, however the direct method was most accurate. The direct method has great potential for operational application in forest management inventories, in which models are already commonly applied to predict a range of forest attributes. Models for predicting SI can then be used alongside others, the only difference being that 3D data from a previous point in time is needed. The indirect method may prove highly beneficial in inventories where ground reference values of SI are not available, and SI estimation will have to be based on Hdom estimates from two points in time.

Bitemporal ALS data are highly suitable for detecting changes in forest structure. Changes in Hdom, AGB, forest disturbances and forestry activities were classified with overall accuracies of around 90% or higher. The results were particularly relevant from an operational point of view, because a classification of the suitability of forest areas is needed to ensure that predictions of SI are limited to undisturbed forest.

By combining the direct method proposed in paper I with the forest disturbance classification shown in paper II, a practical method for predicting and mapping SI in large-area inventories was demonstrated in paper III. Operational validation confirmed the conclusions drawn from paper I in that there were strong statistical relationships between ground reference values of SI and changes in 3D point cloud data. Bitemporal ALS data were used to predict and map SI at a much finer spatial resolution than what is common in operational forest management inventories.

When using remotely sensed 3D data for SI estimation in forest management inventories, the choice of method has great impact on both the accuracy and the economic utility of the produced estimates. Both in terms of accuracy and economic utility, direct SI estimation from bitemporal 3D data provided a substantial improvement from conventional practices. DAP proved to be a suitable source of tree height data for SI estimation, which is encouraging from a cost-saving perspective, as DAP provides a low-cost means to update previous ALS-based inventories. Although the methods presented here are restricted to forest areas in which Hdom growth has remained undisturbed, they can be applied over large areas of forest automatically, with greater accuracy than conventional practices and at a smaller total cost.

6.2 Future perspectives

Future operational trials of the methods proposed in this thesis may clarify a number of issues. First, stratification based on forest attributes other than tree species alone (e.g. development class, altitude, changes in 3D data, SI estimates obtained from a previous inventory) may improve the accuracy of SI estimates. Second, the proposed methods have yet to be tested on inventory data from countries other than Norway. Third, remote sensing based and cell level classifications of tree species, development stage and other potential stratification criteria may pave the way to a more efficient operational workflow. Regarding the classification of forest disturbances, no guideline has been set for the minimum proportion of undisturbed forest within a given stand for reliable SI estimation. Lastly, there are several theoretical considerations that should be taken into account when aggregating cell level predictions of SI to stand level. In theory, SI is defined at the scale of 1 ha, and when predicting or estimating SI for areas of different sizes, an even distribution of site trees is assumed, while in fact site trees are likely to be clustered to some extent. Questions regarding whether stand level SI estimates should simply be an average of SI predictions, or perhaps be weighed by cell level predictions of, for example, basal area therefore require more investigation.

More research is needed in developing suitable methods of SI estimation in regeneration stands. SI models in most parts of the world are not valid for regeneration forests, because they have not been calibrated with such data, and field methods of SI estimation in such forests have not been studied extensively, let alone the linkage to remotely sensed 3D data. In addition, further research may clarify whether

the methods proposed here may be combined with data acquired from other platforms. Data obtained from spaceborne platforms such as ICESat-2, GEDI and TanDEM-X may prove highly suitable for the assessment of forest productivity over spatial scales extending beyond those of forest management inventories. Also, the methods proposed in this thesis have been based on bitemporal datasets with temporal resolutions of 10-15 years, however it may prove beneficial to further develop the methods for application on time series of 3D data with shorter time intervals. Growing conditions and forest productivity may be more dynamic than previously assumed, and tracking changes in forest areas with higher frequency and over longer periods of time may therefore contribute to more reliable forest change monitoring. It is therefore important to push the development of remote sensing toward the front line of change applications, especially when assessing forest productivity under changes in growing conditions.

References

Ali-Sisto, D. and Packalen, P. (2016). Forest change detection by using point clouds from dense image matching together with a lidar-derived terrain model. *IEEE Journal of Selected Topics in Applied Earth Observations and Remote Sensing*, 10(3):1197–1206.

Andersen, H. E., Barrett, T., Winterberger, K., Strunk, J., and Temesgen, H. (2009). Estimating forest biomass on the western lowlands of the kenai peninsula of alaska using airborne lidar and field plot data in a model-assisted sampling design. In *Proceedings of the IUFRO Division 4 Conference: "Extending Forest Inventory and Monitoring over Space and Time*, pages 19–22.

Batho, A. and García, O. (2006). De perthuis and the origins of site index: a historical note. *Forest Biometry, Modelling and Information Science*, 1:1–10.

Berrill, J. P. and O'Hara, K. L. (2014). Estimating site productivity in irregular stand structures by indexing the basal area or volume increment of the dominant species. *Canadian journal of forest research*, 44(1):92–100.

Bohlin, J., Wallerman, J., and Fransson, J. E. (2012). Forest variable estimation using photogrammetric matching of digital aerial images in combination with a high-resolution dem. *Scandinavian Journal of Forest Research*, 27(7):692–699.

Boisvenue, C. and Running, S. W. (2006). Impacts of climate change on natural forest productivity–evidence since the middle of the 20th century. *Global Change Biology*, 12(5):862–882.

Bufton, J. L., Garvin, J. B., Cavanaugh, J. F., Ramos-Izquierdo, L. A., Clem, T. D., and Krabill, W. B. (1991). Airborne lidar for profiling of surface topography. *Optical Engineering*, 30(1):72–79.

Cajander, A. (1909). Über waldtypen. *Acta Forestalia Fennica*, 1(1):1–175.

Carmean, W. H. (1975). Forest site quality evaluation in the united states. In *Advances in agronomy*, volume 27, pages 209–269. Elsevier.

Cover, T. and Hart, P. (1967). Nearest neighbor pattern classification. *IEEE transactions on information theory*, 13(1):21–27.

Dalponte, M., Bruzzone, L., and Gianelle, D. (2012). Tree species classification in the southern alps based on the fusion of very high geometrical resolution multi-spectral/hyperspectral images and lidar data. *Remote sensing of environment*, 123:258–270.

de Laillevaut, L. d. P. et al. (1803). *Traité de l'aménagement et de la restauration des bois et forêts de la France*. Imprimerie de Madame Huzard.

Eid, T. (1992). Bestandsvis kontroll av skogbruksplandata i hogstklasse iii-v. *Meddelelser Fra Norsk Institutt for Skogforskning*, 45(7).

Eid, T. (1996). Kontroll av skogbruksplandata fra understøttet fototakst. *Norsk Institutt for Skogforskning, og Institutt for Skogfag, Norges Landbrukshøgskole, Ås, Norway, Report*, 8:21.

Eid, T. et al. (2000). Use of uncertain inventory data in forestry scenario models and consequential incorrect harvest decisions. *Silva Fennica*, 34(2):89–100.

Eid, T. and Økseter, P. (1999). *Bestandsuavhengig bonitering og konsekvenser*. Norsk Institutt for Skogforskning (NISK).

Ginzler, C. and Hobi, M. L. (2015). Countrywide stereo-image matching for updating digital surface models in the framework of the swiss national forest inventory. *Remote Sensing*, 7(4):4343–4370.

Gisnås, A. (1982). Skogkartlegging ved fototyding i kartkonstruksjonsinstrument. *Report from Norsk Institutt for skogforskning*, 14(82):209–269.

Gobakken, T., Næsset, E., Nelson, R., Bollandsås, O. M., Gregoire, T. G., Ståhl, G., Holm, S., Ørka, H. O., and Astrup, R. (2012). Estimating biomass in hedmark county, norway using national forest inventory field plots and airborne laser scanning. *Remote Sensing of Environment*, 123:443–456.

Goodbody, T. R., Coops, N. C., and White, J. C. (2019). Digital aerial photogrammetry for updating area-based forest inventories: A review of opportunities, challenges, and future directions. *Current Forestry Reports*, 5(2):55–75.

Hagglund, B. et al. (1981). Evaluation of forest site productivity. *For Abstr.*, 42:515–527.

Hamilton, G. J. (1985). Forest mensuration handbook. Technical report.

Hartig, G. L. (1795). *Anweisung zur Taxation der Forste, oder zur Bestimmung des Holzertrags der Wälder: Ein Beytrag zur höheren Forstwissenschaft: Nebst einer illuminirten Forst-Charte und mehreren Tabellen.* Heyer.

Hartig, R. (1892). *Ueber den Entwicklungsgang der Fichte im geschlossenen Bestande nach höhe, Form und Inhalt.*

Hawryło, P., Tompalski, P., and Wezyk, P. (2017). Area-based estimation of growing stock volume in scots pine stands using als and airborne image-based point clouds. *Forestry: An International Journal of Forest Research*, 90(5):686–696.

Heyer, C. (1883). *Die Waldertrags-Regelung.* Teubner.

Hoen, H. and Eid, T. (1990). En modell for analyse av behandlingsstrategier for en skog ved bestandssimulering og lineær programmering (a model for analysis of treatment strategies for a forest applying standwise simulations and linear programming). *Internal report, Norwegian Forest Research Institute, Ås.*

Hoen, H. and Gobakken, T. (1997). Brukermanual for bestandssimulatoren gaya v1. 20. *Internal Report, Norwegian Forest Research Institute, Ås*, page 59.

Hollaus, M., Eysn, L., Maier, B., and Pfeifer, N. (2015). Site index assessment based on multi-temporal als data. *Proceedings of the Silvilaser.*

Holopainen, M., Vastaranta, M., Haapanen, R., Yu, X., Hyyppä, J., Kaartinen, H., Viitala, R., and Hyyppä, H. (2010). Site-type estimation using airborne laser scanning and stand register data. *Photogrammetric Journal of Finland*, 22(1):16–32.

Huang, S. and Titus, S. J. (1993). An index of site productivity for uneven-aged or mixed-species stands. *Canadian Journal of Forest Research*, 23(3):558–562.

Husch, B. (1956). Use of age at dbh as a variable in the site index concept. *J. For*, 54(5):340.

Hyyppä, J., Yu, X., Rönnholm, P., Kaartinen, H., and Hyyppä, H. (2003). Factors affecting laser-derived object-oriented forest height growth estimation. *The Photogrammetric Journal of Finland*, 18(2):16–31.

Jochem, A., Hollaus, M., Rutzinger, M., and Höfle, B. (2011). Estimation of aboveground biomass in alpine forests: a semi-empirical approach considering canopy transparency derived from airborne lidar data. *Sensors*, 11(1):278–295.

Kandare, K., Ørka, H. O., Dalponte, M., Næsset, E., and Gobakken, T. (2017). Individual tree crown approach for predicting site index in boreal forests using airborne laser scanning and hyperspectral data. *International journal of applied earth observation and geoinformation*, 60:72–82.

Kramer, H. (1959). Die oberhöhe als bestandesmerkmal. *Allgemeine Forst- und Jagdzeitung*, 130(10):241–255.

Kvaalen, H., Solberg, S., and May, J. (2015). Aldersuavhengig bonitering med laserskanning av enkelttrær. *Nibio Report*, 1(67):31.

Lillesand, T., Kiefer, R. W., and Chipman, J. (2015). *Remote sensing and image interpretation*. John Wiley & Sons.

Magnussen, S. and Boudewyn, P. (1998). Derivations of stand heights from airborne laser scanner data with canopy-based quantile estimators. *Canadian journal of forest research*, 28(7):1016–1031.

Maltamo, M., Næsset, E., and Vauhkonen, J. (2014). Forestry applications of airborne laser scanning. *Concepts and case studies. Managing Forest Ecosystems*, 27:460.

Matérn, B. (1976). Om skattning av ovre hojden. *Sveriges Skogvardsforbunds Tidskrift*.

McRoberts, R. E., Bollandsås, O. M., and Næsset, E. (2014). Modeling and estimating change. In *Forestry Applications of Airborne Laser Scanning*, pages 293–313. Springer.

McRoberts, R. E., Cohen, W. B., Naesset, E., Stehman, S. V., and Tomppo, E. O. (2010). Using remotely sensed data to construct and assess forest attribute maps and related spatial products. *Scandinavian Journal of Forest Research*, 25(4):340–367.

McRoberts, R. E., Næsset, E., and Gobakken, T. (2013). Inference for lidar-assisted estimation of forest growing stock volume. *Remote Sensing of Environment*, 128:268–275.

Messaoud, Y. and Chen, H. Y. (2011). The influence of recent climate change on tree height growth differs with species and spatial environment. *PLoS one*, 6(2).

Miller, C. I. and Beers, T. W. (1982). *Forest mensuration*. Wiley.

Monserud, R. A. (1981). Variations on a theme of site index. *General Technical Report NC.*, page 419.

Næsset, E. (1994). Sammenlikning av ulike boniteringer av et skogområde. *Rapport fra Skogforsk*, 11:21.

Næsset, E. (1997a). Determination of mean tree height of forest stands using airborne laser scanner data. *ISPRS Journal of Photogrammetry and Remote Sensing*, 52(2):49–56.

Næsset, E. (1997b). Estimating timber volume of forest stands using airborne laser scanner data. *Remote Sensing of Environment*, 61(2):246–253.

Næsset, E. (2002). Predicting forest stand characteristics with airborne scanning laser using a practical two-stage procedure and field data. *Remote sensing of environment*, 80(1):88–99.

Næsset, E. (2004a). Accuracy of forest inventory using airborne laser scanning: evaluating the first nordic full-scale operational project. *Scandinavian Journal of Forest Research*, 19(6):554–557.

Næsset, E. (2004b). Practical large-scale forest stand inventory using a small-footprint airborne scanning laser. *Scandinavian Journal of Forest Research*, 19(2):164–179.

Næsset, E. (2007). Airborne laser scanning as a method in operational forest inventory: Status of accuracy assessments accomplished in scandinavia. *Scandinavian Journal of Forest Research*, 22(5):433–442.

Næsset, E. (2014). Area-based inventory in norway–from innovation to an operational reality. In *Forestry applications of airborne laser scanning*, pages 215–240. Springer.

Næsset, E., Bollandsås, O. M., Gobakken, T., Gregoire, T. G., and Ståhl, G. (2013). Model-assisted estimation of change in forest biomass over an 11 year period in a sample survey supported by airborne lidar: A case study with

post-stratification to provide "activity data". *Remote Sensing of Environment*, 128:299–314.

Næsset, E. and Gobakken, T. (2005). Estimating forest growth using canopy metrics derived from airborne laser scanner data. *Remote sensing of environment*, 96(3-4):453–465.

Niklasson, M. (2002). A comparison of three age determination methods for suppressed norway spruce: implications for age structure analysis. *Forest Ecology and Management*, 161(1-3):279–288.

Nilsson, M. (1996). Estimation of tree heights and stand volume using an airborne lidar system. *Remote sensing of environment*, 56(1):1–7.

Noordermeer, L., Bollandsås, O. M., Ørka, H. O., Næsset, E., and Gobakken, T. (2019). Comparing the accuracies of forest attributes predicted from airborne laser scanning and digital aerial photogrammetry in operational forest inventories. *Remote sensing of environment*, 226:26–37.

Ørka, H. O. (2020). skogr - norwegian forestry functions. *R package*, https://github.com/hansoleorka/skogR.

Ørka, H. O., Dalponte, M., Gobakken, T., Næsset, E., and Ene, L. T. (2013). Characterizing forest species composition using multiple remote sensing data sources and inventory approaches. *Scandinavian Journal of Forest Research*, 28(7):677–688.

Packalén, P., Mehtätalo, L., and Maltamo, M. (2011). Als-based estimation of plot volume and site index in a eucalyptus plantation with a nonlinear mixed-effect model that accounts for the clone effect. *Annals of Forest Science*, 68(6):1085.

Paulsen, J. C. (1795). *Kurze praktische Anweisung zum Forstwesen: oder Grundsäzze über die vortheilhafteste Einrichtung der Forsthaushaltung und über Ausmittelung des Werths vom Forstgrunde besonders auf die Grafschaft Lippe angewendet*. Selbstverl. d. Hrsg.

Persson, H. J. and Fransson, J. E. (2016). Estimating site index from short-term tandem-x canopy height models. *IEEE Journal of Selected Topics in Applied Earth Observations and Remote Sensing*, 9(8):3598–3606.

Pitt, D. G., Woods, M., and Penner, M. (2014). A comparison of point clouds derived from stereo imagery and airborne laser scanning for the area-based estimation of forest inventory attributes in boreal ontario. *Canadian Journal of Remote Sensing*, 40(3):214–232.

Rahlf, J., Breidenbach, J., Solberg, S., Næsset, E., and Astrup, R. (2017). Digital aerial photogrammetry can efficiently support large-area forest inventories in norway. *Forestry: An International Journal of Forest Research*, 90(5):710–718.

Rothermel, M., Wenzel, K., Fritsch, D., and Haala, N. (2012). Sure: Photogrammetric surface reconstruction from imagery. In *Proceedings LC3D Workshop, Berlin*, volume 8, page 2.

Sharma, R. P., Brunner, A., Eid, T., and Øyen, B.-H. (2011). Modelling dominant height growth from national forest inventory individual tree data with short time series and large age errors. *Forest Ecology and Management*, 262(12):2162–2175.

Skovsgaard, J. P. and Vanclay, J. K. (2008). Forest site productivity: a review of the evolution of dendrometric concepts for even-aged stands. *Forestry: An International Journal of Forest Research*, 81(1):13–31.

Skowronski, N. S., Clark, K. L., Gallagher, M., Birdsey, R. A., and Hom, J. L. (2014). Airborne laser scanner-assisted estimation of aboveground biomass change in a temperate oak–pine forest. *Remote Sensing of Environment*, 151:166–174.

Socha, J. (2008). Effect of topography and geology on the site index of picea abies in the west carpathian, poland. *Scandinavian Journal of Forest Research*, 23(3):203–213.

Solberg, S. (2010). Mapping gap fraction, lai and defoliation using various als penetration variables. *International Journal of Remote Sensing*, 31(5):1227–1244.

Solberg, S., Kvaalen, H., and Puliti, S. (2019). Age-independent site index mapping with repeated single-tree airborne laser scanning. *Scandinavian Journal of Forest Research*, pages 1–8.

Spurr, S. H., Barnes, B. V., et al. (1973). Forest ecology. *Forest ecology.*, (2. ed.).

St-Onge, B. and Vepakomma, U. (2004). Assessing forest gap dynamics and growth using multi-temporal laser-scanner data. *Power*, 140:173–178.

Stearns-Smith, S. (2002). Making sense of site index estimates in british columbia: A quick look at the big picture. *Journal of Ecosystems and Management*, 1(2).

Straub, C., Stepper, C., Seitz, R., and Waser, L. T. (2013). Potential of ultracamx stereo images for estimating timber volume and basal area at the plot level in mixed european forests. *Canadian Journal of Forest Research*, 43(8):731–741.

Tompalski, P., Coops, N. C., Marshall, P. L., White, J. C., Wulder, M. A., and Bailey, T. (2018). Combining multi-date airborne laser scanning and digital aerial photogrammetric data for forest growth and yield modelling. *Remote Sensing*, 10(2):347.

Tomppo, E., Gschwantner, T., Lawrence, M., McRoberts, R. E., Gabler, K., Schadauer, K., Vidal, C., Lanz, A., Ståhl, G., and Cienciala, E. (2010). National forest inventories. *Pathways for Common Reporting. European Science Foundation*, pages 541–553.

Tveite, B. (1976). Bonitetskurver for furu. norwegian forest research institute. Technical report, Ås, Internal report. 40 p.(In Norwegian.).

Tveite, B. (1977). Bonitetskurver for gran: Site-index curves for norway spruce (picea abies (l.) karst).

Valbuena, R., Maltamo, M., and Packalen, P. (2016). Classification of multilayered forest development classes from low-density national airborne lidar datasets. *Forestry: An International Journal of Forest Research*, 89(4):392–401.

van Ewijk, K. Y., Treitz, P. M., and Scott, N. A. (2011). Characterizing forest succession in central ontario using lidar-derived indices. *Photogrammetric Engineering & Remote Sensing*, 77(3):261–269.

Vasilescu, M. M. (2013). Standard error of tree height using vertex iii. *Bulletin of the Transilvania University of Brasov. Forestry, Wood Industry, Agricultural Food Engineering. Series II*, 6(2):75.

Véga, C. and St-Onge, B. (2009). Mapping site index and age by linking a time series of canopy height models with growth curves. *Forest Ecology and Management*, 257(3):951–959.

Villalba, R. and Veblen, T. T. (1997). Improving estimates of total tree ages based on increment core samples. *Ecoscience*, 4(4):534–542.

Wakeley, P. C. (1954). The growth intercept method of site classification. In *Proc. 3rd Ann. For. Symp. Louisiana State Univ., Baton Rouge*, pages 32–33.

Watt, M. S., Palmer, D. J., Kimberley, M. O., Höck, B. K., Payn, T. W., and Lowe, D. J. (2010). Development of models to predict pinus radiata productivity throughout new zealand. *Canadian Journal of Forest Research*, 40(3):488–499.

Weise, W. (1880). *Ertragstafeln für die Kiefer: Im Auftrage des Vereins deutscher forstlicher Versuchs-Anstalten bearbeitet durch die Königlich Preussische Hauptstation des forstlichen Versuchswesens.* Springer-Verlag.

White, J. C., Tompalski, P., Coops, N. C., and Wulder, M. A. (2018). Comparison of airborne laser scanning and digital stereo imagery for characterizing forest canopy gaps in coastal temperate rainforests. *Remote Sensing of Environment*, 208:1–14.

White, J. C., Wulder, M. A., Varhola, A., Vastaranta, M., Coops, N. C., Cook, B. D., Pitt, D., and Woods, M. (2013a). A best practices guide for generating forest inventory attributes from airborne laser scanning data using an area-based approach. *The Forestry Chronicle*, 89(6):722–723.

White, J. C., Wulder, M. A., Vastaranta, M., Coops, N. C., Pitt, D., and Woods, M. (2013b). The utility of image-based point clouds for forest inventory: A comparison with airborne laser scanning. *Forests*, 4(3):518–536.

Woods, M., Pitt, D., Penner, M., Lim, K., Nesbitt, D., Etheridge, D., and Treitz, P. (2011). Operational implementation of a lidar inventory in boreal ontario. *The Forestry Chronicle*, 87(4):512–528.

Yu, X., Hyyppä, J., Holopainen, M., and Vastaranta, M. (2010). Comparison of area-based and individual tree-based methods for predicting plot-level forest attributes. *Remote Sensing*, 2(6):1481–1495.

Yu, X., Hyyppä, J., Kaartinen, H., and Maltamo, M. (2004). Automatic detection of harvested trees and determination of forest growth using airborne laser scanning. *Remote sensing of Environment*, 90(4):451–462.

Yu, X., Hyyppä, J., Kukko, A., Maltamo, M., and Kaartinen, H. (2006). Change detection techniques for canopy height growth measurements using airborne laser scanner data. *Photogrammetric Engineering & Remote Sensing*, 72(12):1339–1348.

Zhao, K., Suarez, J. C., Garcia, M., Hu, T., Wang, C., and Londo, A. (2018). Utility of multitemporal lidar for forest and carbon monitoring: Tree growth, biomass dynamics, and carbon flux. *Remote Sensing of Environment*, 204:883–897.

Paper I

Direct and indirect site index determination for Norway spruce and Scots pine using bitemporal airborne laser scanner data

Lennart Noordermeer*, Ole Martin Bollandsås, Terje Gobakken, Erik Næsset

Faculty of Environmental Sciences and Natural Resource Management, Norwegian University of Life Sciences, NMBU, P.O. Box 5003, NO-1432 Ås, Norway

A B S T R A C T

Forest site productivity, usually represented by site index (SI), is a fundamental resource variable in forest management planning as it is a quantitative measure of the production capacity of forest land. Site index is usually derived from estimates of dominant height (H_{dom}) at a given reference age using empirical age-height curves. However, it is commonly quantified with large uncertainty in forest management inventories, resulting in economic losses due to incorrect management decisions. In this study, we used bitemporal airborne laser scanner (ALS) data acquired for a study area in southeastern Norway with a time interval of 15 years to estimate SI by means of an area-based approach. We present two practical methods for SI determination, i.e., the (1) direct and (2) indirect method. With the direct method, we regressed field observations of age-height SI against canopy height metrics derived from ALS data from the first point in time and changes in ALS metrics reflecting canopy height growth during the observation period. With the indirect method, we first modelled H_{dom} for the two points in time using the respective ALS metrics as predictors. We then derived SI from the initial H_{dom}, the estimated H_{dom} increment, and the length of the observation period using empirical SI curves. We used bitemporal field data collected from 80 georeferenced sample plots of size 232.9 m² to fit the species-specific regression models for SI and H_{dom}. We then applied the models to an independent dataset comprising 42 georeferenced validation plots of size ∼3700 m², for which ground reference values were collected at both points in time, to assess the precision of both methods. Both the proposed methods produced SI estimates with satisfactory precision. For the direct method, the independent validation revealed root mean squared errors (RMSE) of 1.78 and 1.08 m for Norway spruce and Scots pine, respectively, compared to 1.82 m obtained for both tree species using the indirect method. The indirect method can provide a good alternative to the direct method as field observations of SI are not required to calibrate the regression models.

1. Introduction

Forest site productivity (SP) is a fundamental resource variable in forest management planning. Site productivity is a quantitative estimate of the potential for biomass production capacity given a specific genotype and management regime, and therefore reflects the general quality of the growing conditions for a given unit of land (Skovsgaard and Vanclay, 2008). Accurate data on SP are crucial for sustainable forest management, the assessment of current and future yields, and monitoring carbon stocks of forests (Avery and Burkhart, 1994; Coops, 2015). Numerous silvicultural treatment decisions rely on SP, such variables as optimal rotation age, target tree species during regeneration, planting density, thinning regime, and form of final felling (Bontemps and Bouriaud, 2013). In operational forest management inventories (FMIs), however, SP is often quantified with large uncertainty, which can result in considerable financial losses due to

incorrect management decisions (Eid, 1991, 1992, 2000). In fact, SP is among the most sub-optimally determined resource variables with respect to losses in monetary terms (Eid, 2000).

Site productivity is most commonly represented by site index (SI), which is usually based on, or derived from, the stand height at a given reference age using age-height curves (Hägglund and Lundmark, 1981; Monserud, 1984; Ralston, 1964; Skovsgaard and Vanclay, 2008; Spurr, 1952). Classification of SI by dominant height (H_{dom}) at a given reference age is a common practice in forestry, and is the predominant methodology for quantifying SP in forest management planning (Hägglund and Lundmark, 1977; Monserud, 1984; Rayner and Turner, 1990; Schönau, 1987). Stand height is generally accepted as the most suitable indicator of SI, because tree height is more easily measured than timber volume, and the relation between stand height and age resembles the relation between standing volume and age (Baur, 1881; Skovsgaard and Vanclay, 2008). The current study was conducted in

---

Norway, where SI is characterized by the H40 system in which species-specific SI is derived from the H_{dom} at a breast height age of 40 years using empirical age-height curves (Sharma et al., 2011; Tveite, 1977; Tveite and Braastad, 1981). H_{dom} is defined as the mean height of the 100 largest trees per hectare according to stem diameter (Fries, 1969; Tveite, 1977). Such age-height SI, derived from the estimated H_{dom} at a given age, represents the effects of all environmental factors that determine height growth at a given geographic location, from the moment a stand reaches breast height to the moment SI is determined.

Site index is traditionally estimated by collecting core samples from dominant trees to determine the age at breast height, along with measurements of the corresponding tree heights, and then deriving the SI class from species-specific age-height curves. However, this method is both costly and unreliable on the long run for several reasons. Firstly, local changes in SI over time caused by atmospheric and climatic factors may affect growth rate (Boisvenue and Running, 2006; Kvaalen et al., 2015; Messaoud and Chen, 2011; Sharma et al., 2011). For example, growth rates of tree species in Europe have accelerated considerably during the last decennia due to a combination of environmental factors such as increased carbon- and nitrogen deposition and increasing temperatures and precipitation (Hunter and Schuck, 2002). Secondly, age determination can be challenging in forest stands due to retention trees left after the previous final harvest (Kvaalen et al., 2015). Thirdly, SI curves are not valid for mixed species stands (Tveite, 1977), stands in which H_{dom} growth has been suppressed, stands that have been fertilized, and stands younger than 20 years at breast height (Tveite and Braastad, 1981). Finally, SI cannot be determined correctly when dominant trees are not present in a stand, when dominant trees have been subject to injuries (Nigh and Love, 1999), or when the stand has recently been harvested.

As an alternative to the more conventional age-height approach, periodic height growth might be a more reliable indicator of SI in stands where the age is unknown, where the potential for volume growth is not well reflected by stand height, or where H_{dom} growth has been restricted (Skovsgaard and Vanclay, 2008). Several age-independent methods for SI determination have been proposed, the growth intercept method being the most widely used (Arias-Rodil et al., 2015; Bull, 1931; Ferree et al., 1958; Wakeley, 1954). Through the growth intercept method, SI can be estimated as a function of internodal distances, beginning at a given lower part of the stem such as breast height, typically using a five year intercept (Wakeley and Marrero, 1958; Warrack and Fraser, 1955). However, the growth intercept method is only applicable to regeneration stands, and fails to describe age-height relationships at mature stand ages (Ferree et al., 1958). For practical utilization, the growth intercept method is only suitable for trees that have distinct annual branch whorls visible on the lower stem, i.e., young coniferous trees (Hägglund, 1976).

Site index is directly related to H_{dom} growth over time (Husch et al., 1982; Tveite, 1977). The use of the accumulated growth in H_{dom} over a given time period as an indicator for SI, independent of stand age, has been proposed as an alternative to the growth intercept method (Hollaus et al., 2015; Kvaalen et al., 2015). Through such height-differential SI determination, SI is derived from the initial H_{dom} and the H_{dom} growth over a known period. A major advantage of this approach is that, in contrast to the growth intercept method, it is applicable to mature stands. Moreover, in contrast to the age-height approach, recent changes in environmental and climatic conditions can be captured, and the produced SI estimates might therefore be more relevant than estimates derived from the total accumulated height growth in the period since the tree reached breast height. Furthermore, this method does not entail additional field work as it is age-independent, and collection of core samples is therefore not required.

As it is not cost effective to acquire field-based observations of SI for each individual stand in modern Norwegian FMIs, SI is often determined through manual and subjective interpretation of aerial images. This process is also time- and resource consuming, and error

margins associated with SI can be considerable (Eid, 1992). In stand-based FMIs, most resource variables such as H_{dom}, timber volume, basal area, mean tree height, mean diameter, and stem number are commonly estimated by using remotely sensed three-dimensional data, through the development of regression models that are applied for prediction wall-to-wall over an area of interest (Næsset, 2004b). A strong demand currently exists for the development of such a method for SI determination as well, which can be incorporated in operational practices for forest resource mapping.

Providing detailed three-dimensional data in the form of georeferenced point clouds depicting forest structure and terrain surface, airborne laser scanner (ALS) systems have proven useful for producing precise estimates of numerous forest stand attributes in stand-based FMIs (Magnussen and Boudewyn, 1998; Means et al., 2000; Næsset, 2002; White et al., 2013). ALS data are known to be suitable for estimating H_{dom} in forest stands of various types of ages, species compositions and SI classes (Martins et al., 2010; Næsset, 2004a; Næsset and Bjerknes, 2001). Site index is directly related to the accumulated H_{dom} growth over a defined period (Husch et al., 1982; Tveite, 1977), and determination of SI by using canopy height metrics derived from multi-temporal ALS data might therefore provide a suitable alternative to conventional methods.

Airborne laser scanning acquisitions have become an integral part of stand-based FMIs in Norway and numerous other countries (Maltamo et al., 2014). The area-based approach is the prevailing method for ALS-based forest inventory, comprising two stages (Næsset, 2002). In the first stage, a sample of field plots is selected within the area of interest. Ground reference values of various forest attributes are collected for georeferenced sample plots, and plot-level ALS metrics are derived from the ALS point cloud. Predictive models are then calibrated, using the ground reference data, i.e., field data collected to describe the targeted forest attributes, as response variables and ALS metrics as predictor variables. In the second stage, the models are applied for prediction over a regular grid covering the entire area of interest, where grid cells and sample plots are identical in size, to generate wall-to-wall predictions of the desired forest inventory attributes. Predictions for individual grid cells within stands are then aggregated to provide stand-level estimates of the desired attributes, which are used primarily for forest management planning purposes.

Numerous studies have demonstrated that multi-temporal ALS data are suitable for monitoring forest growth (Hopkinson et al., 2008; Hyyppä et al., 2003; Næsset and Gobakken, 2005; Yu et al., 2004, 2006). Previous attempts to determine SI based on ALS data and the individual tree crown approach have produced promising results (Hollaus et al., 2015; Kandare et al., 2017; Kvaalen et al., 2015). In other studies, SI was determined using a combination of registered stand age and ALS data (Chen and Zhu, 2012; Holopainen et al., 2010; Packalén et al., 2011), or stand age derived from annual Landsat time series in combination with H_{dom} predictions based on ALS data (Tompalski et al., 2015). Véga and St-Onge (2009) quantified SI and stand age using time series of canopy height models produced using digital photogrammetry and ALS. Socha et al. (2017) used bitemporal ALS data and age estimated using stand register data to model H_{dom} growth and SI for a forest area in a sample-based inventory. However, no attempts have been made to develop a method for SI determination using data from repeated ALS surveys with the area-based approach. This is a considerable research gap, as such a method could potentially revolutionize operational practices for SI determination.

The main objective of this study was to develop, validate, and compare two different methods for SI determination using bitemporal ALS data; (1) through direct SI determination: field observations of age-height SI were regressed against combinations of ALS-derived canopy height metrics from the initial point in time (T1) and differences from the corresponding ALS-derived metrics from the second point in time (T2); (2) through indirect SI determination: SI is derived from stand-level estimates of H_{dom} at T1, the estimated H_{dom} increment, and the length of the observation period.
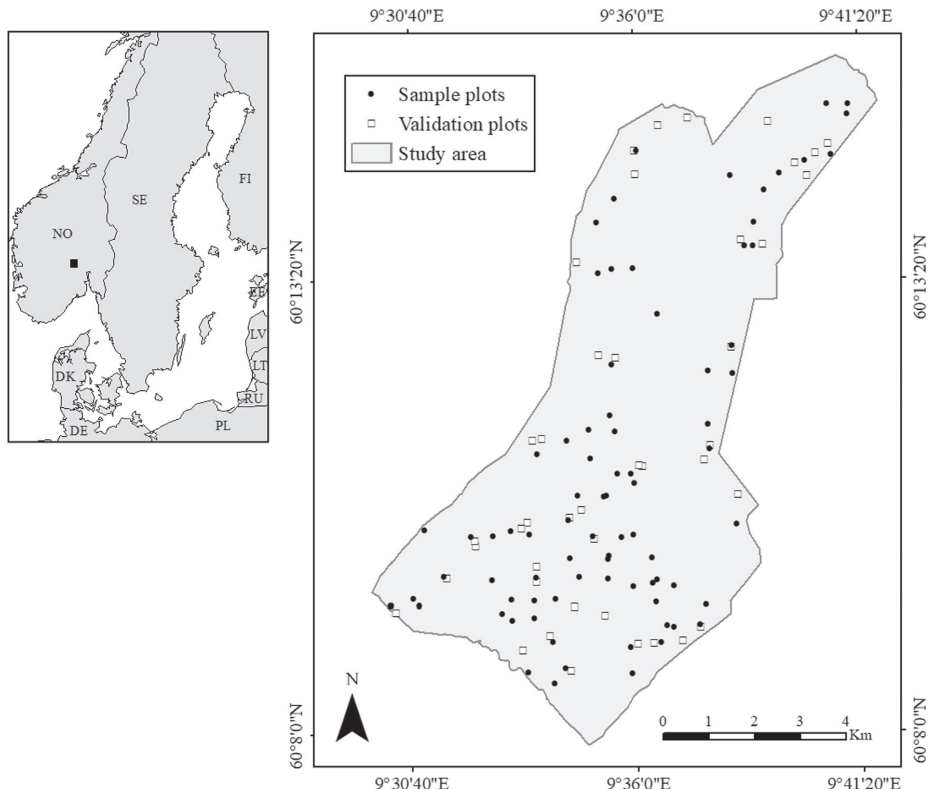
Fig. 1. Outline of the study area for which airborne laser scanner data were acquired in 2001 and 2016, and locations of sample- and validation plots used in this study from which ground reference data were acquired in 2001 and 2016.

2. Materials and methods

2.1. Study area

The study was conducted in the municipality of Krødsherad (60°10′N, 9°35′E, 130–660 m above sea level) in southeastern Norway (Fig. 1). The most common tree species in the study area are Norway spruce (*Picea abies* (L.) Karst.) and Scots pine (*Pinus sylvestris* L.). The study area of approximately 50 km² is characterized by an actively managed forest landscape typically seen in Nordic boreal forests. Pine-dominated stands are usually regenerated naturally after final felling, and spruce-dominated stands are usually planted after clear-felling. Other common silvicultural practices include scarification, pre-commercial and commercial thinning.

2.2. Field data

Ground reference data were obtained from georeferenced sample plots for both points in time, the first point in time (T1) being the year 2001 and the second point in time (T2) being the year 2016. The ground reference data for T2 were collected during the summers of 2016 and 2017. As part of a commercial forest management inventory at T1, a systematic stratified sampling design was applied to distribute 116 circular sample plots with an area of 232.9 m² throughout the study area.

The sample plot survey covered three pre-defined strata in young and mature forest stands. The first stratum comprised 39 plots in young

forest, the second stratum contained 38 plots in mature forests for which the H40 SI was interpreted to be ≤11 m, and the third stratum contained 38 plots in mature forest for which the H40 SI was interpreted to be > 11 m. The strata were classified manually by means of interpretation of aerial images. Regular grids were created independently for each stratum, based on the equal allocation principle, where the spacing of the grid varied according to the number of plots within each stratum, and the total area of each stratum. Regeneration stands were excluded. Young and mature stands were discriminated by their development class, defined according to stand age and SI in a national system for characterizing forest development stage (e.g. Anon, 1987; Lexerød, 2005). There are five development classes in this system, where development class I characterizes clear felled stands and class V represents mature stands ready for harvest. In this particular study, we excluded development classes I and II, leaving stands with tree heights of approximately 10 m and higher for further analyses. Young forest included stands in development class III, and mature forest included stands in development classes IV and V.

Additionally, 57 relatively large validation plots were established in young and mature forest stands at T1. Validation plots were selected subjectively to represent different combinations of SI and tree species composition. The validation plots were designed to form squares of 61 × 61 m, resulting in an area of 3721 m². However, due to challenging topography, the final plot coordinates showed that the sides of the squares were not always parallel. Thus, the actual obtained shapes and areas deviated from the initial design to some extent, with areas ranging from 3377 m² to 4086 m² and with a mean of 3760 m². The

validation plots were used as proxies for small stands. Grid-cell predictions were aggregated to the scale of the validation plot so that the results would better reflect area units used in operational forest management inventories.

All sample- and validation plots were revisited and remeasured at T2. A total of 92 sample plots were classified as young or mature forest at both points in time. Of the initial 57 validation plots in young and mature forests, a total of eight had been harvested during the observation period, leaving 49 validation plots that were registered as young or mature forest during the second campaign.

The field measurement procedures used at T1 and T2 were identical, with two exceptions. Firstly, for the large validation plots, field measurements at T1 were only registered to the plot as such without any finer geographical resolution, while at T2 the measurements were geographically referenced to individual subplots. Each validation plot was tessellated into 16 such georeferenced subplots of approximately $233 \, m^2$ in size each. Secondly, age at breast height and tree heights were measured for two and 16 SI sample trees in the sample- and validation plots, respectively, only at T2.

2.3. Tree measurements in sample plots

All trees with a DBH > 4 and 10 cm were calipered in young- and mature forest sample plots, respectively, and the tree species were recorded. Sample trees were selected for height measurement with a probability proportional to stem basal area using a relascope. Tree heights were measured using a Vertex hypsometer, and DBH and species were recorded. For such tree height measurements, the standard error can be expected to be 0.2–0.3 m (Vasilescu, 2013). In addition, two SI sample trees were selected within each sample plot at T2. The SI sample trees were the largest trees of the dominant species within the plot according to DBH. Retention trees from the previous rotation were not accepted as sample trees. The DBH and height were measured for each SI sample tree, and age at breast height was determined using core sampling.

2.4. Tree measurements in validation plots

Within validation plots at T1, and subplots at T2, all trees were calipered as described above, however, sample trees were selected successively as DBHs were measured. Every n^{th} calipered tree in each diameter class was selected for height measurement, where n varied according to the basal area accumulated by including a tree belonging to each of the different diameter classes. At T2, one SI sample tree was selected within each subplot, being the largest tree within the subplot according to DBH, of the dominant species within the large validation plot as a whole. Field measurements for SI sample trees within subplots were identical to those within sample plots, i.e., the DBH, age at breast height and height were recorded for each SI sample tree.

2.5. Plot positioning

During the field measurements at both T1 and T2, planimetric coordinates of sample plot centers and validation plot corners were determined using differential Global Navigation Satellite Systems (dGNSS-GPS and GLONASS). The collection of data lasted 15–30 min for each position. At T1, plot centers of circular sample plots and corners of validation plots were marked with wooden sticks. At T2, real time kinematic satellite navigation was used to locate to the original positions. A total of 30 and 47 of the wooden sticks were recovered for sample- and validation plots respectively, ensuring identical locations for those cases. Sample plot centers and validation plot corners that had not been found at T2 were re-measured using dGNSS. The mean distance between T1 and T2 coordinates was 1.07 m, and distances ranged from 0.04 to 4.46 m with a standard deviation of 0.99 m. For those plots of which the plot centers were not found at T2, we used the computed coordinates for T2 as a reference for calculating ALS metrics at both points in time, as we assumed these to be more precise due to recent advances in GPS technology.

2.6. Computation of field variables

We computed plot-level H_{dom} as the arithmetic mean height of the two largest trees according to DBH, within sample plots and validation subplots. In a $232.9 \, m^2$ plot, the two trees with the largest DBH can be expected to be among the 100 largest trees per ha, conforming to the criteria for dominant trees (Sharma et al., 2011). Tree heights were only available for sample trees, which did not necessarily represent the two trees that had the largest DBH within each plot. We therefore computed the heights of all calipered trees using a ratio estimator as described in Ørka et al. (2018), and obtained height estimates for the calipered trees by using inverted species specific, single tree volume functions proposed by Braastad (1966), Brantseg (1967) and Vestjordet (1967). The inversion enabled the volume functions to predict height instead of volume for all trees, and thus made it possible to obtain tree heights for the two trees with the largest DBH within each plot. We obtained species-specific plot volumes by summing the calculated volumes of individual trees, in order to assign a species label to each plot.

Tree heights were measured at different points in time throughout the growing seasons. We therefore corrected the obtained plot-level H_{dom} estimates with respect to the day in the growing season on which the field data were obtained, using a sigmoid height growth curve proposed by Sharma et al. (2011). We assumed the growing season to start at the end of April at day 115, and height growth to last for 60 days for both spruce (Ekberg et al., 1994; Kozlowski, 1962) and pine (Kilpeläinen et al., 2006; Kozlowski, 1962).

We computed age-height SI for individual SI sample trees using species-specific age-height curves for Norway spruce and Scots pine recommended by Sharma et al. (2011). The curves are based on one of Hossfeld's (1822) functions, describing a two-dimensional relationship between tree height and age at breast height. We computed plot-level age-height SI as the arithmetic mean of individual SI observations within sample plots and subplots, and computed plot-level SI for validation plots as the arithmetic mean of SI values for the individual subplots.

We computed height-differential SI for validation plots as ground-reference, to evaluate the precision of the indirect method. Using ground reference H_{dom} at T1 and T2, we solved the SI by exhaustive search as described in the following. For each validation plot, we first derived the age at breast height needed to reach the estimated H_{dom} at T1 for all SI values ranging from 5 to 30 m, with an interval of 1 m, using empirical age-height curves presented by Sharma et al. (2011) (Fig. 2). The H40 SI system is not defined for values < 5 m (Tveite, 1977), and such sites are labelled "unproductive". Values > 30 m are extreme for Norwegian conditions. We then projected the expected H_{dom} at T2 given each discrete SI value, at the corresponding derived age at T1 added to the length of the observation period. Finally, we interpolated between the two discrete SI values for which the projected H_{dom} at T2 corresponded best to the actual H_{dom} at T2, to obtain plot-level SI estimates as continuous variables. A summary of the obtained ground reference data is shown in Table 1.

2.7. Airborne laser scanner data

Airborne laser scanner data were acquired at T1 and T2. The respective data acquisition parameters are shown in Table 2. Both ALS surveys were carried out under leaf-on conditions.

The contractors, Fotonor AS and Terratec AS, normalized the ALS point clouds acquired at T1 and T2, respectively, and laser returns were classified automatically as ground, canopy, and noise returns. Planimetric coordinates and ellipsoidal heights of laser returns were calculated, and a triangulated irregular network was derived from the
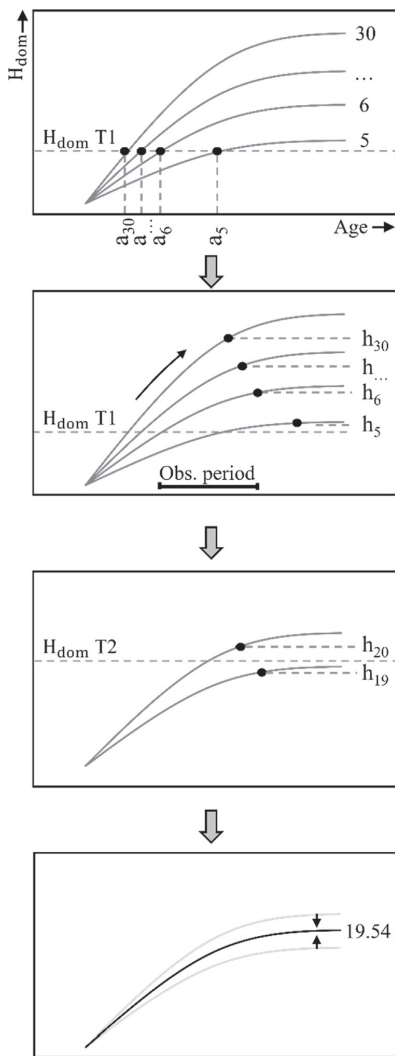
Fig. 2. Schematic representation of the indirect method. H_{dom} = dominant height (m), T1 = the first point in time (2001), T2 = the second point in time (2016), $H_{dom\,T1}$ and $H_{dom\,T2}$ = dominant height (m) at T1 and T2, respectively, Obs. period = the length of the observation period.

laser returns classified as ground. The terrain level was subtracted from the ellipsoidal height of each laser return to calculate the height above the ground for each canopy return.

2.8. ALS metrics

We computed canopy height and density metrics as described in Næsset (2002) and Næsset (2004b), respectively, for all sample plots, for both T1 and T2. Height percentiles (H10, H20, ..., H90) were computed from the laser return height distributions, and the arithmetic mean height (Hmean), maximum height (Hmax), standard deviation (Hsd), and coefficient of variation (Hcv) of return heights for first and last returns separately. We excluded laser returns with a height above the ground < 2 m from the analyses, as they were not considered to

represent canopy returns and were therefore not considered to be relevant when estimating H_{dom} growth. We then divided the height range between the 2 m threshold and H95 into ten identical fractions. We computed canopy density metrics (D0, D1, ..., D9) as the proportion of returns between the lower limit of each fraction and the total number of returns. We computed differential ALS metrics by subtracting the value of each ALS metric computed for T1 from the corresponding value at T2. Thus, for each sample plot, we derived a total of 46 ALS metrics from the ALS data acquired at T1, an additional 46 ALS metrics from the ALS data acquired at T2, and 46 differential ALS metrics.

2.9. Selection of suitable sample plots

Since SI is supposed to represent the growth potential of a stand, it is

Table 1
Summary of ground reference data for sample (232.9 m^2) – and validation (~3700 m^2) plots.

Characteristic[a]	Sample plots			Validation plots		
	n	Range	Mean	n	Range	Mean
Spruce dominated plots	36			21		
SI$_{AH}$		8.19–25.62	17.36		9.91–24.29	16.59
H$_{dom\ T1}$		10.33–25.65	18.99		14.87–24.51	19.87
H$_{dom\ T2}$		16.51–30.28	22.13		12.80–29.81	22.64
V$_{T1}$		26.47–643.87	201.38		77.37–360.62	211.95
V$_{T2}$		12.84–909.15	310.05		17.52–747.03	316.83
Pine dominated plots	44			21		
SI$_{AH}$		4.53–20.26	13.14		6.45–20.09	13.53
H$_{dom\ T1}$		10.40–25.35	18.32		13.15–25.24	18.33
H$_{dom\ T2}$		12.25–28.68	20.33		10.42–28.19	20.24
V$_{T1}$		20.16–437.47	201.87		54.22–308.44	171.66
V$_{T2}$		45.77–565.60	278.82		3.32–667.50	233.05

V$_{T1}$ and V$_{T2}$ = volume (m^3 ha^{-1}) at T1 and T2, respectively.

[a] SI$_{AH}$ = age-height H40 site index (m), H$_{dom\ T1}$ and H$_{dom\ T2}$ = dominant height (m) at T1 and T2, respectively.

Table 2
Specifications of the two airborne laser scanner surveys.

Year of acquisition	2001	2016
Time period	23 June–1 August	7 June–31 July
Aircraft	Piper PA-31	Piper PA-31
Laser scanning system	Optech ALTM 1210	Riegl LMS Q-1560
Average flying altitude	650 m	1280 m
Average flying speed	75 m/s	69 m/s
Pulse repetition frequency	10 kHz	534 kHz
Scanning frequency	30 Hz	115 Hz
Side overlap	50%	20%
Maximum scan angle	15°	20°
Average point density	0.9 points/m^2	11.8 points/m^2

essential that the natural development of H$_{dom}$ of both the ground reference plots for model calibration, and the prediction units where the models are applied, is undisturbed. When estimating SI in an operational setting using an area-based inventory approach, each prediction unit will have to be classified based on whether such disturbance has occurred. In this current experimental study, we have omitted the classification stage, and used ground reference data to classify both sample plots and prediction units as "suitable" or "not suitable" for SI estimation.

In the dataset containing sample plots, denoted from here on as the sample dataset, we removed all observations for which the ground reference H$_{dom}$ had decreased during the observation period. This led to a reduction of the number of observations in the sample dataset from 92 to 80.

In the validation dataset, ground reference values for H$_{dom}$ were not available at subplot-level for T1. To exclude subplots in the validation dataset that were unsuitable for SI determination, we therefore used the ALS data to assess if the H$_{dom}$ development was disturbed. All subplots for which either the mean height of first returns or H90 of first returns had decreased during the observation period, were removed. This lead to a reduction of the number of validation plots from 49 to 47. Furthermore, several subplots within the validation dataset lacked ALS data for one of two points in time and were therefore removed from the analyses. Resultantly, five large validation plots remained with less than four subplots. Given their limited size, we discarded these five validation plots from the analyses as we no longer considered these observations to be suitable proxies for forest stands. Thus, a total of 42 validation plots were included in the analyses. An overview of the sample- and validation datasets is shown in Table 1.

2.10. Data analyses

Because Norwegian SI models are species-specific and applicable to either Scots pine or Norway spruce, we divided the dataset as described in the following. We used the computed species-specific plot volume estimates for the sample- and validation datasets at T2, and assigned a species label to each sample plot and subplot according to the majority proportion of either Norway spruce or Scots pine volume. We then performed the analyses for the direct and indirect methods separately for the two species as described below.

With the direct method, we fitted species-specific multiple regression models to describe relationships between ground reference SI and bitemporal ALS metrics. We fitted the models using age-height SI observations from sample plots as a response variable, and combinations of ALS-derived canopy height metrics computed for T1 and corresponding differential ALS height metrics as predictors. We used the ordinary least squares (OLS) method in R for parameter estimation. We first obtained a number of candidate models during the model selection, which we conducted using the stepwise algorithm 'regsubsets' from the leaps package (Lumley, 2004) in R, and manual experimentation with different combinations of predictors. We only included predictors with a p-value < 0.05. We then performed leave-one-out cross validation (LOOCV) within the sample dataset to evaluate the prediction accuracy of each regression model using the root mean square error (RMSE). We set an upper limit of three predictors for each regression model to avoid overfitting, and assessed multicollinearity by computing and observing the variance inflation factor (VIF) for the individual predictors. We considered any VIF > 10 to indicate multicollinearity problems (Fox and Weisberg, 2011). We then applied the selected species-specific regression models to predict age-height SI for each subplot in the validation dataset.

With the indirect method, we regressed ground reference H$_{dom}$ for both points in time separately against the respective ALS-derived metrics computed for the sample plots, using model selection procedures as described in the previous paragraph. To meet the assumptions of normality and homoscedasticity, we applied a natural logarithmic transformation to both the response- and predictor variables before fitting the regression models for H$_{dom}$. This procedure has been proven to be suitable for model development of H$_{dom}$ using ALS metrics as predictors (Means et al., 2000; Næsset, 2002; Næsset and Bjerknes, 2001; Næsset et al., 2004). We applied the regression models to the validation dataset, generating predictions of H$_{dom}$ for individual subplots. We transformed the obtained predictions back to arithmetic scale, and corrected the conversion bias using the ratio-of-means estimator presented by Snowdon (1992). We then aggregated the predicted values for subplots to obtain laser-estimated, i.e., estimated from the ALS data, H$_{dom}$ within each validation plot. This conforms to the standard procedure in the second phase of the area-based approach, in which predictions for grid cells within stands are aggregated to obtain stand-level estimates of forest attributes. Using the laser-estimated H$_{dom}$ at T1 and T2, and the length of the observation period, we then solved the SI for each validation plot by exhaustive search as we did for computing the ground reference height-differential SI (Fig. 2), the only difference being that we substituted ground reference values of H$_{dom}$ with laser-estimated values of H$_{dom}$. The ground reference values of height-differential SI for three of the pine-dominated validation plots was < 5. These plots were discarded from the analysis because H40 SI is not defined < 5 m (Tveite, 1977). A schematic representation of the study design is shown in Fig. 3.

2.11. Validation

To evaluate the precision of the direct method, we calculated the RMSE and mean differences between ground reference and laser-estimated SI at validation plot-level. We evaluated the statistical
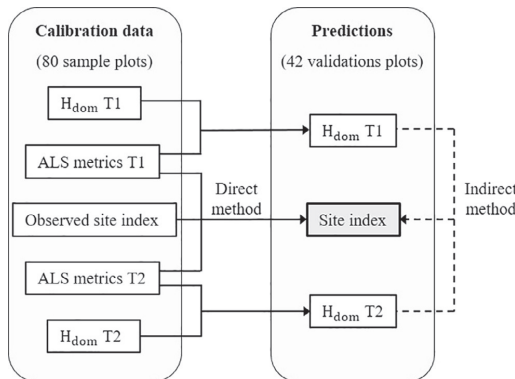
Fig. 3. Study design. Airborne laser scanner (ALS) data and field data were acquired in 2001 (T1) and 2016 (T2). With the direct method, we regressed field observations of site index against bitemporal ALS metrics. We then used the regression models to predict site index for the validation plots. With the indirect method, we modelled dominant height (H_{dom}) at T1 and T2 separately using the respective ALS metrics as predictors, and we derived the site index from the initial predicted H_{dom}, the estimated H_{dom} increment, and the length of the observation period using empirical SI curves.

significance of the mean differences using a paired two-tailed t-tests. For the indirect method, we compared the ground reference height-differential SI, based on ground reference values of H_{dom}, with the height-differential SI based on laser-estimated values of H_{dom}. Again, we evaluated the accuracy of the obtained estimates using the RMSE and mean differences between ground reference and laser-estimated SI as described for the direct approach.

3. Results

The models selected according to the model selection criteria are presented in Table 3. The number of predictor variables in the obtained models varied from two to three. Predictors from both the first and last return data were selected for H_{dom} models during the stepwise selection

Table 3
Selected regression models with corresponding fit statistics and root mean square errors in the cross validation.

Response variable[a]	Predictive model[b]	R^2_{adj}	RMSE
Spruce dominated sample plots			
SI_{AH}	$5.81 + 0.35 * Hmean. F_{T1} + 2.35 * \Delta Hmean. F$	0.77	2.42
$lnH_{dom\ T1}$	$0.88 + 0.72 * lnH90.L_{T1} + 0.16 * lnD4.L_{T1} - 0.12 * lnD9.F_{T1}$	0.90	0.06
$lnH_{dom\ T2}$	$0.92 + 0.42 * lnHmean. F_{T2} + 0.34 * lnHmax. L_{T2}$	0.80	0.08
Pine dominated sample plots			
SI_{AH}	$-0.93 + 0.54 * H90.F_{T1} + 2.27 * \Delta H90.F$	0.80	1.90
$lnH_{dom\ T1}$	$1.06 + 0.69 * lnHmax. L_{T1} + 0.13 * lnD7.F_{T1}$	0.93	0.06
$lnH_{dom\ T2}$	$0.71 + 0.81 * lnH90.F_{T2} + 0.12 * lnD1.F_{T2}$	0.93	0.06

[a] SI_{AH} = age-height H40 site index (m), $H_{dom\ T1}$ and $H_{dom\ T2}$ = dominant height (m) at T1 and T2, respectively.
[b] $Hmean.F_{T1}$ = arithmetic mean of first return laser heights (m) at T1, $\Delta Hmean.F$ = difference in arithmetic mean heights of first returns at T2 and T1 (m), $H90.L_{T1}$ = 90% height percentile of last returns at T1 (m), $H90.F_{T1}$, $H90.F_{T2}$ = 90% height percentile of first returns at T1 and T2 (m), $H90.F$ = difference in 90% height percentile of first returns at T2 and T1 (m), $Hmax.L_{T1}$ = maximum height of last returns at T1 (m), $D4.L_{T1}$ = canopy density corresponding to the proportions of last returns above the 4th fraction at T1, $D7.F_{T1}$, $D9.F_{T1}$, $lnD1.F_{T2}$ = canopy densities corresponding to the proportions of first returns above the 7th and 9th fraction at T1, and 1st fraction at T2.

procedure (Table 3). The models that described the relationship between ALS metrics and SI for both species included combinations of one ALS height metric and the corresponding differential height metric. We considered numerous models containing only differential ALS metrics as predictor variables for both species, but these did not produce a smaller RMSE in the cross validation than the selected models. The highest VIF of 4.63 was calculated for the predictors that belonged to the model for H_{dom} for T2 in pine-dominated forest, i.e., the mean height of first returns at T2 and maximum height of last returns at T2. Nevertheless, this indicated no serious collinearity problems. The VIFs calculated for the SI models were 1.08 and 1.03 for pine and spruce respectively.

All predictor variables in the selected models were statistically significant at the 95%-level (p-value < 0.05). The proportion of the variance in the response variables explained by the predictor variables, adjusted for the number of predictor variables (R^2_{adj}), ranged from 0.77 to 0.93. Prediction models for H_{dom} of pine-dominated forest had the largest R^2_{adj} values (Table 3). The R^2_{adj} obtained for SI models indicated strong correlations between ground reference SI and the Hmean and H90 of first returns at T1 and differential Hmean and H90 of first returns. The results of the LOOCV within the sample dataset revealed a RMSE of 2.42 m for the selected model for age-height SI in spruce-dominated sample plots.

When using the regression models to predict the targeted resource variables for all subplots in the validation data, and aggregating the predictions to obtain estimates for validation plots, the RMSE values ranged from 0.52 to 1.82 m. The highest precision was obtained for H_{dom} predictions in pine-dominated validation plots (Table 4). The mean differences between ground reference and laser-estimated values ranged from −0.67 to 0.82. None of the mean differences were found to be statistically significant (p > 0.05). The mean observed height-differential SI in spruce-dominated validation plots was smaller than the mean ground reference age-height SI (Table 4, Fig. 2). The selected regression model for predicting age-height SI in pine-dominated forest performed better than the model for spruce-dominated forest.

The direct method yielded the best results, with RMSE values of 1.78 and 1.08 m for spruce and pine-dominated validation plots, respectively, compared to 1.82 m obtained for both tree species using the indirect method (Table 4). For most spruce-dominated validation plots, ground reference age-height SI was higher than height-differential SI (Fig. 4).

4. Discussion

The obtained results demonstrated that bitemporal ALS data can be

Table 4
Differences (D) between ground reference and laser-estimated dominant height at T1 and T2, age-height and height-differential H40 site index for all validation plots.

Variable[a]	Observed mean	D		
		Range	Mean	RMSE
Spruce-dominated validation plots				
$H_{dom\ T1}$	18.99	−0.90 to 2.14	0.82[ns]	1.26
$H_{dom\ T2}$	22.13	−1.04 to 2.25	0.62[ns]	1.23
SI_{AH}	17.36	−3.95 to 1.84	−0.67[ns]	1.78
SI_{HD}	14.46	−3.70 to 3.07	−0.13[ns]	1.82
Pine-dominated validation plots				
$H_{dom\ T1}$	18.32	−1.16 to 1.55	0.02[ns]	0.64
$H_{dom\ T2}$	20.33	−0.84 to 1.35	0.03[ns]	0.52
SI_{AH}	13.14	−0.80 to 2.51	0.53[ns]	1.08
SI_{HD}	13.82	−4.19 to 3.23	−0.04[ns]	1.82

ns: not significant (p < 0.05).
[a] $H_{dom\ T1}$ and $H_{dom\ T2}$ = dominant height (m) at T1 and T2, respectively, SI_{AH} = age-height H40 site index (m), SI_{HD} height-differential site index (m).
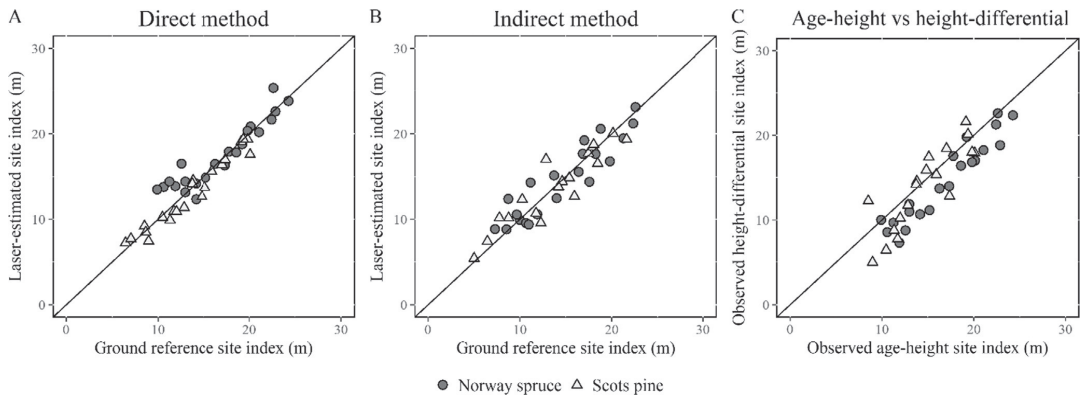
Fig. 4. Ground reference site index plotted against laser-estimated site index obtained using the direct method (A), the indirect method (B), and observed age-height site index plotted against observed height-differential site index (C) for Norway spruce and Scots pine-dominated validation plots.

used to estimate SI by means of an area based approach with adequate precision. Both the proposed methods produced satisfactory precision at the scale of the validation plots used in this study. The independent validation of the models for estimating age-height SI through the direct method revealed strong correlations between field observations of SI and ALS canopy height metrics from T1 in combination with changes in the corresponding height metrics during the observation period. This method produces estimates that reflect growing conditions from the moment a stand reaches breast height to the moment SI is determined, as opposed to estimates produced by the indirect method, which reflect growing conditions over a shorter observation period. Although the independent validation of the indirect method revealed larger errors for both tree species, the method provides a highly relevant alternative as no additional field work is required to calibrate the regression models, and changes in SI can be captured over time.

4.1. Direct method

Consistent with our expectations, the independent validation of the direct method revealed greater precision than the indirect method. Direct estimation of change might be preferred over the indirect alternative, because direct estimates only contain a single set of errors as opposed to prediction errors occurring for both points in time (Bollandsås et al., 2013; Fuller et al., 2003; Skowronski et al., 2014). To obtain adequate accuracies when using the indirect method, precise H_{dom} estimates are needed for both points in time and the occurrence of systematic prediction errors must be limited. We obtained acceptable levels of precision and mean differences between ground reference and laser-estimated H_{dom} at both points in time and for both tree species, but height-differential SI estimates would be considerably less precise when H_{dom} predictions are less accurate, and especially when systematic errors occur in opposite directions for the two points in time. On the other hand, a relatively low precision on grid cell level can still result in accurate SI estimates after aggregating individual predictions within stands, as long as systematic prediction errors are not present.

A disadvantage of the direct method is that stand age can be challenging to determine. The age-height relationships obtained through core samples can be prone to systematic errors, as it is uncertain whether the dominant trees that were sampled were dominant also at the beginning of the rotation cycle (Perin et al., 2013; Sharma et al., 2002). We considered the obtained core samples of SI sample trees to be observations of age without error, but age is often determined with large errors, and can be especially challenging to quantify in uneven-aged stands (Sharma et al., 2011). The indirect method, on the other hand, is age-independent, and the collection of core samples is

therefore not required.

Both of the selected regressions models for predicting age-height SI contained an ALS canopy height metric from T1 and the corresponding differential height metric. Such combinations should be preferred over ALS metrics that are selected in pairs from the two respective points in time separately. Although they contain the same information, and model fit and the produced predictions are identical, such repeated measurements can be correlated and caution must be exercised when they are included in OLS regression models as the assumption of no multicollinearity can be violated.

We used empirical age-height curves recommended by Sharma et al. (2011), which are based on a combination of Norwegian NFI data and long-term experiment data. In Norwegian operational FMIs, the more conventional age-height curves presented by Tveite (1977) and Tveite and Braastad (1981) are most commonly used. These conventional models were calibrated using smaller datasets from exclusively long-term experiments, i.e., a subset of the same calibration data used by Sharma et al. (2011), containing shorter time series. Some dissimilarities exist between the two alternatives, the most notable being faster expected height growth at ages at breast height > 60 years for the more recently fitted curves (Sharma et al., 2011). We used the most recently fitted age-height curves in the current study, because they were calibrated with larger and more timely datasets.

4.2. Indirect method

While computing the ground reference values of height-differential SI, we removed three pine-dominated validation plots from the analysis as their observed height-differential SI values were < 5 m, and SI is theoretically not defined < 5 m (Tveite, 1977). Although the observed age-height SI values for the three validation plots were 6.45, 8.65, and 7.03 m, the observed H_{dom} growth of the respective validation plots was slow considering the observation period of 15 years, i.e., 0.23, 0.40, and 0.14 m. Such cases where the H_{dom} increment is too small to obtain a meaningful height-differential SI must be accounted for also in an operational context, and have two likely explanations: (1) the H_{dom} growth has been suppressed during the observation period due to anthropogenic or natural factors, and (2) the stand age is too high for the age-height curves to be valid. The average ages at breast height of the SI sample trees in these plots were 154, 117, and 169 years for the respective plots, i.e., not exceptionally old, suggesting that the H_{dom} growth within these plots had been disrupted. When plotting the laser returns from these three validation plots from both points in time, we observed a reduction in canopy cover in the former, and very small height increment of canopy laser returns in the latter. This suggested

that mortality had occurred, and a very low productivity plot that had nearly reached maximum H_{dom}, respectively. Such areas are not suitable for SI determination, and methods should therefore be developed to classify them as such so that they can be excluded when generating SI predictions in the second stage of the area-based approach.

When comparing the ground reference age-height and height-differential SI within validation plots, we observed a systematic deviation in spruce-dominated plots. Contrary to our expectations, the observed mean height-differential SI, which reflects H_{dom} growth during recent years, was lower than the observed mean age-height SI for this species. The opposite could be expected because growth rates of European forests have accelerated during the last decennia (Hunter and Schuck, 2002). A number of factors could explain this result. First, the H_{dom} growth rate in spruce-dominated validation plots might have been slower during the observation period than the H_{dom} growth rate throughout the entire rotation. Secondly, height growth of SI sample trees in almost all spruce-dominated validation plots might have been faster than height growth of the two tallest sample trees within subplots. Lastly, the age-height curves that we used for spruce-dominated plots might not coincide with the actually observed growth trajectories of the species in our study area. For pine-dominated validation plots, the height-differential SI was higher than the age-height SI, only because three validation plots with a height-differential SI < 5 m were removed from the analysis. Because this study is limited to the extent of a relatively small study area, future research is advised to test the proposed methods on datasets acquired from different study areas to investigate whether the same systematic differences occur.

4.3. Application of the methods

One of the challenges of estimating H_{dom} and SI using the area-based approach, is that predictions of SI must be generated at the geographical scale of sample plots and equally sized grid cells, even though H_{dom} and SI are not theoretically defined at that specific scale. According to Tveite (1977), H_{dom} and SI are derived from the 100 largest trees per ha, as opposed to the two largest trees per sample plot of 232.9 m^2 used in this study. Therefore, estimates of H_{dom} and SI obtained through the area-based approach assume a relatively homogenous spatial distribution of dominant trees, when in fact the 100 largest trees within a given hectare of forest are likely to be clustered to some extent. Resultantly, both H_{dom} and SI will theoretically be underestimated when the area-based approach is used.

Another challenge when estimating SI in an operational context is that age-height curves used for SI estimation are species specific (Skovsgaard and Vanclay, 2008; Tveite, 1977). However, not all forest stands are monocultures. Furthermore, forests are ecosystems that are not only influenced by management-related factors, but also by naturogenic factors such as mortality, competition among species, diseases, and natural disaster. The latter component is challenging to incorporate in methods for SI determination because natural processes can disrupt H_{dom} growth. The full potential of a given site to produce biomass is never realized (Skovsgaard and Vanclay, 2008), and a certain degree of uncertainty must therefore be accounted for whichever method for SI determination is used.

Both the proposed methods are restricted to forest with undisturbed H_{dom} growth. Stands that have undergone silvicultural treatment or natural calamities are therefore not suitable for SI estimation. In an operational setting, suitable prediction units have to be classified as such, using a calibrated classification model dependent on wall-to-wall, bitemporal, and remotely sensed data. The indirect method is a special case because it fails if the predicted change in H_{dom} is negative. Thus, only a proportion of the grid cells of an area-based inventory will be classified as unsuitable in the classification stage, and additional grid cells will be excluded after the prediction phase if the models for the two respective points in time result in a predicted negative growth. For slow growing forest, this is likely since the model predictions of H_{dom}

are associated with random errors (Næsset, 2002). However, the revision of forest maps is a continuous process, as FMIs are repeated through multiple cycles. Remotely sensed, three-dimensional data are expected to be increasingly available in the future, and forest areas that are unsuitable for SI determination using the proposed methods at a given point in time will therefore likely be included in subsequent surveys. In addition, areas that are not suitable for predicting SI might be in proximity to areas for which predictions can be made. For such cases, interpolation or nearest neighbors techniques might provide suitable alternatives to produce the desired estimates.

In this study, we relied on ground reference data for classifying our data, which means that the level of precision obtained in this study is optimistic, and such precision might not be obtained in operational FMIs. Furthermore, the methods for SI determination proposed in this study were only applied to young and mature stands. The inclusion of stands that are at the regeneration stage at the first point in time is not recommended because the SI curves have not been calibrated on data from such forest. Moreover, since the field observations could not be attributed to grid cell level for the validation plots for T1, we used the change in Hmean and H90 of first returns as a proxy for canopy height. Because of sensor effects (Næsset, 2009; Ørka et al., 2010), this might have caused certain grid cells to be misclassified. In addition, the selection procedure only identified units with an increase in H_{dom} throughout the observation period and did not guarantee undisturbed H_{dom} growth for all subplots that were included in the validation dataset. Future research is needed to develop methods for identifying areas in which H_{dom} growth has not been disturbed substantially by silvicultural treatments or natural disasters during the observation period.

Variations in SI within forest stands are known to be considerable (Eid and Moum, 1999; Eid and Økseter, 1999; Monserud and Rehfeldt, 1990). Although the validation plots used in this study were considerably smaller in size than typical forest stands, the standard deviations of ground reference age-height SI within validation plots was considerable, ranging from 1.21 to 6.42 m with a mean of 2.52 m. Cell-level predictions of SI can provide more detailed geographical information and can potentially increase the utility of the data substantially with regard to optimizing management decisions, especially in relatively large stands. However, cell-level predictions of SI might not produce satisfactory precision, and aggregating individual predictions within stands is therefore advisable. For forest management purposes, it can prove useful to aggregate sections within stands when mapping SI in operational FMIs (Eid and Økseter, 1999). As such, when estimating SI through the area-based approach, a trade-off must be made between the precision of the generated SI estimates and geographic extent to which predictions for individual grid cells are aggregated.

For the proposed methods to be applied in operational FMIs, wall-to-wall data on dominant tree species must be available for the area of interest so that the appropriate regression models can be applied. A number of studies have shown that adequate precision can be achieved when classifying tree species using remotely sensed data (Dalponte et al., 2012, 2013; Heinzel and Koch, 2011). In operational FMIs in Norway, however, dominant tree species in stands are most commonly determined through a combination of field visits and subjective interpretation of aerial photos. In this study, we determined the dominant tree species for all observations in both the sample- and validation datasets by using ground reference timber volume which we computed for each species, because we had no realistic alternative. The level of precision obtained at validation plot-level in this study is therefore optimistic, and an accurate tree species classification is required to match the level of precision reported in this study.

5. Conclusions

We proposed two methods for SI determination. With the direct

method, we regressed field observations of age-height SI against bi-temporal canopy height metrics derived from ALS data. With the indirect method, we derived SI from the initial laser-estimated H_{dom}, the laser-estimated H_{dom} increment, and the length of the observation period using empirical SI curves. Both the proposed methods produced SI estimates with satisfactory precision. The direct method produced higher precision, but the indirect method provides a suitable alternative because no additional fieldwork is required as the collection of core sample are not necessary, and, in addition, changes in SI can be captured over time. Future research is advised to (1) test the proposed methods on datasets acquired from different study areas, (2) develop methods for identifying areas that have been subject to silvicultural treatment or natural calamities during the observation period, and (3) develop methods for tree species classification using remotely sensed data.

Acknowledgements

References

Anon., 1987. Handbok for planlegging i skogbruket. Landbruksforlaget Oslo, Norway.

Arias-Rodil, M., Crecente-Campo, F., Barrio-Anta, M., Diéguez-Aranda, U., 2015. Evaluation of age-independent methods of estimating site index and predicting height growth: a case study for maritime pine in Asturias (NW Spain). Eur. J. For. Res. 134 (2), 223–233.

Avery, T.E., Burkhart, H., 1994. Forest management. For. Manage.

Baur, F., 1881. Die Rothbuche in Bezug auf Ertrag, Zuwachs und Form: unter Zugrundlegung der an der Kgl. Württemberg'schen Forstlichen Versuchsanstalt angestellten Untersuchungen bearbeitet: P. Parey.

Boisvenue, C., Running, S.W., 2006. Impacts of climate change on natural forest productivity – evidence since the middle of the 20th century. Glob. Change Biol. 12 (5), 862–882.

Bollandsås, O.M., Gregoire, T.G., Næsset, E., Øyen, B.-H., 2013. Detection of biomass change in a Norwegian mountain forest area using small footprint airborne laser scanner data. Stat. Methods Appl. 22 (1), 113–129.

Bontemps, J.-D., Bouriaud, O., 2013. Predictive approaches to forest site productivity: recent trends, challenges and future perspectives. Forestry 87 (1), 109–128.

Braastad, H., 1966. Volume tables for birch. Meddr. Norske SkogforsVes. 21, 265–365 Norwegian with English summary.

Brantseg, A., 1967. Volume functions and tables for Scots pine South Norway. Meddelelser fra det Norske Skogforsoksvesen 22, 695.

Bull, H., 1931. The Use of Polymorphic Curves in Determining Site Quality in Young Red Pine Plantations. Government Printing Office, US.

Chen, Y., Zhu, X., 2012. Site quality assessment of a *Pinus radiata* plantation in Victoria, Australia, using LiDAR technology. Southern For.: J. For. Sci. 74 (4), 217–227.

Coops, N.C., 2015. Characterizing forest growth and productivity using remotely sensed data. Curr. For. Rep. 1 (3), 195–205.

Dalponte, M., Bruzzone, L., Gianelle, D., 2012. Tree species classification in the Southern Alps based on the fusion of very high geometrical resolution multispectral/hyperspectral images and LiDAR data. Remote Sens. Environ. 123, 258–270.

Dalponte, M., Orka, H.O., Gobakken, T., Gianelle, D., Næsset, E., 2013. Tree species classification in boreal forests with hyperspectral data. IEEE Trans. Geosci. Remote Sens. 51 (5), 2632–2645.

Eid, T., 1991. Virkninger Av Malefeil Pa Takstresultater, Framskrivninger Og Prioriteringer Av Tiltak i Skogbestand. Norsk Institutt for Skogforskning, Skogforsk(8).

Eid, T., 1992. Bestandsvis kontroll av skogbruksplandata i hogstklasse III-V. Norsk Institutt for Skogforskning, Skogforsk(45.7).

Eid, T., 2000. Use of uncertain inventory data in forestry scenario models and consequential incorrect harvest decisions. Silva Fennica 34 (2), 89–100.

Eid, T., Moum, O., 1999. Bestandsuavhengig bonitering og nøyaktighet, vol. 7 Skogforsk.

Eid, T., Økseter, P., 1999. Bestandsuavhengig bonitering og konsekvenser. Norsk Institutt for Skogforskning, Skogforsk(8/99).

Ekberg, I., Eriksson, G., Namkoong, G., Nilsson, C., Norell, L., 1994. Genetic correlations for growth rhythm and growth capacity at ages 3–8 years in provenance hybrids of *Picea abies*. Scand. J. For. Res. 9 (1–4), 25–33.

Ferree, M., Shearer, T., Stone, E., 1958. A method of evaluating site quality in young red pine plantations. J. For. 56 (5), 328–332.

Fox, J., Weisberg, S., 2011. An R Companion to Applied Regression. Sage Publications.

Fries, J., 1969. Boniteringskurvor för tall och gran. Site index curves for Scots pine and Norway spruce. Skogen 57 (1), 30.

Fuller, R., Smith, G., Devereux, B., 2003. The characterisation and measurement of land cover change through remote sensing: problems in operational applications? Int. J. Appl. Earth Observ. Geoinform. 4 (3), 243–253.

Heinzel, J., Koch, B., 2011. Exploring full-waveform LiDAR parameters for tree species classification. Int. J. Appl. Earth Observ. Geoinform. 13 (1), 152–160.

Hollaus, M., Eysn, L., Maier, B., Pfeifer, N., 2015. Site index assessment based on multitemporal ALS data. SilviLaser 28–30.

Holopainen, M., Vastaranta, M., Haapanen, R., Yu, X., Hyyppä, J., Kaartinen, H., Hyyppä, H., 2010. Site-type estimation using airborne laser scanning and stand register data. Photogr. J. Finland 22 (1), 16–32.

Hopkinson, C., Chasmer, L., Hall, R., 2008. The uncertainty in conifer plantation growth prediction from multi-temporal lidar datasets. Remote Sens. Environ. 112 (3), 1168–1180.

Hossfeld, J., 1822. Mathematik für Forstmänner, Ökonomen und Cameralisten. Gotha 4, 310.

Hunter, I., Schuck, A., 2002. Increasing forest growth in Europe—possible causes and implications for sustainable forest management. Plant Biosyst.-Int. J. Deal. All Aspects Plant Biol. 136 (2), 133–141.

Husch, B., Miller, C.I., Beers, T.W., 1982. Forest Mensuration. John Wiley Sons Inc.

Hyyppä, J., Yu, X., Rönnholm, P., Kaartinen, H., Hyyppä, H., 2003. Factors affecting laser-derived object-oriented forest height growth estimation. Photogr. J. Finland 18 (2), 16–31.

Hägglund, 1976. Skattning av höjdboniteten i unga tall-och granbestånd. Institutionen för Skogsproduktion.

Hägglund, Lundmark, 1977. Site index estimation by means of site properties.

Hägglund, Lundmark, 1981. Handledning i bonitering. National Board of Forestry.

Kandare, K., Ørka, H.O., Dalponte, M., Næsset, E., Gobakken, T., 2017. Individual tree crown approach for predicting site index in boreal forests using airborne laser scanning and hyperspectral data. Int. J. Appl. Earth Obser. Geoinform. 60, 72–82.

Kilpeläinen, A., Peltola, H., Rouvinen, I., Kellomäki, S., 2006. Dynamics of daily height growth in Scots pine trees at elevated temperature and CO_2. Trees 20 (1), 16–27.

Kozlowski, T.T., 1962. Tree growth.

Kvaalen, H., Solberg, S., May, J., 2015. Aldersuavhengig bonitering med laserskanning av enkelttrær.

Lexerød, N.L., 2005. Recruitment models for different tree species in Norway. For. Ecol. Manage. 206 (1–3), 91–108.

Lumley, T., 2004. The leaps package for regression subset selection. R package version 2.9.

Magnussen, S., Boudewyn, P., 1998. Derivations of stand heights from airborne laser scanner data with canopy-based quantile estimators. Can. J. For. Res. 28 (7), 1016–1031.

Maltamo, M., Næsset, E., Vauhkonen, J., 2014. Forestry applications of airborne laser scanning. Concepts and case studies. Manage. For. Ecosyst. 27, 2014.

Martins, F.S., Bock, J., Dambrine, E., Dez, G., Dupouey, J.-L., Georges-Leroy, M., Renaud, J.-P., 2010. Estimativa da altura dominante em povoamentos decíduos através de dados LIDAR com múltiplos retornos. Estimating dominant height in deciduous stands using multi-echo LIDAR data. Ambiência 6 (4), 115–126.

Means, J.E., Acker, S.A., Fitt, B.J., Renslow, M., Emerson, L., Hendrix, C.J., 2000. Predicting forest stand characteristics with airborne scanning lidar. Photogramm. Eng. Remote Sens. 66 (11), 1367–1372.

Messaoud, Y., Chen, H.Y., 2011. The influence of recent climate change on tree height growth differs with species and spatial environment. PLoS One 6 (2), e14691.

Monserud, R.A., 1984. Height growth and site index curves for inland Douglas-fir based on stem analysis data and forest habitat type. For. Sci. 30 (4), 943–965.

Monserud, R.A., Rehfeldt, G.E., 1990. Genetic and environmental components of variation of site index in inland Douglas-fir. For. Sci. 36 (1), 1–9.

Nigh, G.D., Love, B.A., 1999. How well can we select undamaged site trees for estimating site index? Can. J. For. Res. 29 (12), 1989–1992.

Næsset, E., 2002. Predicting forest stand characteristics with airborne scanning laser using a practical two-stage procedure and field data. Remote Sens. Environ. 80 (1), 88–99.

Næsset, E., 2004a. Accuracy of forest inventory using airborne laser scanning: evaluating the first Nordic full-scale operational project. Scand. J. For. Res. 19 (6), 554–557.

Næsset, E., 2004b. Practical large-scale forest stand inventory using a small-footprint airborne scanning laser. Scand. J. For. Res. 19 (2), 164–179.

Næsset, E., 2009. Effects of different sensors, flying altitudes, and pulse repetition frequencies on forest canopy metrics and biophysical stand properties derived from small-footprint airborne laser data. Remote Sens. Environ. 113 (1), 148–159.

Næsset, E., Bjerknes, K.-O., 2001. Estimating tree heights and number of stems in young forest stands using airborne laser scanner data. Remote Sens. Environ. 78 (3), 328–340.

Næsset, E., Gobakken, T., 2005. Estimating forest growth using canopy metrics derived from airborne laser scanner data. Remote Sens. Environ. 96 (3), 453–465. http://dx.doi.org/10.1016/j.rse.2005.04.001.

Næsset, E., Gobakken, T., Holmgren, J., Hyyppä, H., Hyyppä, J., Maltamo, M., Söderman, U., 2004. Laser scanning of forest resources: the Nordic experience. Scand. J. For. Res. 19 (6), 482–499.

Ørka, H.O., Bollandsås, O.M., Hansen, E.H., Næsset, E., Gobakken, T., 2018. Effects of terrain slope and aspect on the error of ALS-based predictions of forest attributes. For.: Int. J. For. Res. 91 (2), 225–237.

Ørka, H.O., Næsset, E., Bollandsås, O.M., 2010. Effects of different sensors and leaf-on and leaf-off canopy conditions on echo distributions and individual tree properties derived from airborne laser scanning. Remote Sens. Environ. 114 (7), 1445–1461.

Packalén, P., Mehtätalo, L., Maltamo, M., 2011. ALS-based estimation of plot volume and site index in a eucalyptus plantation with a nonlinear mixed-effect model that accounts for the clone effect. Ann. For. Sci. 68 (6), 1085.

Perin, J., Hébert, J., Brostaux, Y., Lejeune, P., Claessens, H., 2013. Modelling the top-height growth and site index of Norway spruce in Southern Belgium. For. Ecol. Manage. 298, 62–70.

Ralston, C.W., 1964. Evaluation of forest site productivity. Int. Rev. For. Res. 1, 171–200.

Rayner, M., Turner, B., 1990. Growth and yield modelling of Australian eucalypt forests II. Future trends. Aust. For. 53 (4), 238–247.

Schönau, A., 1987. 7. Problems in using vegetation or soil classification in determining site quality. S. Afr. For. J. 141 (1), 13–18.

Sharma, Brunner, Eid, Øyen, 2011. Modelling dominant height growth from national forest inventory individual tree data with short time series and large age errors. For. Ecol. Manage. 262 (12), 2162–2175.

Sharma, M., Amateis, R.L., Burkhart, H.E., 2002. Top height definition and its effect on site index determination in thinned and unthinned loblolly pine plantations. For. Ecol. Manage. 168 (1), 163–175.

Skovsgaard, J.P., Vanclay, J.K., 2008. Forest site productivity: a review of the evolution of dendrometric concepts for even-aged stands. For.: Int. J. For. Res. 81 (1), 13–31.

Skowronski, N.S., Clark, K.L., Gallagher, M., Birdsey, R.A., Hom, J.L., 2014. Airborne laser scanner-assisted estimation of aboveground biomass change in a temperate oak–pine forest. Remote Sens. Environ. 151, 166–174.

Snowdon, P., 1992. Ratio methods for estimating forest biomass. N. Z. J. For. Sci. 22 (1), 54–62.

Socha, J., Pierzchalski, M., Bałazy, R., Ciesielski, M., 2017. Modelling top height growth and site index using repeated laser scanning data. For. Ecol. Manage. 406, 307–317.

Spurr, S.H., 1952. Forest Inventory. The Ronald Press Co., New York, pp. 476.

Tompalski, P., Coops, N.C., White, J.C., Wulder, M.A., Pickell, P.D., 2015. Estimating forest site productivity using airborne laser scanning data and Landsat time series. Can. J. Rem. Sens. 41 (3), 232–245.

Tveite, B., 1977. Bonitetskurver for gran: Site-index curves for Norway spruce (Picea abies (L.) Karst). Norsk Inst. for Skogforskning.

Tveite, B., Braastad, H., 1981. Bonitering for gran, furu og bjørk. Norsk Skogbruk.

Vasilescu, M.M., 2013. Standard error of tree height using vertex III. Bull. Transilvania University of Brașov, Ser. II: For. Wood Ind. Agric. Food Eng. 6 (6).

Véga, C., St-Onge, B., 2009. Mapping site index and age by linking a time series of canopy height models with growth curves. For. Ecol. Manage. 257 (3), 951–959.

Vestjordet, 1967. Functions and tables for volume of standing trees. Norway spruce. Meddelelser fra det Norske Skogforsoksvesen 22 545-&.

Wakeley, P.C., 1954. The growth intercept method of site classification. Paper presented at the Proceedings of 3rd Annual Forestry Symposium, Louisiana State University, Baton Rouge, La.

Wakeley, P.C., Marrero, J., 1958. Five-year intercept as site index in southern pine plantations. J. For. 56 (5), 332–336.

Warrack, G.C., Fraser, A., 1955. Estimation of Site Quality in Juvenile Douglas Fir Stands. Department of Lands and Forests.

White, J.C., Wulder, M.A., Varhola, A., Vastaranta, M., Coops, N.C., Cook, B.D., Woods, M., 2013. A best practices guide for generating forest inventory attributes from airborne laser scanning data using an area-based approach. For. Chronicle 89 (6), 722–723.

Yu, X., Hyyppä, J., Kaartinen, H., Maltamo, M., 2004. Automatic detection of harvested trees and determination of forest growth using airborne laser scanning. Remote Sens. Environ. 90 (4), 451–462.

Yu, X., Hyyppä, J., Kukko, A., Maltamo, M., Kaartinen, H., 2006. Change detection techniques for canopy height growth measurements using airborne laser scanner data. Photogramm. Eng. Remote Sens. 72 (12), 1339–1348.

Paper II

MDPI

Article

Classifications of Forest Change by Using Bitemporal Airborne Laser Scanner Data

Lennart Noordermeer *, Roar Økseter, Hans Ole Ørka, Terje Gobakken[ID], Erik Næsset and Ole Martin Bollandsås

Faculty of Environmental Sciences and Natural Resource Management, Norwegian University of Life Sciences, NMBU, P.O. Box 5003, NO-1432 Ås, Norway; roar.okseter@nmbu.no (R.Ø.); hans-ole.orka@nmbu.no (H.O.Ø.); terje.gobakken@nmbu.no (T.G.); erik.naesset@nmbu.no (E.N.); ole.martin.bollandsas@nmbu.no (O.M.B.)
* Correspondence: lennart.noordermeer@nmbu.no

check for updates

Abstract: Changes in forest areas have great impact on a range of ecosystem functions, and monitoring forest change across different spatial and temporal resolutions is a central task in forestry. At the spatial scales of municipalities, forest properties and stands, local inventories are carried out periodically to inform forest management, in which airborne laser scanner (ALS) data are often used to estimate forest attributes. As local forest inventories are repeated, the availability of bitemporal field and ALS data is increasing. The aim of this study was to assess the utility of bitemporal ALS data for classification of dominant height change, aboveground biomass change, forest disturbances, and forestry activities. We used data obtained from 558 field plots and four repeated ALS-based forest inventories in southeastern Norway, with temporal resolutions ranging from 11 to 15 years. We applied the k-nearest neighbor method for classification of: (i) increasing versus decreasing dominant height, (ii) increasing versus decreasing aboveground biomass, (iii) undisturbed versus disturbed forest, and (iv) forestry activities, namely untouched, partial harvest, and clearcut. Leave-one-out cross-validation revealed overall accuracies of 96%, 95%, 89%, and 88% across districts for the four change classifications, respectively. Thus, our results demonstrate that various changes in forest structure can be classified with high accuracy at plot level using data from repeated ALS-based forest inventories.

Keywords: forest change; ALS; classification; dominant height; aboveground biomass; forest disturbance; forestry activity

---

1. Introduction

Changes in land use and land cover have great implications on a range of ecosystem functions [1–3]. Particularly changes in forest areas have received considerable research attention in recent years, due to their impacts on biodiversity and carbon pools [4,5]. Resultantly, the development of reliable and timely systems for monitoring forest change across different spatial and temporal scales has become a central task in forestry. Primary motives have been the provision of data for national users such as government and conservation agencies, forest organizations and industries, and international reporting in accordance with treaties and conventions. Although forest changes typically are monitored in national programs [6,7] and reported at a national level, forest management decisions that directly induce those changes are made locally, namely at the level of municipalities, forest properties, and stands, i.e., treatment units. At such local scales, sampling rates of national monitoring programs are too low to obtain the necessary information [8], and local inventories are carried out to inform forest management.

Remote sensing provides a means to collect large amounts of information on forest attributes, and recent decades have witnessed substantial innovations in remote sensing technologies and

data processing algorithms [9,10]. This has greatly facilitated the use of remotely sensed data for forest monitoring across various spatial and temporal scales. At global and national levels, coarse resolution optical satellite imagery provides useful information for estimating forest cover [11,12] and biomass [13,14]. At the level of forest properties and stands, high-resolution three-dimensional data have proven particularly useful for forest inventory applications [15]. Airborne laser scanning (ALS) provides accurate three-dimensional data on terrain surface and vegetation height, and in forest management inventories in numerous countries across the globe, it is common practice to use ALS data in estimating and mapping forest attributes [16] for local management needs.

ALS-based forest management inventories typically cover areas in the range of 100–1000 km^2 per project [17], in which forest attributes are commonly estimated and mapped using the area-based approach [18,19]. This approach involves developing statistical relationships between forest attributes and ALS metrics at the level of sample plots and predicting the attributes over a grid tessellating the entire inventory area into smaller cells. In stand-level forest inventories, model predictions for grid cells within stands are typically aggregated to obtain stand estimates. Alternatively, cell-level predictions can be used for wall-to-wall mapping of forest attributes [20], or as auxiliary information in probability-based sampling designs [21]. Parametric modeling techniques such as linear regression have widely been used due to their familiarity and practicality; however, they require assumptions regarding the distribution of the response variable, the model errors, and the absence of multicollinearity and autocorrelation. Because such assumptions may be violated in certain forest inventory applications for which remotely sensed data are used, nonparametric approaches have been studied extensively, such as nearest neighbor methods [22], regression trees [23], and neural networks [24]. Among these, nearest neighbor methods have become very popular in the field of forest inventory because they can easily be used for a wide range of applications, including classification, univariate and multivariate prediction, imputation, mapping, and inference [25].

The availability of multitemporal ALS data is increasing as ALS-based forest inventories are repeated through multiple cycles. Bitemporal ALS data have proven useful for estimating forest height growth [26,27] and aboveground biomass (AGB) change [28–30]. Although the quantification of changes in the mentioned attributes is highly relevant for forest planning, many applications in forestry require classification into discrete categories. Categorical variables such as dominant tree species, forest development class, and forest productivity have long been fundamental in forest planning. As ALS-based forest inventories are starting to be repeated in many countries, possibilities for new classification systems emerge that allow for temporal change monitoring.

A range of forest inventory applications may benefit from change classification. First, recent studies have shown that canopy height growth as depicted by bitemporal ALS data enables the estimation of forest productivity [31–33]. Forest productivity is among the most essential variables in forest management and is expensive to record in field surveys. The estimation of forest productivity requires the height of dominant trees (Hdom) to have increased during the observation period, as forest productivity would be underestimated in cases where Hdom growth has been disrupted. This calls for a classification of forest into positive and negative Hdom development prior to the estimation of forest productivity itself. Second, AGB change classes can be used as post-strata in AGB change estimation [34], and changes can be projected spatially to identify areas where changes have occurred, their spatial extents alone being relevant reporting units. Third, forest disturbance events such as storm damage and harvest have gained relevance due to their impacts on forest ecosystems [35–38] and carbon balances [30,39]. Finally, classification of forestry activities such as untouched, partial harvest, and clearcut are crucial for estimating and reporting net forest carbon fluxes, given that carbon emissions and removals must be attributed to certain offset activities [34].

Previous research has shown that single-date ALS data can be used to indicate past forest disturbances and silvicultural operations. For example, d'Oliveira et al. [40] used structural ALS metrics over a tropical forest in Brazil to identify selective logging. Other studies using single-date ALS data discriminated between forest development classes [41–43] and forest/non-forest classes for

the purpose of stand delineation [44–46]. To monitor changes in forest structure over time, however, multitemporal data are needed. Bitemporal ALS data have been used to identify single harvested trees [47] and monitor canopy gap dynamics [48–50]. Næsset et al. [34] used bitemporal ALS data with a temporal resolution of 11 years to classify untouched, partial harvest, and clearcut forest at plot-level in a boreal forest in southeastern Norway using multinomial logistic regression. To the best of our knowledge, however, no further research has been done on the use of multitemporal ALS data for forest change classification. Here, we present the first study assessing the use of bitemporal ALS data for classification of various changes in forest structure. We used data acquired as part of repeated operational inventories carried out by a forest owner's cooperative and demonstrated how such data can be used for local forest change monitoring.

The objective of this study was to assess the utility of bitemporal ALS data for classification of Hdom change, AGB change, forest disturbances and forestry activities. We distinguished between the following change classes: (i) increasing versus decreasing Hdom, (ii) increasing versus decreasing AGB, (iii) undisturbed versus disturbed forest and (iv) forestry activities namely untouched, partial harvest and clearcut.

2. Material and Methods

2.1. Study Areas

We used bitemporal field and ALS data acquired as part of four repeated forest inventories in southeastern Norway (Figure 1). The inventories were carried out by Viken Skog SA, a Norwegian forest owner's cooperative, and were among the first commercial ALS-based trials in the early 2000s [17]. They were also among the first repeated ALS-based inventories. District 1 was part of the municipality of Krødsherad (60°10′N 9°35′E, 130–660 m above sea level) and comprised about 5000 ha productive forest [51]. The dominant tree species in the area are Norway spruce (*Picea abies* (L.) Karst.) and Scots pine (*Pinus sylvestris* L.). District 2 comprised about 49,000 ha productive forest in the municipality of Nordre Land (60°50′N 10°5′E, 140–900 m above sea level) [52], also mainly composed of Norway spruce and Scots pine. District 3, the district of Tyristrand (60°6′N 10°2′E, 150–480 m above sea level), comprised about 13,000 ha productive forest where Scots pine is the main species [17]. Lastly, District 4 was part of the municipality of Hole (60°1′N 10°20′E, 240–540 m above sea level) which comprises 6500 ha productive forest, dominated by Norway spruce [53].
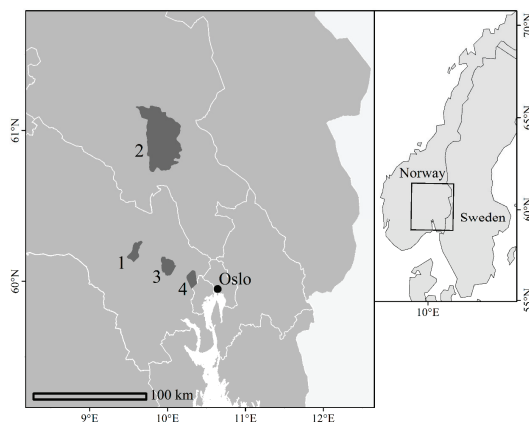
Figure 1. Map of southeastern Norway showing the location of the four districts. White lines represent county borders.

2.2. Field Data

During the first inventory cycle (t_1), circular sample plots were distributed systematically throughout the districts by means of systematic stratified sampling designs. The sample plots had a radius of 8.61 m for district 1 and 8.92 m for the remaining districts, resulting in plot sizes of 233 m^2 and 250 m^2, respectively (Table 1). These are typical plot sizes in Norwegian operational forest inventories [54]. Stratification was carried out according to dominant tree species, site productivity, and forest development class as interpreted from aerial images, for details see [17,51–53]. In Norway, development classes represent the succession of production forest [55], where class 1 represents clear-felled stands, class 2 represents regeneration forests, typically with a height <10 m, class 3 represents young forest, class 4 represents mature forest, and class 5 represents forest ready for harvest. Development class 1 was omitted from the inventories, and at t_1, development class 2 was only included in the inventory of district 1. During the second inventory cycle (t_2), all plots were revisited, and they were remeasured unless a final harvest recently had taken place. For plots that had been subject to final harvest, those for which sufficient time had passed for regeneration to occur were remeasured if the regenerated forest had reached a height >0.5 m. Table 1 provides an overview of the inventories and the number of plots within forest development classes.

Table 1. Summary of the inventories and number of plots within forest development classes.

District	Name	Plot Size (m^2)	First Inventory Cycle			Second Inventory Cycle		
			Year	No. of Plots, Development Class * 2	No. of Plots, Development Classes 3–5	Year	No. of Plots, Development Class 2	No. of Plots, Development Classes 3–5
1	Krødsherad	233	2001	39	111	2016	19	131
2	Nordre Land	250	2003	0	198	2017	21	177
3	Tyristrand	250	2006	0	111	2017	3	108
4	Hole	250	2005	0	99	2017	12	87

* development class 2 = regeneration forest, class 3 = young forest, class 4 = mature forest, class 5 = forest ready for harvest.

2.3. Plot Positioning

At t_1, plot center coordinates were determined using differential global navigation satellite systems (dGNSS) with Javad Legacy 20-channel receivers. The receivers measured pseudorange and carrier phase observables of the global positioning system (GPS) and the global navigation satellite system (GLONASS). A Javad Legacy served as a local base station. During post-processing, the coordinates were corrected against the collected reference data, and average accuracies of the planimetric plot center coordinates were <50 cm according to the positional standard errors reported by the Pinnacle 1.0 post-processing software. Plot centers were marked with wooden sticks. Upon revisiting the plots at t_2, a 226-channel Topcon HiPer SR was used in real-time kinematic mode to navigate to the plot centers. In case the wooden stick was not found, the position was remeasured using a Topcon Legacy E 40-channel receiver. During post-processing, the coordinates were corrected against reference data from the base stations of the Norwegian Mapping Authority using the software Magnet Tools [56].

2.4. Tree Measurements

On plots within forest development classes 3–5, the diameter at breast height (DBH) of trees exceeding given lower caliper limits was measured using a caliper during both inventory cycles. The lower caliper limits varied across districts and forest development classes, however on all plots, trees with a DBH ≥10 cm were calipered. For consistency, we excluded trees with a DBH <10 cm from the analysis across all districts and development classes. Furthermore, a sample of about 10 trees per plot was selected using a relascope and their heights were measured using a Vertex hypsometer.

On regeneration plots in district 1 and 2, four circular subplots of 40 m^2 were measured in cardinal directions from the plot center at a distance of 5.10 m. In district 3 and 4, three subplots of 40 m^2 were measured in north, southwest, and southeast directions at a distance of 5.35 m from the plot center.

The radius around subplot centers was determined using a telescopic rod of 3.57 m. The subplots were divided into four quadrants in cardinal directions, and tree measurements were carried out within the separate quadrants. DBHs were not measured, as plot volumes were not calculated for regeneration plots in the inventories. The heights of the first tree in each quadrant, counting in a clockwise direction, and the first subjectively chosen dominant tree in each quadrant were measured using a height pole for trees with a height <8 m and a Vertex hypsometer for taller trees. A maximum of two dominant trees were selected in each quadrant.

2.5. Computation of Forest Attributes

Tree heights had only been measured for sample trees on plots of development classes 3–5. Thus, we estimated the heights of all calipered trees using a ratio estimator described in detail in Ørka et al. [57], based on the ratio between heights predicted with empirical DBH-height models and field-measured heights. We then computed Hdom as the mean predicted height of the trees corresponding to the largest 100 trees per ha, according to DBH [58]. Furthermore, we computed N as the number of calipered trees on each plot, scaled to a per hectare basis. Lastly, we predicted the AGB of individual trees using allometric models estimated by Marklund [59], and computed plot-level AGB as the sum of biomass predictions scaled to a per hectare basis.

For regeneration plots, we computed Hdom as the mean heights of dominant trees. We assumed values of AGB on regeneration plots to be negligible and thus zero. A summary of the computed field plot data is shown in Figure 2.
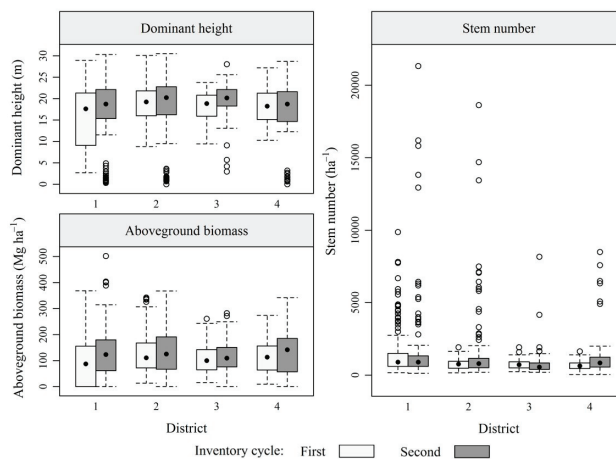
Figure 2. Box plots showing the distribution of computed field plot data.

2.6. Field Data Classification

We assigned forest change classes to each plot according to changes in the computed forest attributes, dividing the plots into distinct change classes for the four classification schemes. The classification schemes were aimed at distinguishing between different changes in forest structure with increasing complexity. For classification of Hdom change, we discriminated between plots on which Hdom had increased and decreased during the observation period (Table 2). For classification of AGB change, the classes were defined as increased or decreased AGB. For the classification of forest disturbance, the classes were defined as undisturbed plots or disturbed plots, using changes in forest structure as proxies for disturbances. We applied the rule that a decrease in Hdom or AGB, or a reduction in N of at least 30% indicated that a disturbance had taken place during the observation period. Such reductions in forest attributes would rule out a natural succession and corresponding

growth and mortality rates, and would therefore indicate that a substantial disturbance such as storm damage or thinning had occurred. For the classification of forestry activity, we further separated these changes by distinguishing between untouched, partial harvest and clearcut classes. The untouched class comprised plots on which no activity had taken place, i.e., undisturbed plots. The partial harvest class included plots that had been subject to a temporary reduction in Hdom, AGB, or N. The undisturbed class comprised plots on which the same reductions had occurred, and additionally, a reduction in AGB of at least 90%.

Table 2. Criteria for the classification schemes and numbers of plots within classes.

Classification	Class	Criteria *	No. of Plots			
			District 1	District 2	District 3	District 4
Dominant height change	Increase	$Hdom_{t2} > Hdom_{t1}$	118	165	99	83
	Decrease	All other plots	32	33	12	16
Aboveground biomass change	Increase	$AGB_{t2} > AGB_{t1}$	118	148	81	79
	Decrease	All other plots	32	40	30	20
Forest disturbance	Undisturbed	$Hdom_{t2} > Hdom_{t1}$ & $AGB_{t2} > AGB_{t1}$ & $N_{t2} > 0.7 \times N_{t1}$	75	149	68	77
	Disturbed	All other plots	75	49	43	22
Forestry activity	Untouched	$Hdom_{t2} > Hdom_{t1}$ & $AGB_{t2} > AGB_{t1}$ & $N_{t2} > 0.7 \times N_{t1}$	75	149	68	77
	Partial harvest	$Hdom_{t2} < Hdom_{t1}$ or $AGB_{t2} < AGB_{t1}$ or $N_{t2} < 0.7 \times N_{t1}$ & $AGB_{t2} \geq 0.1 AGB_{t1}$	56	28	40	10
	Clearcut	$Hdom_{t2} < Hdom_{t1}$ or $AGB_{t2} < AGB_{t1}$ or $N_{t2} < 0.7 \times N_{t1}$ & $AGB_{t2} < 0.1 AGB_{t1}$	19	21	3	12

* $Hdom_{t2}$ and $Hdom_{t1}$ = dominant height (m) during the second and first inventory cycles, respectively, AGB_{t2} and AGB_{t1} = aboveground biomass (Mg ha^{-1}) and, N_{t2} and N_{t1} = stem number (ha^{-1}), during the second and first inventory cycles, respectively.

2.7. ALS Data

At t_1, four ALS surveys were carried out using the Optech instruments ALTM 1233 and ALTM 3100 in the years 2001–2005, the acquisition parameters are shown in Table 3. At t_2, two ALS surveys were flown with a Riegl LMS Q-1560 scanner, where one of two surveys covered districts 1, 3, and 4. All ALS data were acquired under leaf-on conditions. The contractors Fotonor AS and TerraTec AS processed the ALS data and generated terrain surface models as triangulated irregular networks from laser returns classified as ground. Heights relative to the ground were computed for the remaining laser returns by subtracting the terrain height from ellipsoidal height.

Table 3. Airborne laser scanning acquisition parameters.

District	Year	Flight Dates	Instrument	PRF [a] (kHz)	Scanning Frequency (Hz)	Mean Flying Altitude (m)	Return Density (m^{-2})
			First inventory cycle				
1	2001	June 23–August 1	Optech ALTM 1233	50	21	650	1
2	2003	July 10–August 26	Optech ALTM 1233	33	40	800	1
3	2005	October 14	Optech ALTM 3100	50	32	1600	1
4	2004	September 16	Optech ALTM 1233	50	21	1200	1
			Second inventory cycle				
1	2016	June 7–July 31	Riegl LMS Q-1560	534	115	1300	12
2	2016	September 5–13	Riegl LMS Q-1560	400	100	2900	4
3	2016	June 7–July 31	Riegl LMS Q-1560	534	115	1300	8
4	2016	June 7–July 31	Riegl LMS Q-1560	534	115	1300	10

[a] Pulse repetition frequency.

2.8. ALS Metrics

For each plot, we extracted the laser returns for both points in time using the plot coordinates measured at t_2. We computed ALS metrics from the height distributions of first returns only because

we expected them to be most sensitive to canopy changes. Considering all first returns with a height >2 m relative to the ground as vegetation returns, we computed heights at the 10th, 20th, ... , 90th percentiles, denoted h_{10}, h_{20}, ... , h_{90}, and the maximum and mean vegetation return heights, denoted h_{max} and h_{mean}, respectively. Furthermore, we computed the standard deviation, kurtosis, coefficient of variation, and skewness of the vegetation return height distributions, denoted h_{sd}, h_{kurt}, h_{cv}, and $h_{skewness}$, respectively. We computed canopy density metrics by partitioning the range of vegetation return heights into 10 vertical fractions of equal height and dividing the cumulative number of returns within each fraction by the total number of returns. Density metrics were denoted d_0, d_1, ... , d_9. We also computed the total number of vegetation returns, denoted n. ALS metrics from the first and second inventory cycles were denoted _t1 and _t2, respectively. Finally, we computed differential (Δ) ALS metrics as the differences between corresponding ALS metrics computed for t_1 and t_2.

2.9. Forest Change Classification

We used the k-nearest neighbor (kNN) method [60] to classify forest change at plot-level on the basis of the computed ALS metrics described in the previous section. The method is known to be well suited to datasets with large numbers of ALS height and density metrics that may be correlated [61]. In kNN classification, each target unit is classified based on the k closest reference units in the feature space. The reference set comprises a set of labeled examples, and proximity must be determined on the basis of the distance between reference and target units using a given distance metric. Many distance metrics have been proposed, the Euclidian metric being the most common in forestry applications where nearest neighbor approaches are applied to remotely sensed data [22]. We used the Minkowski metric:

$$\text{distance} = \left(\sum_{i=1}^{m} |\mathbf{x}_i - \mathbf{y}_i|^p \right)^{1/p}$$

where $\mathbf{x}_i$ and $\mathbf{y}_i$ are m-dimensional vectors of ALS metrics and p is the Minkowski parameter. Note that the Minkowski metric equals the Manhattan metric given p = 1 and the Euclidian metric given p = 2. We performed the classification for each district separately, using the kknn package in R. Allowing a maximum of three ALS metrics to avoid overfitting, we implemented a grid search over all potential combinations of ALS metrics, k = 1, 3, 5, 7, and 9, and p = 1 and 2 to select the classifier that yielded the highest kappa [62] in leave-one-out cross-validation. We considered kappa to be a suitable criterion due to the uneven class sizes (Table 2).

2.10. Accuracy Assessment

We assessed the performance of the classifiers according to their overall accuracy, user's accuracy, and kappa as obtained from leave-one-out cross-validation. We computed the overall accuracy as the percentage of correct classifications, the user's accuracy as the percentage of correct classifications in each predicted class, and the kappa as the chance-standardized version of the overall accuracy [63]. We also computed accuracies across the four districts using aggregated confusion matrices for each classification scheme.

3. Results

The ALS metrics and classification parameters that yielded the highest kappa values are shown in Table 4. Differential ALS metrics were selected for most classifiers, frequently in combination with an ALS metric from t_1 or t_2. For most classifications, the highest kappa was obtained by including three ALS metrics and one or three nearest neighbors. In most cases, a Minkowski distance parameter of 2 was selected, although in many cases, a Minkowski parameter of 1 and/or other combinations of ALS metrics produced similar or identical values of kappa.

Table 4. k-nearest neighbor classification parameters.

District	Dominant Height Change			Aboveground Biomass Change			Forest Disturbance			Forestry Activity		
	ALS Metrics	k	p	ALS Metrics	k	p	ALS Metrics	k	p	ALS Metrics	k	p
1	$d_{3\_t1} + \Delta h_{sd} + \Delta d_6$	1	2	$\Delta h_{skewness} + \Delta h_{60} + \Delta d_2$	1	2	$h_{Sd\_t2} + d_{0\_t2} + \Delta d_3$	5	2	$d_{5\_t1} + \Delta h_{sd} + \Delta d_4$	1	2
2	$d_{0\_t1} + d_{1\_t2} + \Delta h_{50}$	3	2	$d_{7\_t1} + d_{2\_t2}$	3	1	$h_{max\_t2} + d_{4\_t2} + \Delta d_6$	3	2	$h_{max\_t2} + d_{4\_t2} + \Delta d_6$	3	2
3	$h_{20\_t1} + \Delta d_6 + \Delta n$	1	1	$h_{80\_t1} + d_{2\_t1} + \Delta d_5$	1	1	$h_{sd\_t1} + d_{7\_t2} + \Delta d_2$	3	1	$h_{10\_t2} + d_{0\_t2} + \Delta d_0$	3	2
4	$h_{50\_t1} + \Delta h_{max} + \Delta d_4$	1	2	$h_{10\_t2} + n_{\_t2} + \Delta d_0$	1	2	$h_{10\_t2} + \Delta d_5 + \Delta n$	1	2	$d_{2\_t2} + \Delta d_0 + \Delta n$	1	1

k = number of nearest neighbors, p = Minkowski parameter, see 2.8 for a description of ALS metrics.

Overall accuracies obtained for Hdom and AGB change classifications were similar across the four districts, however, highest for district 4 (Figure 3). For forest disturbance and forestry activity classifications, overall accuracies differed substantially across districts, also being highest for district 4. For the classification of forestry activity, the lowest accuracies were obtained for class A, i.e., untouched forest. Classifications of clearcut plots were 100% accurate in districts 2, 3, and 4; however, in district 1, one clearcut plot was misclassified as partially harvested.
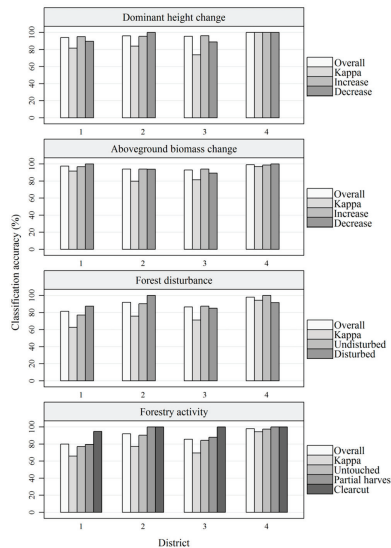
Figure 3. Classification accuracies.

Regarding the accuracies calculated from aggregated confusion matrices for the four districts, user's accuracies tended to be similar across classes (Table 5, Table 6, Table 7, and Table 8). However, the forestry activity class "clearcut" stood out with particularly high accuracy. The misclassifications of forestry activity were mainly caused by confusion between "untouched" and "partial harvest" classes.

Table 5. Aggregated confusion matrix of dominant height change classifications for the four districts.

Predicted	Reference		Total	User's Accuracy (%)
	Increase	Decrease		
Increase	462	20	480	96
Decrease	3	73	76	96
Total	465	93	558	
Kappa			0.83	
Overall accuracy (%)			96	

Table 6. Aggregated confusion matrix of aboveground biomass change classifications for the four districts.

Predicted	Reference		Total	User's Accuracy (%)
	Increase	Decrease		
Increase	429	22	451	95
Decrease	7	100	107	93
Total	436	122	558	
Kappa			0.83	
Overall accuracy (%)			95	

Table 7. Aggregated confusion matrix of forest disturbance classifications for the four districts.

Predicted	Reference		Total	User's Accuracy (%)
	Undisturbed	Disturbed		
Undisturbed	350	44	394	89
Disturbed	19	145	164	88
Total	369	189	558	
Kappa			0.74	
Overall accuracy (%)			89	

Table 8. Aggregated confusion matrix of forestry activity classifications for the four districts.

Predicted	Reference			Total	User's Accuracy (%)
	Untouched	Partial Harvest	Clearcut		
Untouched	355	50	1	406	87
Partial harvest	14	83	1	98	85
Clearcut	0	1	53	54	98
Total	369	134	55	558	
Kappa				0.74	
Overall accuracy (%)				88	

4. Discussion

Our results show that bitemporal data acquired as part of repeated ALS-based forest inventories are highly suitable for plot-level forest change classification. Forest planning systems in Norway, as well as many other countries, rely on information acquired in local forest inventories, and monitoring forest change at local levels is fundamental for sustainable forest management. The kNN method proved to be a practical and effective way of classifying the different changes in forest structure and yielded high accuracies. This is encouraging because the availability of bitemporal datasets will increase as local ALS-based forest inventories are repeated. The area-based approach is the most common method for predicting forest attributes from ALS data, and the methods proposed here can thus easily be applied in repeated ALS-based inventories.

Changes in ALS data proved to be good indicators of various types of forest change. This was expected because the ALS metrics that we computed characterize the height and density of the canopy at t_1 and t_2, and changes therein. Some sources of uncertainty must, however, be anticipated at the separate points in time, such as measurement errors, co-location errors between field and ALS data, and allometric errors. Moreover, additional sources of uncertainty arise when employing bitemporal field and ALS data for change detection, such as co-location errors between t_1 and t_2 plot center coordinates which may have influenced classifications negatively. Although state of the art positioning systems were used during both inventory cycles, the locations of plot centers differed in cases where the center mark was not found at t_2. In those cases, mean distances between post-processed t_1 and t_2 center coordinates were minimal, i.e., 1.1, 0.5, 0.3, and 0.5 m for districts 1–4, respectively. Nevertheless, even small positional errors will likely result in trees being in- or excluded in the plot data from the respective inventory cycles, and will therefore have caused inconsistencies in the classification of field data into change classes. Furthermore, changes in boundary effects may have added to this uncertainty.

Different portions of the canopy returns within plots will have belonged to trees of which the stem was located outside of the plot and vice versa, and such boundary effects will not have been constant for t_1 and t_2.

In spite of the abovementioned challenges, classifications of Hdom change yielded high overall accuracies, and even 100% accuracy for both Hdom change classes in district 4. Local differences in species compositions may partly explain the obtained accuracies being particularly high in district 4, as it is spruce-dominated and noticeably homogenous compared to other districts. Resultantly, the forest canopy structure can also be expected to be relatively homogeneous. Crown shapes of spruce and pine trees differ, which is known to influence the values of ALS height and density metrics [64]. Tree crowns of spruce trees are narrower, longer, and more cone-shaped than those of pine and deciduous trees, which will generally skew ALS height and density metrics toward lower values [51]. Therefore, stratification according to species and forest productivity is common practice in Norwegian forest inventories, and the two are strongly linked because spruce typically grows on high productivity sites and pine on poorer sites. Stratification can potentially improve the accuracy of ALS-based predictions [65], and stratification by dominant tree species may have improved classification accuracies in other districts. However, we chose to pool all plots together to maintain large reference sets covering a broad and continuous range of forest change examples, and thus to limit the number of classifications for target units of which ALS metrics fall outside the range of the reference set.

We obtained high overall accuracies for classifications of AGB change. A kappa value of 0.87 across districts indicated an "almost perfect" agreement between observed and predicted classes according to Landis and Koch [66]. This result was expected, as ALS is a proven tool for AGB estimation [67–70], and bitemporal ALS data can therefore be expected to be well suited for classification of AGB change. The classification for district 4 yielded the highest overall accuracy, likely due to the homogeneity of the species composition. Findings presented by Næsset and Gobakken [17] also support this, as they found that tree species had a strong effect on relationships between AGB and ALS data. The classifier for district 1 performed nearly as well, with an overall accuracy of 97%, which may be explained by the relatively large portion of plots that had been harvested during the observation period (Table 1), in which case changes in AGB are particularly distinct.

Using decreases in Hdom, AGB, and N as proxies for forest disturbances, our results demonstrated that such changes in forest structure can be detected reliably from bitemporal ALS data. The use of remotely sensed data for forest disturbance detection has been studied extensively, although most studies have focused on the use of spectral-temporal information derived from time series of satellite imagery. The overall accuracy of 89% across districts is in line with accuracies reported in many of those studies. Using the Landsat archive, high overall accuracies have been reported for stand-replacing forest disturbance classifications, for example 93% [71], 88% [72], 90% [73], and 88% [74]. However, studies that included non-stand replacing disturbances in the classification reported lower overall accuracies; 75% [73] and 80% [75], likely because subtle forest changes do not tend to display a clear spectral change that can be linked to a change in land cover class [76,77]. Thus far, however, no study has investigated the use of bitemporal ALS data for the classification of structural forest changes that indicate disturbance at plot-level, and our results demonstrate that also minor decreases in Hdom, ABG, and N can be detected reliably using such data.

It must be noted, however, that defining forest disturbance on the basis of forest inventory data is not trivial. Essentially, a forest disturbance can be any event that leads to a substantial reduction in structural forest attributes and can be caused by a range of anthropogenic or naturogenic factors. Different types and intensities of disturbances can occur, and particularly minor disturbances may be challenging to detect from bitemporal ALS data with time intervals >10 years. For example, selective harvest, disease, or insect damage may have disturbed even those plots for which field-based criteria indicated they were undisturbed. A shorter observation period may ensure that such minor disturbances are detected; Yu et al. [47] showed that single harvested trees can be detected reliably from bitemporal

ALS data with a temporal resolution of two years. In this study, however, we used bitemporal data with intervals of 11–15 years, which are common temporal resolutions in repeated ALS-based forest management inventories, meaning that minor disturbances may not always be captured.

We obtained high overall accuracies for the classification of forestry activities, which revealed that disturbed plots can reliably be further classified into "partial harvest" and "clearcut". Clearcut plots were easily identified, which can be expected because a substantial loss of AGB should be easy to detect from changes in ALS metrics that reflect canopy height and density. Overall accuracies ranged from 80% to 98% across districts, with a mean of 88%. These results are similar to findings reported by Næsset et al. [34], who obtained an overall accuracy of 94% for classification of the same activity classes from bitemporal ALS data. In the mentioned study, identical field-based criteria were used to define the activity classes, a temporal resolution similar to those used in this study was used; 11 years, however, the study area was substantially smaller. Comparable to their results, discriminating between untouched and partially harvested plots proved difficult in comparison to discriminating between partially harvested and clearcut plots. This may be expected as certain subtle changes in Hdom, AGB, and especially N may not be detectable from bitemporal ALS data at temporal resolutions >10 years. ALS data are poorly suited to characterize N in comparison to other forest attributes commonly estimated in forest inventories [53], and the detection of changes in N can therefore be expected to be more challenging than changes in Hdom and AGB.

5. Conclusions

Our results show that bitemporal data acquired as part of repeated ALS-based forest inventories can be used to classify various changes in forest structure reliably. At the spatial resolution of plots used in this study and at temporal resolutions of 11–15 years, changes in Hdom and AGB can be expected to be classified with overall accuracies >90%. Forest disturbances and forestry activities were classified with overall accuracies of 89 and 88%, respectively. These results are encouraging because the availability of bitemporal field and ALS data can be expected to increase as local forest inventories are repeated, enabling the operational application of the methods proposed here.

References

1. Foley, J.A.; DeFries, R.; Asner, G.P.; Barford, C.; Bonan, G.; Carpenter, S.R.; Gibbs, H.K. Global consequences of land use. *Science* **2005**, *309*, 570–574. [CrossRef] [PubMed]

2. Meyer, W.B.; Turner, B.L. Human Population Growth and Global Land-Use/Cover Change. *Annu. Rev. Ecol. Syst.* **1992**, *23*, 39–61. [CrossRef]

3. Yang, S.; Zhao, W.; Liu, Y.; Wang, S.; Wang, J.; Zhai, R. Influence of land use change on the ecosystem service trade-offs in the ecological restoration area: Dynamics and scenarios in the Yanhe watershed, China. *Sci. Total Environ.* **2018**, *644*, 556–566. [CrossRef] [PubMed]

4. Chaplin-Kramer, R.; Sharp, R.P.; Mandle, L.; Sim, S.; Johnson, J.; Butnar, I.; Mueller, C. Spatial patterns of agricultural expansion determine impacts on biodiversity and carbon storage. *Proc. Natl. Acad. Sci. USA* **2015**, *112*, 7402–7407. [CrossRef] [PubMed]

5. Mazor, T.; Doropoulos, C.; Schwarzmueller, F.; Gladish, D.W.; Kumaran, N.; Merkel, K.; Gagic, V. Global mismatch of policy and research on drivers of biodiversity loss. *Nat. Ecol. Evol.* **2018**, *2*, 1071. [CrossRef] [PubMed]

6. Tomppo, E.; Gschwantner, T.; Lawrence, M.; McRoberts, R.E.; Gabler, K.; Schadauer, K.; Cienciala, E. *National Forest Inventories. Pathways for Common Reporting*; European Science Foundation: Strasbourg, France, 2010; pp. 541–553.

7. Vidal, C.; Alberdi, I.; Redmond, J.; Vestman, M.; Lanz, A.; Schadauer, K. The role of European National Forest Inventories for international forestry reporting. *Ann. For. Sci.* **2016**, *73*, 793–806. [CrossRef]

8. Breidenbach, J.; Astrup, R. Small area estimation of forest attributes in the Norwegian National Forest Inventory. *Eur. J. For. Res.* **2012**, *131*, 1255–1267. [CrossRef]

9. Houborg, R.; Fisher, J.B.; Skidmore, A.K. *Advances in Remote Sensing of Vegetation Function and Traits*; Elsevier: Amsterdam, The Netherlands, 2015.

10. White, J.C.; Coops, N.C.; Wulder, M.A.; Vastaranta, M.; Hilker, T.; Tompalski, P. Remote sensing technologies for enhancing forest inventories: A review. *Can. J. Remote Sens.* **2016**, *42*, 619–641. [CrossRef]

11. Hansen, M.C.; Potapov, P.V.; Moore, R.; Hancher, M.; Turubanova, S.A.; Tyukavina, A.; Townshend, J.R.G. High-Resolution Global Maps of 21st-Century Forest Cover Change. *Science* **2013**, *342*, 850–853. [CrossRef]

12. Sexton, J.O.; Song, X.P.; Feng, M.; Noojipady, P.; Anand, A.; Huang, C.; DiMiceli, C. Global, 30-m resolution continuous fields of tree cover: Landsat-based rescaling of MODIS vegetation continuous fields with lidar-based estimates of error. *Int. J. Digit. Earth* **2013**, *6*, 427–448. [CrossRef]

13. Duncanson, L.; Armston, J.; Disney, M.; Avitabile, V.; Barbier, N.; Calders, K.; Crowther, T. The importance of consistent global forest aboveground biomass product validation. *Surv. Geophys.* **2019**, *40*, 979–999. [CrossRef] [PubMed]

14. Herold, M.; Carter, S.; Avitabile, V.; Espejo, A.B.; Jonckheere, I.; Lucas, R.; McRoberts, R.; Næsset, E.; Nightingale, J.; Petersen, R.; et al. The Role and Need for Space-Based Forest Biomass-Related Measurements in Environmental Management and Policy. *Surv. Geophys.* **2019**, *40*, 757–778. [CrossRef]

15. Vauhkonen, J.; Maltamo, M.; McRoberts, R.; Næsset, E. Introduction to Forestry Applications of Airborne Laser Scanning. In *Forestry Applications of Airborne Laser Scanning*; Maltamo, M., Næsset, E., Vauhkonen, J., Eds.; Springer: Dordrecht, The Netherlands, 2014; Volume 27, pp. 1–16.

16. Maltamo, M.; Næsset, E.; Vauhkonen, J. *Forestry Applications of Airborne Laser Scanning. Concepts and Case Studies*; Managing Forest Ecosystems; Springer: Dordrecht, The Netherlands, 2014; Volume 27, p. 460.

17. Næsset, E.; Gobakken, T. Estimation of above-and below-ground biomass across regions of the boreal forest zone using airborne laser. *Remote Sens. Environ.* **2008**, *112*, 3079–3090. [CrossRef]

18. Næsset, E. Predicting forest stand characteristics with airborne scanning laser using a practical two-stage procedure and field data. *Remote Sens. Environ.* **2002**, *80*, 88–99. [CrossRef]

19. White, J.C.; Wulder, M.A.; Varhola, A.; Vastaranta, M.; Coops, N.C.; Cook, B.D.; Woods, M. A best practices guide for generating forest inventory attributes from airborne laser scanning data using an area-based approach. *For. Chron.* **2013**, *89*, 722–723. [CrossRef]

20. Niemi, M.; Vastaranta, M.; Peuhkurinen, J.; Holopainen, M. Forest inventory attribute prediction using airborne laser scanning in low-productive forestry-drained boreal peatlands. *Silva Fenn.* **2015**. [CrossRef]

21. Ståhl, G.; Holm, S.; Gregoire, T.G.; Gobakken, T.; Næsset, E.; Nelson, R. Model-based inference for biomass estimation in a LiDAR sample survey in Hedmark County, Norway. *Can. J. For. Res.* **2010**, *41*, 96–107. [CrossRef]

22. Chirici, G.; Mura, M.; McInerney, D.; Py, N.; Tomppo, E.O.; Waser, L.T.; McRoberts, R.E. A meta-analysis and review of the literature on the k-Nearest Neighbors technique for forestry applications that use remotely sensed data. *Remote Sens. Environ.* **2016**, *176*, 282–294. [CrossRef]

23. Xu, M.; Watanachaturaporn, P.; Varshney, P.K.; Arora, M.K. Decision tree regression for soft classification of remote sensing data. *Remote Sens. Environ.* **2005**, *97*, 322–336. [CrossRef]

24. Niska, H.; Skon, J.P.; Packalen, P.; Tokola, T.; Maltamo, M.; Kolehmainen, M. Neural networks for the prediction of species-specific plot volumes using airborne laser scanning and aerial photographs. *IEEE Trans. Geosci. Remote Sens.* **2009**, *48*, 1076–1085. [CrossRef]

25. McRoberts, R.E. Estimating forest attribute parameters for small areas using nearest neighbors techniques. *For. Ecol. Manag.* **2012**, *272*, 3–12. [CrossRef]

26. Næsset, E.; Gobakken, T. Estimating forest growth using canopy metrics derived from airborne laser scanner data. *Remote Sens. Environ.* **2005**, *96*, 453–465. [CrossRef]

27. Yu, X.; Hyyppä, J.; Kukko, A.; Maltamo, M.; Kaartinen, H. Change detection techniques for canopy height growth measurements using airborne laser scanner data. *Photogramm. Eng. Remote Sens.* **2006**, *72*, 1339–1348. [CrossRef]

28. Økseter, R.; Bollandsås, O.M.; Gobakken, T.; Næsset, E. Modeling and predicting aboveground biomass change in young forest using multi-temporal airborne laser scanner data. *Scand. J. For. Res.* **2015**, *30*, 458–469. [CrossRef]

29. Skowronski, N.S.; Clark, K.L.; Gallagher, M.; Birdsey, R.A.; Hom, J.L. Airborne laser scanner-assisted estimation of aboveground biomass change in a temperate oak–pine forest. *Remote Sens. Environ.* **2014**, *151*, 166–174. [CrossRef]

30. Zhao, K.; Suarez, J.C.; Garcia, M.; Hu, T.; Wang, C.; Londo, A. Utility of multitemporal lidar for forest and carbon monitoring: Tree growth, biomass dynamics, and carbon flux. *Remote Sens. Environ.* **2018**, *204*, 883–897. [CrossRef]

31. Bollandsås, O.M.; Ørka, H.O.; Dalponte, M.; Gobakken, T.; Næsset, E. Modelling Site Index in Forest Stands Using Airborne Hyperspectral Imagery and Bi-Temporal Laser Scanner Data. *Remote Sens.* **2019**, *11*, 1020. [CrossRef]

32. Noordermeer, L.; Bollandsås, O.M.; Gobakken, T.; Næsset, E. Direct and indirect site index determination for Norway spruce and Scots pine using bitemporal airborne laser scanner data. *For. Ecol. Manag.* **2018**, *428*, 104–114. [CrossRef]

33. Solberg, S.; Kvaalen, H.; Puliti, S. Age-independent site index mapping with repeated single-tree airborne laser scanning. *Scand. J. For. Res.* **2019**, 1–31. [CrossRef]

34. Næsset, E.; Bollandsås, O.M.; Gobakken, T.; Gregoire, T.G.; Ståhl, G. Model-assisted estimation of change in forest biomass over an 11 year period in a sample survey supported by airborne LiDAR: A case study with post-stratification to provide "activity data". *Remote Sens. Environ.* **2013**, *128*, 299–314. [CrossRef]

35. Daskalova, G.N.; Myers-Smith, I.H.; Bjorkman, A.D.; Blowes, S.A.; Supp, S.R.; Magurran, A.; Dornelas, M. Forest loss as a catalyst of population and biodiversity change. *bioRxiv* **2018**, 473645. [CrossRef]

36. Franklin, J.F.; Spies, T.A.; Van Pelt, R.; Carey, A.B.; Thornburgh, D.A.; Berg, D.R.; Shaw, D.C. Disturbances and structural development of natural forest ecosystems with silvicultural implications, using Douglas-fir forests as an example. *For. Ecol. Manag.* **2002**, *155*, 399–423. [CrossRef]

37. Seidl, R.; Thom, D.; Kautz, M.; Martin-Benito, D.; Peltoniemi, M.; Vacchiano, G.; Honkaniemi, J. Forest disturbances under climate change. *Nat. Clim. Chang.* **2017**, *7*, 395. [CrossRef]

38. Thom, D.; Seidl, R. Natural disturbance impacts on ecosystem services and biodiversity in temperate and boreal forests. *Biol. Rev.* **2016**, *91*, 760–781. [CrossRef]

39. Raymond, C.L.; Healey, S.; Peduzzi, A.; Patterson, P. Representative regional models of post-disturbance forest carbon accumulation: Integrating inventory data and a growth and yield model. *For. Ecol. Manag.* **2015**, *336*, 21–34. [CrossRef]

40. d'Oliveira, M.V.; Reutebuch, S.E.; McGaughey, R.J.; Andersen, H.E. Estimating forest biomass and identifying low-intensity logging areas using airborne scanning lidar in Antimary State Forest, Acre State, Western Brazilian Amazon. *Remote Sens. Environ.* **2012**, *124*, 479–491. [CrossRef]

41. Falkowski, M.J.; Evans, J.S.; Martinuzzi, S.; Gessler, P.E.; Hudak, A.T. Characterizing forest succession with lidar data: An evaluation for the Inland Northwest, USA. *Remote Sens. Environ.* **2009**, *113*, 946–956. [CrossRef]

42. Valbuena, R.; Maltamo, M.; Packalen, P. Classification of multilayered forest development classes from low-density national airborne lidar datasets. *For. Int. J. For. Res.* **2016**, *89*, 392–401. [CrossRef]

43. Van Ewijk, K.Y.; Treitz, P.M.; Scott, N.A. Characterizing forest succession in Central Ontario using LiDAR-derived indices. *Photogramm. Eng. Remote Sens.* **2011**, *77*, 261–269. [CrossRef]

44. Eysn, L.; Hollaus, M.; Schadauer, K.; Pfeifer, N. Forest delineation based on airborne LIDAR data. *Remote Sens.* **2012**, *4*, 762–783. [CrossRef]

45. Olofsson, K.; Holmgren, J. Forest stand delineation from lidar point-clouds using local maxima of the crown height model and region merging of the corresponding Voronoi cells. *Remote Sens. Lett.* **2014**, *5*, 268–276. [CrossRef]

46. Sačkov, I.; Kardoš, M. Forest delineation based on LiDAR data and vertical accuracy of the terrain model in forest and non-forest area. *Ann. For. Res.* **2014**, *57*, 119–136. [CrossRef]

47. Yu, X.; Hyyppä, J.; Kaartinen, H.; Maltamo, M. Automatic detection of harvested trees and determination of forest growth using airborne laser scanning. *Remote Sens. Environ.* **2004**, *90*, 451–462. [CrossRef]

48. Nyström, M.; Holmgren, J.; Olsson, H. Change detection of mountain birch using multi-temporal ALS point clouds. *Remote Sens. Lett.* **2013**, *4*, 190–199. [CrossRef]

49. Solberg, S. Mapping gap fraction, LAI and defoliation using various ALS penetration variables. *Int. J. Remote Sens.* **2010**, *31*, 1227–1244. [CrossRef]

50. St-Onge, B.; Vepakomma, U. Assessing forest gap dynamics and growth using multi-temporal laser-scanner data. *Int. Arch. Photogramm. Remote Sens. Spat. Inf. Sci.* **2004**, *36*, 173–178.

51. Næsset, E. Practical large-scale forest stand inventory using a small-footprint airborne scanning laser. *Scand. J. For. Res.* **2004**, *19*, 164–179. [CrossRef]

52. Næsset, E. Accuracy of forest inventory using airborne laser scanning: Evaluating the first Nordic full-scale operational project. *Scand. J. For. Res.* **2004**, *19*, 554–557. [CrossRef]

53. Næsset, E. Airborne laser scanning as a method in operational forest inventory: Status of accuracy assessments accomplished in Scandinavia. *Scand. J. For. Res.* **2007**, *22*, 433–442. [CrossRef]

54. Gobakken, T.; Næsset, E. Assessing effects of laser point density, ground sampling intensity, and field sample plot size on biophysical stand properties derived from airborne laser scanner data. *Can. J. For. Res.* **2008**, *38*, 1095–1109. [CrossRef]

55. Anonymous. *Handbok for Planlegging I Skogbruket*; Landbruksforlaget: Oslo, Norway, 1987; Available online: https://www.nb.no/nbsok/nb/c55d16a811d846645632638cb893d749 (accessed on 23 August 2019).

56. Topcon Positioning Systems. *MAGNET Tools 1.0.*; Topcon Positioning Systems Inc.: Livermore, CA, USA, 2012.

57. Ørka, H.O.; Bollandsås, O.M.; Hansen, E.H.; Næsset, E.; Gobakken, T. Effects of terrain slope and aspect on the error of ALS-based predictions of forest attributes. *For. Int. J. For. Res.* **2018**, *91*, 225–237. [CrossRef]

58. García, O. Estimating top height with variable plot sizes. *Can. J. For. Res.* **1998**, *28*, 1509–1517. [CrossRef]

59. Marklund, L.G. *Biomass Functions for Pine, Spruce and Birch in Sweden*; Rapport-Sveriges Lantbruksuniversitet, Institutionen foer Skogstaxering: Uppsala, Sweden, 1988.

60. Cover, T.M.; Hart, P. Nearest neighbor pattern classification. *IEEE Trans. Inf. Theory* **1967**, *13*, 21–27. [CrossRef]

61. Maltamo, M.; Malinen, J.; Packalén, P.; Suvanto, A.; Kangas, J. Nonparametric estimation of stem volume using airborne laser scanning, aerial photography, and stand-register data. *Can. J. For. Res.* **2006**, *36*, 426–436. [CrossRef]

62. Cohen, J. A coefficient of agreement for nominal scales. *Educ. Psychol. Meas.* **1960**, *20*, 37–46. [CrossRef]

63. Hand, D.J. Assessing the Performance of Classification Methods. *Int. Stat. Rev.* **2012**, *80*, 400–414. [CrossRef]

64. Nelson, R. Modeling forest canopy heights: The effects of canopy shape. *Remote Sens. Environ.* **1997**, *60*, 327–334. [CrossRef]

65. Næsset, E. Area-based inventory in Norway–from innovation to an operational reality. In *Forestry Applications of Airborne Laser Scanning*; Springer: Berlin/Heidelberg, Germany, 2014; pp. 215–240.

66. Landis, J.R.; Koch, G.G. The measurement of observer agreement for categorical data. *Biometrics* **1977**, *33*, 159–174. [CrossRef]

67. Aardt, J.A.V; Wynne, R.H.; Oderwald, R.G. Forest volume and biomass estimation using small-footprint lidar-distributional parameters on a per-segment basis. *For. Sci.* **2006**, *52*, 636–649.

68. Bortolot, Z.J.; Wynne, R.H. Estimating forest biomass using small footprint LiDAR data: An individual tree-based approach that incorporates training data. *ISPRS J. Photogramm. Remote Sens.* **2005**, *59*, 342–360. [CrossRef]

69. Gregoire, T.G.; Ståhl, G.; Næsset, E.; Gobakken, T.; Nelson, R.; Holm, S. Model-assisted estimation of biomass in a LiDAR sample survey in Hedmark County, Norway. *Can. J. For. Res.* **2010**, *41*, 83–95. [CrossRef]

70. Jochem, A.; Hollaus, M.; Rutzinger, M.; Höfle, B. Estimation of aboveground biomass in alpine forests: A semi-empirical approach considering canopy transparency derived from airborne LiDAR data. *Sensors* **2011**, *11*, 278–295. [CrossRef]

71. Cohen, W.B.; Fiorella, M.; Gray, J.; Helmer, E.; Anderson, K. An efficient and accurate method for mapping forest clearcuts in the Pacific Northwest using Landsat imagery. *Photogramm. Eng. Remote Sens.* **1998**, *64*, 293–299.

72. Cohen, W.B.; Spies, T.A.; Alig, R.J.; Oetter, D.R.; Maiersperger, T.K.; Fiorella, M. Characterizing 23 years (1972–95) of stand replacement disturbance in western Oregon forests with Landsat imagery. *Ecosystems* **2002**, *5*, 122–137. [CrossRef]

73. Ahmed, O.S.; Wulder, M.A.; White, J.C.; Hermosilla, T.; Coops, N.C.; Franklin, S.E. Classification of annual non-stand replacing boreal forest change in Canada using Landsat time series: A case study in northern Ontario. *Remote Sens. Lett.* **2017**, *8*, 29–37. [CrossRef]

74. Huo, L.Z.; Boschetti, L.; Sparks, A.M. Object-Based Classification of Forest Disturbance Types in the Conterminous United States. *Remote Sens.* **2019**, *11*, 477. [CrossRef]

75. Huang, C.; Goward, S.N.; Masek, J.G.; Thomas, N.; Zhu, Z.; Vogelmann, J.E. An automated approach for reconstructing recent forest disturbance history using dense Landsat time series stacks. *Remote Sens. Environ.* **2010**, *114*, 183–198. [CrossRef]

76. Franklin, S.E.; Ahmed, O.S.; Wulder, M.A.; White, J.C.; Hermosilla, T.; Coops, N.C. Large area mapping of annual land cover dynamics using multitemporal change detection and classification of Landsat time series data. *Can. J. Remote Sens.* **2015**, *41*, 293–314. [CrossRef]

77. Hermosilla, T.; Wulder, M.A.; White, J.C.; Coops, N.C.; Hobart, G.W. Regional detection, characterization, and attribution of annual forest change from 1984 to 2012 using Landsat-derived time-series metrics. *Remote Sens. Environ.* **2015**, *170*, 121–132. [CrossRef]

Paper III

Predicting and mapping site index in operational forest inventories using bitemporal airborne laser scanner data

Lennart Noordermeer, Terje Gobakken, Erik Næsset, Ole Martin Bollandsås

Faculty of Environmental Sciences and Natural Resource Management, Norwegian University of Life Sciences, NMBU, P.O. Box 5003, NO-1432 Ås, Norway

ABSTRACT

Forest productivity reflects the wood production capacity of a given site and provides crucial information for forest management planning. The most widely accepted measure of forest productivity is site index (SI), defined as the average height of dominant trees at a given index age. In forest management inventories, SI is commonly interpreted manually from aerial images. While the use of airborne laser scanner (ALS) data has revolutionized operational practices for estimating many forest attributes relevant to forest management planning, practices for determining SI remain unchanged. The main objective of this study was to demonstrate a practical method for predicting and mapping SI in repeated ALS-based forest inventories. We used data acquired as part of three operational large-scale forest inventories in southeastern Norway. First, we identified areas in which forest growth had remained undisturbed since the initial inventory. We then regressed field predictions of SI against bitemporal ALS canopy metrics and used the regression models to predict SI for forest areas classified as undisturbed. The result was SI maps constructed with a spatial resolution of 15.81 m. User accuracies of class predictions of undisturbed forest in the three districts were 92%, 95% and 89%. Plot-level validation revealed root mean squared errors of SI predictions ranging from 1.72 to 2.84 m for Norway spruce, and 1.35 to 1.73 m for Scots pine. The method presented here can be used to map SI over large areas of forest automatically, depicting forest productivity at a much finer spatial resolution than what is common in operational inventories.

1. Introduction

Forest productivity indicates the magnitude of wood production that can be realized at a given site and provides crucial information for forest management planning. It is an aggregated expression of all biotic and abiotic factors that influence the growth rate of a forest, and is essential for determining the economically optimal rotation age, thinning regime, form of final felling, choice of tree species in regeneration, the sustainable yield and other management decisions in forestry (Bontemps and Bouriaud, 2013; Pretzsch et al., 2007). Besides its operational implications, forest productivity is also a key input variable in yield tables, growth simulators and forest property taxation.

The most widely accepted measure of forest productivity is site index (SI), defined as the dominant height (H_{dom}) at a given index age for a given species (Hägglund and Lundmark, 1981; Monserud, 1984; Ralston, 1964; Skovsgaard and Vanclay, 2008). H_{dom} is defined as the average height of the largest 100 trees per ha according to stem diameter at breast height (DBH) (Rennolls, 1978). In Norway, SI is predicted from empirical age-height curves and expressed as the expected H_{dom} at the index age of 40 years (Tveite, 1977). The traditional way of predicting SI requires tree height measurements of dominant trees, i.e., site trees, and age at breast height of the same trees. Such field measurements are, however, expensive to acquire, and the development of cost-effective methods for SI determination thus remains a fundamental task in forest inventory.

In Norwegian forest management inventories, SI is most commonly interpreted manually from aerial images. The interpreter typically uses indications of growing conditions as observed in the aerial images, and in some cases the assessment is supported by subjective field observations, plot measurements and information derived from previous inventories (Eid, 2000). This method has remained unchanged since the 1970′s, and is commonly implemented in large-scale inventories covering forest areas with a typical size of around 50–100 km² (Næsset, 2014), and in recent years sometimes up to 500–1000 km² or greater. Besides being time and resource consuming, photo interpretation of SI is known to entail considerable levels of uncertainty. Several studies have been conducted in Norway, in which stand-level values of photo-interpreted SI were compared with corresponding values of field-predicted SI (Eid, 1992, 1996; Eid and Nersten, 1996). The studies reported mean differences of 2–18% and standard deviations of the differences of 10–22%. This ranks SI among the most error-prone resource variables used in forest management planning (Eid, 1992), with potentially great economic losses as a consequence of incorrect management decisions (Eid, 2000). This calls for the development of practical methods for estimating and mapping SI that can be adopted in operational inventories.

Airborne laser scanning (ALS) is known to provide accurate three-dimensional forest canopy information over large areas and at a low cost (Maltamo et al., 2014). In operational forest inventories, forest attributes are commonly estimated by means of models dependent on ALS metrics that characterize the height and density of the canopy (Hyyppä et al., 2012; McRoberts et al., 2010). The estimates are typically obtained according to a model-based framework, in which the models are applied for predicting forest attributes over a grid

tessellating the inventory area into grid cells, and then aggregated to stand level.

In the pioneering work by Næsset (1997a, 1997b), the first evidence of the potential of ALS data for the estimation of mean tree height and stand volume was provided. Later, proof-of-concept studies (Næsset, 2002a, 2002b), and full-scale demonstrations (Næsset, 2004b) were published. Finally, full-scale application in an operational context (Næsset, 2004a) showed that most forest attributes relevant for forest management planning can be estimated with unprecedented accuracy and at a lower costs than conventional methods (Eid et al., 2004), yet with a finer spatial resolution and with complete cover over large areas of forests. Since the first ALS-based operational inventory was conducted in Nordre Land municipality in 2003 (Næsset, 2004a), ALS data have become an integral part of commercial forest inventories on all continents (Maltamo et al., 2014). However, while the use of ALS data has revolutionized operational practices for estimating and mapping most of the forest stand attributes relevant for forest management planning, operational practices for determining SI remain unchanged.

In previous studies, various types of remotely sensed data have been used for estimating and mapping SI. Véga et al. (2009) demonstrated how SI can be estimated and mapped across Jack pine stands in a 4.5 km^2 forested sector using a series of canopy height models from scanned black-and-white aerial photographs and a digital terrain model derived from ALS data. Other studies have used H$_{dom}$ estimates derived from single-date ALS data in combination with registered stand age (Chen and Zhu, 2012; Holopainen et al., 2010b; Packalén et al., 2011) or age derived from Landsat time series (Tompalski et al., 2015) to predict SI. Persson and Fransson (2016) used multi-temporal X-band SAR data and bitemporal ALS data to construct canopy height models and predict SI from canopy height growth trajectories at plot-level. Socha et al. (2017) used bitemporal ALS data with a five-year interval and age estimated using stand register data to model H$_{dom}$ growth and SI for Norway spruce. They showed that local SI models can be fitted with tree height data obtained from repeated ALS surveys and age obtained from stand register data.

Other studies have investigated the use of bitemporal ALS data for the prediction of SI at individual tree level (Hollaus et al., 2015; Kvaalen et al., 2015; Solberg et al., 2019). However, individual tree methods require a laser echo density > 5–10 echoes m^{-2} for tree segmentation and to obtain a sufficient sampling rate within each individual tree segment (Yu et al., 2010). Such sampling densities surpass what is commonly available from previous ALS-based inventories, typically carried out 10–15 years earlier. Echo density has been one of the main drivers of the acquisition costs of ALS data (Gobakken and Næsset, 2008; Maltamo et al., 2014), and currently, echo densities in large-scale ALS acquisitions in Norway rarely exceed 5 echoes m^{-2}. Also, caution must be exercised when using ALS metrics as direct proxies for tree heights, as laser echo heights should be calibrated with ground reference data to obtain reliable tree height estimates (Magnussen and Boudewyn, 1998; Rönnholm et al., 2004). Without such calibration, tree heights will typically be underestimated because canopy echoes are unlikely to originate from the crown apex (Gaveau and Hill, 2003; Hyyppä, 1999; Lim et al., 2003; Næsset, 1997; Popescu et al., 2003). ALS metrics computed from different acquisitions can differ systematically due to different instruments, technical specifications and parameters being used during the respective acquisitions, and can vary across a range of forest structures (Kotivuori et al., 2016; Latypov, 2002; Næsset, 2009; Wulder et al., 2008; Yu et al., 2006). When using ALS metrics, such as the maximum echo height or the 99th percentile, as a direct proxy for tree height and/or tree height growth in determination of SI, a systematic error will consequently be introduced.

Recently, two studies were conducted in which SI was modelled and predicted at plot-level using bitemporal ALS data (Noordermeer et al., 2018) and a combination of bitemporal ALS data and single-date hyperspectral data (Bollandsås et al., 2019). The former study proposed a direct method for SI prediction, in which SI is regressed against

bitemporal canopy height metrics, and an indirect method, where SI is predicted from the H$_{dom}$ at the start of the observation period, the H$_{dom}$ increment, and the length of the period. The latter study used the direct method. Both studies found that SI was highly correlated with bitemporal ALS metrics, a promising result given that the direct method can easily be incorporated in operational ALS-based inventories in which regression models are already commonly applied wall-to-wall to predict a range of forest attributes.

Although the abovementioned proof-of-concept studies provided promising results, a full-scale demonstration in an operational context is missing to date. The operational application of the proposed method requires wall-to-wall data on dominant tree species to ensure that the species-specific predictive models are applied to the right forest area. Furthermore, when predicting SI, it is essential that forest growth has remained relatively undisturbed (e.g. Carmean et al., 2006, Stearns-Smith, 2002). Therefore, the suitability of spatial units (grid cells) for SI prediction must be classified based on whether any substantial disturbances have occurred to ensure that predictions of SI are limited to undisturbed forest.

The main objective of this study was to demonstrate a practical method for predicting and mapping SI in repeated ALS-based forest inventories. We used bitemporal datasets acquired as part of three repeated operational inventories conducted by a commercial forest owners' cooperative. In the inventories, aerial data, field data and ALS data were acquired at two points in time. We classified forest areas into disturbed and undisturbed on the basis of changes in the ALS data. Then, we used wall-to-wall data on dominant tree species as interpreted from the aerial imagery, and applied species-specific models to predict SI for undisturbed forest areas. Our specific objectives were to (i) assess the accuracy of forest disturbance classification, (ii) assess the accuracy of SI prediction and (iii) demonstrate a practical method for predicting and mapping SI in operational forest inventories using bitemporal ALS data.

2. Methods

2.1. Inventory areas

Consecutive ALS-based forest inventories were conducted in the districts of Nordre Land, Hole and Tyristrand, hereafter referred to as districts A, B and C respectively. The districts are located in the boreal forest zone in southeastern Norway (Fig. 1), with altitudes ranging from 140 to 900 m above sea level (Table 1). The inventories were carried out by Viken Skog SA, one of the larger Norwegian forest owners' cooperatives. The main tree species in district A are Norway spruce (*Picea abies* (L.) Karst.) and Scots pine (*Pinus sylvestris* L.). District B is a Norway spruce-dominated area with only sparse populations of Scots pine and deciduous trees, mainly birch (*Betula pendula* Roth and *B. pubescens* Ehrh). District C comprises mainly low-productivity forests dominated by Scots pine.

2.2. Aerial images and photo interpretation

During the inventories at the first point in time (T1), black-and-white aerial images were acquired for district A, and red–green–blue (RGB) images for districts B and C, with different image resolutions (Table 2). All stands within the inventory areas were identified manually, their boundaries were delineated using stereoscopic photo interpretation, and the stand polygons were stored in a geographic information system. For each stand, the dominant tree species, SI, age and development class were subjectively interpreted from the aerial images. The development class was determined on the basis of stand age and SI conforming to the Norwegian classification system that describes the stages of production forest (Anon, 1987). In this system, class 1 represents clear-felled stands, class 2 represents regeneration forests, typically with a height < 10 m, class 3 represents young forest, class 4
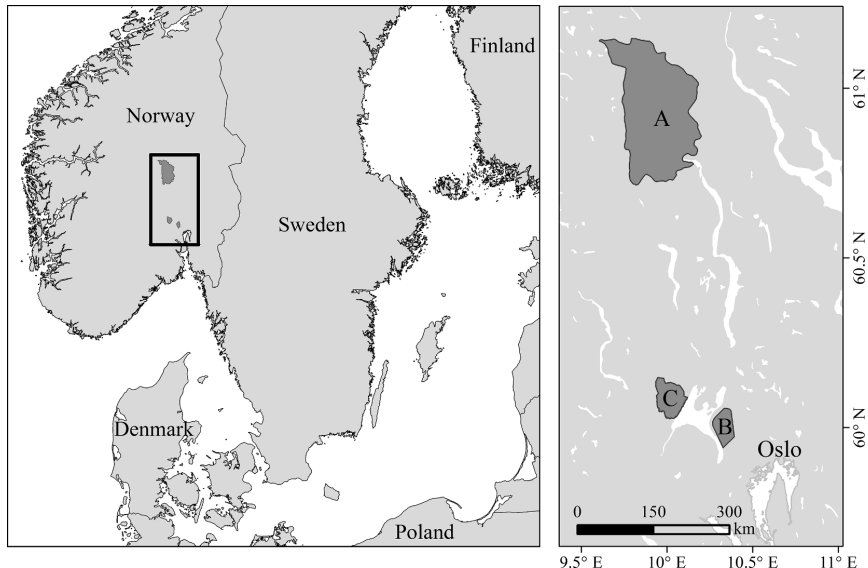
Fig. 1. The locations of the three districts.

Table 1
Overview of the districts and plot surveys.

District	Name	Geographical coordinates	Height above sea level (m)	Area (km²)	Year of first plot survey (T1)	No. of plots (T1)	Year of second plot survey (T2)	No. of plots (T2)
A	Nordre Land	60°50′ N, 10°85′ E	140–900	950	2003–2004	265	2017	180
B	Hole	60°1′ N, 10°20′ E	240–540	59	2005	120	2017	90
C	Tyristrand	60°6′ N, 10°2′ E	150–480	92	2006	120	2017	108

Table 2
Aerial image acquisition parameters.

	First acquisition			Second acquisition		
District	Date	Color[a]	Resolution (m)	Date	Color	Resolution (m)
A	June 6, 2002	B/W	0.25	October 3, 2016	RGB	0.25
B	July 31-August 7, 2003	RGB	0.20	August 17, 2016	RGB	0.25
C	August 15, 2004	RGB	0.25	March 10, 2016	RGB	0.25

[a] B/W = black-and-white, RGB = red, green and blue.

represents mature forest, and class 5 represents forest ready for harvest. At the second point in time (T2), RGB aerial images covering the districts were obtained, all with a resolution of 0.25 m. Digital stereo photogrammetry was used to update the existing inventory maps in terms of stand boundaries, tree species, development class and SI.

2.3. Field plot surveys and stratification

Ground reference data were collected during the summers of 2003–2004, 2005 and 2006 for districts A, B and C, respectively. Circular sample plots with an area of 250 m² were distributed throughout the three districts at T1, the number of plots varying among districts (Table 1). Sample plots were spatially distributed by means of stratified systematic sampling designs, using separate regular sampling grids for the different strata.

In district A, 265 sample plots were distributed over four pre-defined strata according to the proportional allocation principle, i.e., the sample size assigned to each stratum varied in proportion to the total

area of the stratum. The first stratum was defined as spruce-dominated forests of development classes 4–5 for which the SI was interpreted to be > =14, and comprised 74 plots. The second stratum, development classes 4–5 for which the SI was interpreted to be < 14, comprised 67 plots. The thirds stratum was of development class 3, comprising 72 plots, and the fourth was pine-dominated forests of development classes 4–5 and comprised 52 plots.

Approximately 97% of forest stands in district B were classified as spruce-dominated and 79% of stands in district C were classified as pine-dominated during the initial photo interpretations. Due to the homogeneity of the species compositions, no discrimination was made between species in the pre-defined strata. For both districts, a total of 120 sample plots were distributed evenly throughout three strata, i.e., each stratum comprised 40 sample plots. The first stratum comprised forests of development classes 4–5 for which the SI was interpreted to be > =14 m, the second stratum comprised forests of development classes 4–5 of which the SI was interpreted to be < 14 m and the third stratum comprised development class 3 forests.
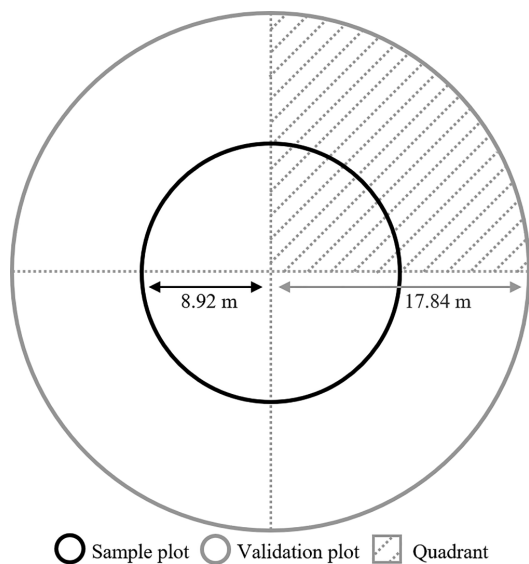
Fig. 2. Illustration of plot design.

In districts A and B, a selection of sample plot centers also served as validation plot centers, for which ground reference data were registered separately to the sample plot of 250 m^2 and the validation plot of 1000 m^2 (Fig. 2). In both districts, 40 validation plots were distributed equally over the two pre-defined strata considered to be most important from an economical perspective. In district A, these strata were (i) spruce- and (ii) pine-dominated forests of development classes 4–5. In district B, these strata were development class 4–5 forests for which the SI was interpreted to be (i) > = 14 m and (ii) < 14 m. All plots were revisited during the summer of 2017, however some plots were located in stands that had been harvested since T1 and were therefore not re-measured at T2.

2.4. Plot positioning

During the field plot surveys at T1, planimetric coordinates of plot centers were determined using Global Positioning System (GPS) and Global Navigation Satellite System (GLONASS) measurements, and plot centers were marked with wooden sticks. Dual-frequency 20-channel Javad Legacy receivers were used as base and rover receivers, and data collection lasted approximately 15–30 min for each plot location. During the plot surveys at T2, 26, 17 and 16 of the wooden sticks were found in districts A, B and C, respectively, ensuring identical plot locations. For the remaining plot centers, we navigated to the coordinates using a real-time kinematic global positioning system Topcon Hiper SR receiver. A 40-channel Topcon Legacy E + receiver was then used to measure planimetric coordinates of all plot centers, with receivers collecting data for a minimum of 30 min. Coordinates were corrected with real-time base station reference data to ensure sub-meter accuracy. Mean distances between T1 and T2 plot center coordinates were 0.47 m, 0.50 m and 0.32 m for districts A, B and C, respectively.

2.5. Tree measurements

Within the sample plots and at both T1 and T2, all trees with DBH > 4 and > 10 cm were calipered in plots of development classes 3 and 4–5, respectively. DBH was measured to the closest mm with a digital caliper, and tree species were recorded. Approximately 10

sample trees were selected within the plots using a relascope, i.e., sample trees were selected with a probability proportional to stem basal area. For sample trees, tree heights were measured using a Vertex hypsometer and recorded to the nearest dm.

At T2, all plots were revisited using identical tree measurement procedures. In addition to the sample trees, two site trees were selected within each sample plot. The selected site trees were the largest trees according to DBH of the dominant species on the plot. The height of each site tree was measured and the age at breast height was determined by coring.

Within validation plots, field procedures for the inner circle (Fig. 2) were first carried out. All trees with a DBH > 10 cm within the outer ring of 750 m^2 were then calipered, and tree species were recorded. Ten additional sample trees were selected for the outer ring using a relascope. At T2, age and height measurements from an additional two site trees were collected within the outer ring of the validation plots.

2.6. Calculation of ground reference values

Because tree heights had only been measured for sample trees, we estimated heights for all trees within plots using a ratio estimator. First, we predicted the so-called base height of all trees using DBH-height models constructed by Vestjordet (1968) and Fitje and Vestjordet (1977). Next, we predicted the so-called base volume for all trees using single-tree allometric volume models constructed by Braastad (1966), Brantseg (1967) and Vestjord (1967), using the DBH and the base heights. We then predicted the "true" volumes of sample trees using the observed instead of the base heights, and calculated the ratio between the true volume and the base volume. Then, for each plot, species-specific mean ratios were calculated and the true volume of each tree was estimated as the base volume multiplied by the appropriate mean ratio. Finally, we inverted the single-tree allometric volume models to predict height instead of volume, and thus obtain heights for all trees.

We computed H$_{dom}$ and aboveground biomass (AGB) at T1 and T2 as measures of forest structure, to identify areas in which forest disturbances had occurred. Areas in which substantial reductions in these forest attributes occurred can be considered unsuitable for SI determination, because disturbances such as forestry activities (harvesting, thinning) or natural calamities (storm damage, insect defoliation) would likely have occurred. For each plot, we calculated the H$_{dom}$ as the mean height of those sample trees that corresponded to the 100 largest trees per ha according to DBH. Thus, H$_{dom}$ estimates were based on the three and ten largest trees for sample and validation plots, respectively. We predicted the AGB of individual trees using species-specific allometric biomass models (Marklund, 1988) with DBH and tree height as predictors, and computed plot-level AGB as the sum of predicted values of tree-level AGB, scaled to per ha units.

Finally, we predicted tree-level SI for site trees using models developed by Sharma et al. (2011), with age and height as predictors. We then computed plot-level SI as the mean of SI values of individual trees within plots. The plot-level ground reference data are summarized in Table 3.

2.7. Airborne laser scanner data

Wall-to-wall ALS data were acquired in 2003, 2004 and 2005 for districts A, B and C, respectively. In 2016, an ALS survey covering district A was carried out, and another survey covering districts B and C. Thus, there were 13, 12 and 11 years between the subsequent ALS surveys. An overview of the ALS data acquisitions is shown in Table 4. For the initial ALS surveys, first and last echo data were supplied separately by the contractor, Fotonor AS, and terrain surface models were constructed for each ALS dataset separately as triangulated irregular networks from the last echo data. For the subsequent ALS acquisitions, all laser echoes were classified automatically as "ground", "unclassified", "noise", "bridge", or "snow" by the contractor, Terratec AS,

Table 3
Summary of ground reference data.

		Sample plots			Validation plots	
Characteristic	n	Range	Mean	n	Range	Mean
District A, spruce dominated	145			9		
SI (m)		4.84–23.43	12.41		8.76–20.63	13.70
H_{domT1} (m)		8.78–30.07	18.32		15.84–27.62	23.73
H_{domT2} (m)		9.49–30.48	20.71		16.89–29.98	24.01
AGB_{T1} (Mg ha^{-1})		13.34–342.86	120.38		48.83–292.08	195.08
AGB_{T2} (Mg ha^{-1})		21.12–367.73	157.11		24.02–358.15	178.74
District A, pine dominated	34			12		
SI (m)		5.85–20.70	13.05		7.37–20.83	13.61
H_{domT1} (m)		13.39–24.80	19.16		13.93–27.02	21.06
H_{domT2} (m)		14.38–29.85	21.17		16.63–25.14	22.44
AGB_{T1} (Mg ha^{-1})		23.43–237.97	105.01		42.46–192.10	124.14
AGB_{T2} (Mg ha^{-1})		41.15–434.87	137.02		56.56–209.12	141.74
District B, spruce dominated	82			29		
SI (m)		4.17–24.18	13.81		4.46–23.96	12.52
H_{domT1} (m)		10.27–27.19	17.74		10.89–24.72	19.49
H_{domT2} (m)		12.26–28.67	20.26		12.44–27.44	20.89
AGB_{T1} (Mg ha^{-1})		9.94–274.51	112.10		29.62–226.89	133.23
AGB_{T2} (Mg ha^{-1})		36.52–342.07	163.03		53.56–296.39	161.70
District C, spruce dominated	15					
SI (m)		7.13–25.13	16.46			
H_{domT1} (m)		10.91–23.69	19.40			
H_{domT2} (m)		16.18–28.01	21.39			
AGB_{T1} (Mg ha^{-1})		23.27–219.27	130.02			
AGB_{T2} (Mg ha^{-1})		41.18–282.38	154.74			
District C, pine dominated	91					
SI (m)		4.97–24.00	13.65			
H_{domT1} (m)		9.44–23.75	18.01			
H_{domT2} (m)		9.09–25.56	20.00			
AGB_{T1} (Mg ha^{-1})		16.10–261.03	102.77			
AGB_{T2} (Mg ha^{-1})		36.59–271.53	113.13			

*SI = site index. H_{domT1} and H_{domT2} = dominant height at the first point in time (T1) and the second point in time (T2), respectively. AGB_{T1} and AGB_{T2} = aboveground biomass at T1 and T2, respectively.

and terrain surface models were constructed from the echoes classified as ground. The echo heights relative to the ground were computed as the difference between laser echo height values and the terrain height.

2.8. ALS metrics

We extracted all first echoes within each plot using the geographical coordinates of plot centers measured at T2, and created height distributions from the echo heights. We omitted last echoes for the computation of ALS metrics as we expected first echoes to better characterize the upper layer of the canopy, and thus the dominant height, and to better reflect the changes therein. We computed canopy height

metrics from the echoes considered to belong to the canopy, i.e., echoes with a height above the ground > 2 m. We computed the heights at the 10th, 20th, …, and 90th percentile of the first echo height distributions at both points in time ($H10_{T1}$, $H10_{T2}$, $H20_{T1}$, $H20_{T2}$, …, $H90_{T1}$, $H90_{T2}$), and the height of the highest echo ($Hmax_{T1}$, $Hmax_{T2}$), mean height ($Hmean_{T1}$, $Hmean_{T2}$), standard deviation (Hsd_{T1}, Hsd_{T2}) and coefficient of variation (Hcv_{T1}, Hcv_{T2}) of laser echo heights. We then divided the height range between the 2 m threshold and H95, which we used only for the computation of canopy density metrics, into 10 fractions of equal height. We computed canopy density metrics at both points in time ($D0_{T1}$, $D0_{T2}$, $D1_{T1}$, $D1_{T2}$, …, $D9_{T1}$, $D9_{T2}$) as the proportion of echoes between the lower limit of each faction to the total number of echoes. Finally, we computed differential (Δ) ALS metrics as the difference between values of each ALS metric computed for T2 and the corresponding value computed for T1, for which, for example, ΔHmean denotes the difference in mean echo height.

2.9. Forest disturbance classification

We defined forest disturbance as a change in biophysical structure, following Clark (1990). We considered H_{dom} and AGB to be the most relevant forest attributes for characterizing forest structural changes. Thus, we used plot-level changes in H_{dom} and AGB as indicators of forest disturbance under the rule that a decrease in either of the two variables meant that a disturbance had taken place. As demonstrated by Noordermeer et al. (2019b), we used the non-parametric k-Nearest Neighbors (kNN) method to classify forest disturbance on the basis of bitemporal ALS metrics. The method has been shown to be effective for predicting, classifying and mapping forest attributes, particularly when used with remotely sensed data (e.g. Breidenbach et al., 2012; Holopainen et al., 2010a; McRoberts et al., 2015). kNN classification involves predicting the class label of a target unit according to the class labels of k reference units that are most similar, i.e., closest in feature space. To apply kNN for classification, four parameters need to be determined: a function for weighing neighbors, a distance measure, the feature variables and k. We used non-weighted kNN, meaning that the class of the target unit was assigned by majority vote. We used the Euclidean metric as a distance measure for which the distance between two plots $i = (x_{i1}, x_{i2,…}, x_{im})$ and $j = (x_{j1}, x_{j2,…}, x_{jm})$ with m ALS metrics can be calculated as:

$$d(i, j) = \sqrt{(x_{i1} - x_{j1})^2 + (x_{i2} - x_{j2})^2 + \cdots + (x_{im} - x_{jm})^2} \tag{1}$$

For each of the three calibration datasets, we searched exhaustively for the optimum combination of any one or two ALS metrics and k = 1, 3, 5, 7 and 9, by maximizing the Cohen's kappa (Landis and Koch, 1977) in leave-one-out cross validation. We used the kknn package in R (Schliep and Hechenbichler, 2014) for performing the classification. To assess the classification accuracies, we computed the overall accuracy as the percentage of correct classifications, the user's and producer's accuracy as the percentage of correct classifications in each predicted and observed class, respectively, and the kappa as the inter-rated agreement, accounting for the possibility of agreement occurring by chance (Hand, 2012).

Table 4
Airborne laser scanner specifications and acquisition parameters.

District	Instrument	Year	Flight dates	Pulse repetition frequency (kHz)	Scanning frequency (Hz)	Mean flying altitude (m)	Echo density (m^{-2})
First acquisition							
A	Optech ALTM 1233	2003	July 10–Aug. 26	33	40	800	1
B	Optech ALTM 1233	2004	Sept. 16	50	21	1200	1
C	Optech ALTM 3100	2005	Oct. 14	50	32	1600	1
Second acquisition							
A	Riegl LMS Q-1560	2016	Sept. 5–13	400	100	2900	4
B	Riegl LMS Q-1560	2016	June 7–July 31	534	115	1300	10
C	Riegl LMS Q-1560	2016	June 7–July 31	534	115	1300	8

2.10. Modelling site index

For each district, we regressed plot-level SI against bitemporal ALS metrics for pine- and spruce-dominated plots separately. In districts A and C, we modelled SI for both species. However, in district B there were only four pine-dominated sample plots which would be too few to fit a regression model. Thus, in district B we omitted pine-dominated forests, see details in section 2.12. We used the ordinary least squares method to estimate the model parameters. Similar to the feature selection applied in the forest disturbance classification, we selected ALS metrics as predictor variables by exhaustively searching for the combination of any one or two ALS metrics that optimized the predictive performance of the models in leave-one-out-cross validation. We assessed the predictive performance of each candidate model using the root mean square error (RMSE):

$$RMSE = \sqrt{\frac{1}{n} \sum_{i=1}^{n} (SI_i - \widehat{SI_i})^2} \tag{2}$$

where n is the sample size, SI_i is the ground reference SI for the out-of-sample plot i and $\widehat{SI_i}$ is the corresponding predicted SI. We selected the model that yielded the smallest RMSE. Furthermore, we estimated the mean differences between ground reference and predicted values (MD) and the RMSE relative to the ground reference mean (RMSE%) as:

$$MD = \frac{1}{n} \sum_{i=1}^{n} (SI_i - \widehat{SI_i}) \tag{3}$$

$$RMSE\% = 100 * RMSE/\overline{SI} \tag{4}$$

where $\overline{SI}$ is the mean of ground reference SI values in the sample.

2.11. Validation plots

We divided the validation plots into four quadrants of 250 m² and applied the kNN classifiers to each quadrant for disturbance classification. Because each validation plot contained a sample plot from which data was used for model fitting, we used a leave-one-out fitting and refitting procedure in which we left out sample plots located within validation plots one at a time while calibrating kNN classifiers and regression models and predicting for the corresponding quadrants. This procedure ensured that the models had not been calibrated with data obtained from within the spatial extent of the validation plot subject to predictions and thereby avoiding the accuracy assessment being too optimistic. Finally, we estimated SI at validation plot-level as mean values of SI predictions generated for undisturbed quadrants. We compared the obtained values with ground reference values. The assessment was based on RMSE, MD and RMSE%.

2.12. Mapping

We generated regular grids by tessellating the districts into 250 m² cells and intersected the grids with the stand layer maps. Thus, each grid cell was assigned a photo-interpreted species, development class and SI label. We omitted grid cells of forest types that were not represented in the calibration data, i.e., development classes 1 and 2, birch-dominated forests, and pine-dominated forests in district B. We also discarded smaller sliver polygons (incomplete border cells with an area < 50 m²), as is common practice in ALS-based operational inventories in Norway. Next, we applied the kNN classifiers to all remaining grid cells and applied the regression models for predicting SI for those grid cells classified as undisturbed. We omitted predictions of SI that fell outside the range of ground reference SI values to avoid extrapolation errors. Finally, we compared species-wise mean values of SI predictions with corresponding mean values of photo-interpreted values of SI to assess whether they differed substantially.

3. Results

3.1. Forest disturbance classification

The selected ALS metrics and number of nearest neighbors are shown in Table 5 and confusion matrices obtained from leave-one-out cross validation are shown in Tables 6, 7 and 8. Both height and density ALS metrics were selected for the classification in districts A and B. For district C, the difference in the cumulative canopy density above the 5th fraction (ΔD5) was selected as the only ALS metric. The overall accuracy obtained for district B was largest, and user accuracies of undisturbed forest class predictions were 92%, 95% and 89%.

3.2. Modelling site index

The parameter estimates, predictor variables and fit statistics of the regression models selected by the automated variable selection procedure are shown in Table 9. All models comprised two predictor variables. The combination of the 90th height percentiles from the two

Table 5
Selected airborne laser scanner (ALS) metrics and number of nearest neighbors (k) selected for the forest disturbance classification, and overall accuracy and kappa obtained from leave-one-out cross validation.

District	ALS metrics*	k	Overall accuracy	Kappa
A	H40$_{T1}$, ΔD5	3	0.89	0.52
B	ΔH70, ΔD0	1	0.94	0.71
C	ΔD5	5	0.87	0.68

*H40$_{T1}$ = 40th height percentile (m) at the first point in time (T1). ΔD0 and ΔD5 = differences in canopy densities corresponding to the proportions of vegetation echoes and vegetation echoes above the 5th fraction, respectively. ΔH70 = difference in the 70th height percentile (m).

Table 6
Confusion matrix of forest disturbance classification in district A.

kNN classifier	Field			
	Undisturbed	Disturbed	Total	User's accuracy
Undisturbed	148	13	161	0.92
Disturbed	6	13	19	0.68
Total	154	26	180	
Producer's accuracy:	0.96	0.50		

Table 7
Confusion matrix of forest disturbance classification in district B.

kNN classifier	Field			
	Undisturbed	Disturbed	Total	User's accuracy
Undisturbed	76	4	80	0.95
Disturbed	1	7	8	0.86
Total	77	11	88	
Producer's accuracy:	0.99	0.64		

Table 8
Confusion matrix of forest disturbance classification in district C.

kNN classifier	Field			
	Undisturbed	Disturbed	Total	User's accuracy
Undisturbed	71	9	80	0.89
Disturbed	5	23	28	0.82
Total	76	32	108	
Producer's accuracy:	0.93	0.72		

Table 9
Fitted regression models, sample sizes (n), fit statistics (R^2), mean differences (MD) and root mean square errors (RMSE) between ground reference and predicted site index, and RMSE relative to the ground reference mean (RMSE%) in leave-one-out cross validation.

District	Species	n	Predictive model*	R^2	MD	RMSE	RMSE%
A	Spruce	127	$2.89 - 2.14 * H90_{T1} + 2.38 * H90_{T2}$	0.67	0.00	2.35	18.63
A	Pine	26	$3.24 + 0.36 * Hmean_{T2} + 2.35 * \Delta H60$	0.87	0.00	1.73	13.79
B	Spruce	72	$-0.82 + 0.53 * H60_{T2} + 2.82 * \Delta H90$	0.69	0.02	2.84	20.03
C	Spruce	11	$6.18 - 3.19 * H50_{T1} + 3.46 * Hmean_{T2}$	0.91	-0.05	1.72	9.83
C	Pine	63	$-2.64 - 3.02 * H90_{T1} + 3.55 * H90_{T2}$	0.87	-0.01	1.61	11.78

*$H90_{T1}$ and $H90_{T2}$ = 90th height percentile (m) at the first point in time (T1) and the second point in time (T2), respectively. $Hmean_{T2}$ = mean echo height (m) at T2. $\Delta H60$ and $\Delta H90$ = differences in 60th and 90th height percentiles (m). $H60_{T2}$ = 60th height percentile (m) at T2. $H50_{T1}$ = 50th height percentile (m) at T1.

points in time or the difference between their values was selected for three out of five models. The model fitted with data obtained from 11 spruce-dominated plots in district C provided the best fit, with an R^2 of 0.91. Both models for pine-dominated forests had R^2 values of 0.87. Values of RMSE obtained from leave-one-out cross validation ranged from 1.61 to 2.84 m, being smallest for pine-dominated forest in districts A and C, and spruce-dominated forest in district C. Values of RMSE% ranged from 9.83 to 20.03.

3.3. Validation plots

At T2, 21 and 29 validation plots were remeasured in districts A and B, respectively. After applying the kNN classifiers to the 250 m^2 quadrants, four validation plots were labeled disturbed in district A and none in district B. The accuracy values of aggregated predictions of SI for validation plots were greater than the accuracies obtained for sample plots (Table 10, Fig. 3). The smallest RMSE of 1.35 m was obtained for pine-dominated validation plots in district A.

3.4. Mapping

Forest areas of approximately 337, 24 and 70 km^2 were classified as

Table 10
Comparison of ground reference and predicted site index for validation plots.

District	Species	n	MD	RMSE	RMSE%
A	Spruce	8	0.80	2.22	16.17
A	Pine	9	0.63	1.35	9.77
B	Spruce	29	0.05	1.93	15.41

undisturbed in districts A, B and C, respectively. These areas corresponded to 80%, 39% and 74% of the total forest area for which the development class was interpreted to be > 2 at T2, however substantial parts of the districts (particularly district 2) were not covered by both ALS surveys and were therefore omitted from the SI maps. The SI predictions provided quasi-continuous maps of forest productivity (Fig. 4) in stands of spruce and pine with development classes 3–5, with a spatial resolution of 15.81 m. Mean values of SI predictions were smallest in district A, which corresponded to the district-wise mean photo-interpreted SI values. Mean values of SI predictions within spruce-dominated forests were higher than corresponding values obtained by photo interpretation, but almost identical in pine-dominated forests. Nearly all SI predictions fell within the range of 5–25 m, which are typical values for Norwegian production forests.

4. Discussion

We demonstrated a method for predicting and mapping SI at the spatial scale of sampling units, using data from repeated ALS-based forest inventories, which can potentially replace existing practices for SI determination. In the method, undisturbed forest areas were first identified. Field measurements of SI were then regressed against bi-temporal ALS canopy metrics. Finally, the regression models were applied to forest areas classified as undisturbed to generate quasi-continuous maps of forest productivity.

As mentioned, this study is not the first to demonstrate a method for predicting and mapping SI using remotely sensed data. Although previous studies using single-date ALS and stand register data have shown that site types can be classified (Holopainen et al., 2010b) and that SI can be spatially projected (Chen and Zhu, 2012; Packalén et al., 2011),
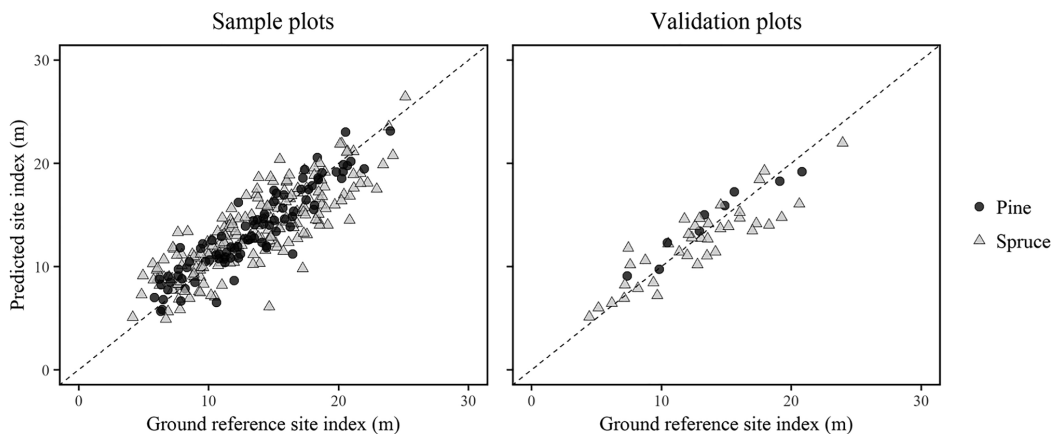
Fig. 3. Ground reference values of site index plotted against predicted values for sample plots (250 m^2) and validation plots (1000 m^2), as obtained by leave-one-out cross validation.
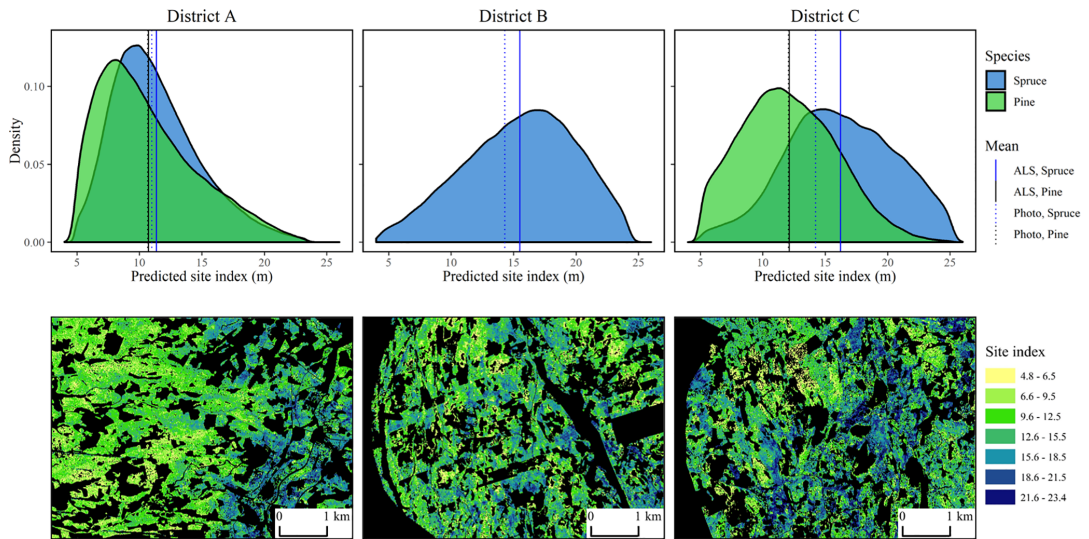
Fig. 4. Density plots showing the distribution of site index predictions, mean values of predictions and corresponding photo-interpreted values, and site index maps for smaller portions of the districts constructed from ALS predictions.

such methods rely on stand age data, which may not always be available, and which is commonly quantified with large uncertainty (Sharma et al., 2011). Furthermore, age-height relationships in stands with an uneven age structure are often weak, and the concept of stand age may be regarded as meaningless in such stands (Huang and Titus, 1993; Monserud, 1988). Also, most SI models require age at breast height as predictor variable as opposed to total age, which must resultantly be derived from the year of regeneration causing additional uncertainty.

4.1. Forest disturbance classification

We used plot-level decreases in H_{dom} or AGB as an indication of forest disturbance, and our results show that a decrease in either of the two variables can be detected with acceptable accuracy from bitemporal ALS data. However, non-decreasing H_{dom} or AGB does not ensure undisturbed forest growth. A wide range of anthropogenic and naturogenic factors may influence forest growth, such as harvest, disease and insect damage. Any of these factors might have disrupted forest growth even on those plots classified as undisturbed, and minor growth disturbances will in some cases not be detectable from bitemporal ALS data. Alternatively, disturbance classes can be registered at plot-level during field work, which would be a subjective assessment to some extent. However, no such data were collected in the current inventories, and the issue of determining whether forest growth has been disturbed arises when using any method for SI determination, including conventional field measurements and photo interpretation. A certain degree of uncertainty must therefore be anticipated when determining whether forest growth has been disturbed, be it based on field assessment, photo interpretation or ALS data.

We obtained large user accuracy values of the classification of undisturbed forest. User accuracies of undisturbed class predictions are particularly important for mapping of SI, to ensure that predictions are limited to undisturbed forest. Omission errors, i.e., undisturbed cells classified as disturbed, do not necessarily affect the certainty of SI predictions, but rather decrease the total area of cells with SI predictions. In some cases, such omissions occurred in sample plots with relatively large age values and small SI values in which forest growth presumably was limited to such a level that it might be difficult to

detect from bitemporal ALS data.

4.2. Modelling

Paired 90th height percentiles from the two points in time or the difference in their values were selected by the automated variable selection procedure for three out of five models. These metrics can be expected to be good predictors of SI, as they represent the height of the upper canopy layer occupied by site trees, while limiting the effect of understory vegetation and extreme values of echo height. Previous studies (Bollandsås et al., 2019; Noordermeer et al., 2018) also found these metrics to be good predictors of SI. As expected from those studies, we found strong correlations between ground reference SI and bitemporal ALS metrics for both spruce- and pine-dominated plots in all districts. The values of RMSE% obtained in leave-one-out cross validation ranged from 9.83 to 20.03, which is within the range of prediction errors that may be expected for ALS-based volume predictions in the same operational inventories (Noordermeer et al., 2019a). Given that volume is commonly predicted wall-to-wall in ALS-based inventories, this result highlights the potential of the proposed method for operational application.

For the 250 m^2 sample plots, we obtained values of RMSE in the range of 1.61–2.84 m, and for the 1000 m^2 validation plots, we obtained slightly smaller values of RMSE in the range of 1.35–2.22 m. Using the same model-based approach for predicting SI, Noordermeer et al. (2018) obtained RMSEs of 1.99–2.42 m for 233 m^2 plots and 1.08–1.78 m for validation plots of size ~ 3700 m^2, while Bollandsås et al. (2019) reported values of RMSE from cross validation of 2.2–3 m for 400 m^2 plots. Persson and Fransson (2016) obtained an RMSE value of 2.3 m at the spatial scale of 5000 m^2 plots by predicting SI from two canopy height models constructed from ALS data with a time interval of three years. The mentioned levels of accuracy provide sufficient basis to infer that bitemporal ALS data are highly suitable for SI determination. However, the spatial scale of the analysis is known to affect the prediction accuracy of ALS models, where accuracies increase with plot size (Gobakken and Næsset, 2008). Thus, when mapping SI, a compromise must be made between prediction accuracy and the spatial resolution at which SI is predicted and subsequently estimated.

We obtained greater accuracy values for pine-dominated plots than spruce-dominated plots, which is in accordance with other studies that assessed forest productivity for those species (Bollandsås et al., 2019; Holopainen et al., 2010b; Noordermeer et al., 2018). This may be explained by differences in canopy structure. The vertical structure of pine forests is more homogeneous than the vertical structure of spruce forests, and changes in canopy height may therefore be more distinguishable in pine forests. In districts A and C, there was considerably less variation in the ALS height metrics computed for pine-dominated plots than the corresponding metrics computed for spruce-dominated plots. ALS height metrics represent the vertical structure of the canopy, and the smaller degree of variation indicates a more homogeneous vertical structure in pine-dominated forests. Changes in canopy height may thus be more distinguishable in pine-dominated forests.

4.3. Mapping

We constructed SI maps with spatial resolutions of 15.81 m, depicting forest productivity at a much higher spatial resolution than what is common in stand-level inventories. Cell-level information provides a means to monitor within-stand dynamics, increasing the utility of the information for forest management planning. For example, the generated maps can be used to update stand boundaries, which is currently done by means of photo interpretation alone. It should be noted, however, that SI, like H_{dom}, is theoretically defined at the scale of 1 ha. When predictions of SI are made at a finer spatial resolution, a homogeneous spatial distribution of site trees is assumed, while the 100 largest trees within a ha may be clustered together (e.g. Ronnolls, 1978). In previous studies, SI maps with resolutions of 10 m (Socha et al., 2017; Solberg et al., 2019) and 20 m (Véga et al., 2009) have been generated. Alternatively, predictions can be aggregated to a larger, but still sub-stand extent, such as the 1000 m^2 validation plots used in this study for which greater certainty can be expected. Although we have not done so in our analysis, it is common practice to aggregate predictions of forest attributes within stands to obtain stand-level estimates. However, caution must be exercised when omitting empty cells from stand-level estimates, as a systematic error may be introduced. Low-productivity forest may be more likely to be classified as disturbed than high-productivity forest because increasing canopy height and density in such forests may be less likely to be detected.

In spruce-dominated forests in districts B and C, mean values of SI predictions were substantially larger than mean photo-interpreted values. As explained above, the means of predicted values may be systematically shifted towards greater values of SI because of low-productivity forests being more likely to be classified as disturbed, resulting in omission from the map. Values of SI can potentially be imputed for empty cells based on values predicted for neighboring cells, however this may not be appropriate in all cases. For example, some forest areas will have reached old age for which height and AGB increment are limited to such an extent that the increment is not captured by bitemporal ALS data with a time interval of, say, 11–13 years. Such areas will consequently be classified as "unsuitable" and omitted from the map, and for those cases, imputed values of SI based on neighboring areas may cause a systematic shift towards greater values of SI.

For the classification of tree species, we used stand-level data on dominant tree species as interpreted from aerial imagery and supported by field visits. In the case of another species being dominant within a given cell, the wrong model will resultantly have been applied, potentially resulting in under- or over-prediction of SI. When determining SI by means of photo-interpretation or conventional field assessments, the same problem is likely to arise because pure monocultures are rare in most forest landscapes, at least in Norway. Alternatively, in addition to the classification of forest disturbance, dominant tree species may be classified for individual grid cells using remotely sensed data (Dalponte et al., 2012; Heinzel and Koch, 2011), which may prove highly beneficial if combined with the approach demonstrated in this paper.

5. Conclusions

The main conclusions of this study were:

1. Changes in ALS data over time were useful for identifying undisturbed forest.
2. Ground reference values of SI were strongly correlated with bitemporal ALS height metrics.
3. SI can be predicted at plot-level with accuracies that are within the range of accuracies obtained for other forest attributes that are commonly predicted from ALS data.
4. The method proposed here can be implemented in repeated ALS-based forest inventories to map SI automatically over large areas at a much finer spatial resolution than what is common in operational inventories.

CRediT authorship contribution statement

Lennart Noordermeer: Conceptualization, Methodology, Software, Validation, Formal analysis, Data curation, Writing - original draft, Writing - review & editing, Visualization. **Terje Gobakken:** Conceptualization, Methodology, Software, Writing - review & editing, Supervision, Project administration, Funding acquisition. **Erik Næsset:** Conceptualization, Methodology, Writing - review & editing, Supervision, Project administration, Funding acquisition. **Ole Martin Bollandsås:** Conceptualization, Methodology, Writing - review & editing, Supervision, Project administration.

Declaration of Competing Interest

The authors declare that they have no known competing financial interests or personal relationships that could have appeared to influence the work reported in this paper.

Acknowledgements

References

Anon. (1987). Handbok for planlegging i skogbruket. In. Landbruksforlaget Oslo, Norway.

Bollandsås, O.M., Ørka, H.O., Dalponte, M., Gobakken, T., Næsset, E., 2019. Modelling Site Index in Forest Stands Using Airborne Hyperspectral Imagery and Bi-Temporal Laser Scanner Data. Remote Sens. 11 (9), 1020.

Bontemps, J.-D., Bouriaud, O., 2013. Predictive approaches to forest site productivity: recent trends, challenges and future perspectives. Forestry 87 (1), 109–128.

Braastad, H., 1966. Volume tables for birch. Meddelelser fra det Norske Skogforsøksvesen 21, 23–78.

Brantseg, A., 1967. Volume functions and tables for Scots pine South Norway. Meddelelser fra det Norske Skogforsoksvesen 22, 695.

Breidenbach, J., Næsset, E., Gobakken, T., 2012. Improving k-nearest neighbor predictions in forest inventories by combining high and low density airborne laser scanning data. Remote Sens. Environ. 117, 358–365.

Carmean, W.H., Hazenberg, G., Deschamps, K., 2006. Polymorphic site index curves for black spruce and trembling aspen in northwest Ontario. For. Chronicle 82 (2), 231–242.

Chen, Y., Zhu, X., 2012. Site quality assessment of a Pinus radiata plantation in Victoria, Australia, using LiDAR technology. Southern For.: J. For. Sci. 74 (4), 217–227.

Clark, D.B., 1990. The role of disturbance in the regeneration of neotropical moist forests. Reprod. Ecol. Trop. For. Plants 7, 291–315.

Dalponte, M., Bruzzone, L., Gianelle, D., 2012. Tree species classification in the Southern Alps based on the fusion of very high geometrical resolution multispectral/hyperspectral images and LiDAR data. Remote Sens. Environ. 123, 258–270.

Eid, T., 2000. Use of uncertain inventory data in forestry scenario models and consequential incorrect harvest decisions. Silva Fennica 34 (2), 89–100.

Eid, T., Nersten, S., 1996. Problemer omkring registreringer og planlegging for en skogeiendom i Birkenes kommune. Del 1 Sammenligning av skogbruksplandata og kontrolldata. Del 2 Sammenligning av takster utfoert med 19 aars mellomrom.

Eid, T., Gobakken, T., Næsset, E., 2004. Comparing stand inventories for large areas based on photo-interpretation and laser scanning by means of cost-plus-loss analyses. Scand. J. For. Res. 19 (6), 512–523.

Eid, T. (1992). Bestandsvis kontroll av skogbruksplandata i hogstklasse III-V.

Eid, T., 1996. Kontroll av skogbruksplandata fra «Understøttet fototakst». Norsk Institutt for Skogforskning, og Institutt for Skogfag, Norges Landbrukshøgskole, Ås, Norway, Report, 8, 21.

Fitje, A., Vestjordet, E., 1977. Stand height curves and new tariff tables for Norway spruce. Medd. Nor. inst. skogforsk. 34 (2), 23–68.

Gaveau, D.L., Hill, R.A., 2003. Quantifying canopy height underestimation by laser pulse penetration in small-footprint airborne laser scanning data. Can. J. Remote Sens. 29 (5), 650–657.

Gobakken, T., Næsset, E., 2008. Assessing effects of laser point density, ground sampling intensity, and field sample plot size on biophysical stand properties derived from airborne laser scanner data. Can. J. For. Res. 38 (5), 1095–1109.

Hägglund, & Lundmark, 1981. Handledning i bonitering. National Board of Forestry.

Heinzel, J., Koch, B., 2011. Exploring full-waveform LiDAR parameters for tree species classification. Int. J. Appl. Earth Obs. Geoinf. 13 (1), 152–160.

Hollaus, M., Eysn, L., Maier, B., Pfeifer, N., 2015. Site index assessment based on multi-temporal ALS data. SilviLaser 2015, 159–161.

Holopainen, M., Haapanen, R., Karjalainen, M., Vastaranta, M., Hyyppä, J., Yu, X., Hyyppä, H., 2010a. Comparing accuracy of airborne laser scanning and TerraSAR-X radar images in the estimation of plot-level forest variables. Remote Sens. 2 (2), 432–445.

Holopainen, M., Vastaranta, M., Haapanen, R., Yu, X., Hyyppä, J., Kaartinen, H., Hyyppä, H., 2010b. Site-type estimation using airborne laser scanning and stand register data. Photogrammetric J. Finland 22 (1), 16–32.

Huang, S., Titus, S.J., 1993. An index of site productivity for uneven-aged or mixed-species stands. Can. J. Remote Sens. 23 (3), 558–562.

Hyyppä, J., 1999. Detecting and estimating attributes for single trees using laser scanner. J. Photogramm. J. Finland 16, 27–42.

Hyyppä, J., Yu, X., Hyyppä, H., Vastaranta, M., Holopainen, M., Kukko, A., Koskinen, J., 2012. Advances in forest inventory using airborne laser scanning. Remote Sens. 4 (5), 1190–1207.

Kotivuori, E., Korhonen, L., Packalen, P., 2016. Nationwide airborne laser scanning based models for volume, biomass and dominant height in Finland. Silva Fennica 50 (4).

Kvaalen, H., Solberg, S., May, J., 2015. Aldersuavhengig bonitering med laserskanning av enkelttrær.

Landis, J.R., Koch, G.G., 1977. The measurement of observer agreement for categorical data. Biometrics 159–174.

Latypov, D., 2002. Estimating relative lidar accuracy information from overlapping flight lines. ISPRS J. Photogramm. Remote Sens. 56 (4), 236–245.

Lim, K., Treitz, P., Baldwin, K., Morrison, I., Green, J., 2003. Lidar remote sensing of biophysical properties of tolerant northern hardwood forests. Can. J. Remote Sens. 29 (5), 658–678.

Magnussen, S., Boudewyn, P., 1998. Derivations of stand heights from airborne laser scanner data with canopy-based quantile estimators. Can. J. For. Res. 28 (7), 1016–1031.

Maltamo, M., Næsset, E.,Vauhkonen, J., 2014. Forestry applications of airborne laser scanning. Concepts and case studies. Managing For Ecosystems, 27, 2014.

Marklund, L.G., 1988. Biomass functions for pine, spruce and birch in Sweden. Rapport-Sveriges Lantbruksuniversitet, Institutionen foer Skogstaxering (Sweden).

McRoberts, R.E., Cohen, W.B., Næsset, E., Stehman, S.V., Tomppo, E.O., 2010. Using remotely sensed data to construct and assess forest attribute maps and related spatial products. Scand. J. For. Res. 25 (4), 340–367.

McRoberts, R.E., Næsset, E., Gobakken, T., 2015. Optimizing the k-Nearest Neighbors technique for estimating forest aboveground biomass using airborne laser scanning data. Remote Sens. Environ. 163, 13–22.

Monserud, R.A., 1984. Height growth and site index curves for inland Douglas-fir based on stem analysis data and forest habitat type. Forest Science 30 (4), 943–965.

Monserud, R.A., 1988. Variations on a Theme of Site Index. USDA Forest Service General Technical Report NC-North. Central Forest Experiment Station.

Naesset, E., 1997. Estimating timber volume of forest stands using airborne laser scanner data. Remote Sens. Environ. 61 (2), 246–253.

Næsset, E., 1997. Determination of mean tree height of forest stands using airborne laser scanner data. ISPRS J. Photogramm. Remote Sens. 52 (2), 49–56.

Næsset, E., 2002Ea. Determination of mean tree height of forest stands by digital photogrammetry. Scand. J. For. Res. 17 (5), 446–459.

Næsset, E., 2002Eb. Predicting forest stand characteristics with airborne scanning laser using a practical two-stage procedure and field data. Remote Sens. Environ. 80 (1), 88–99.

Næsset, E., 2004Ea. Accuracy of forest inventory using airborne laser scanning: evaluating the first Nordic full-scale operational project. Scand. J. For. Res. 19 (6), 554–557.

Næsset, E., 2004Eb. Practical large-scale forest stand inventory using a small-footprint airborne scanning laser. Scand. J. For. Res. 19 (2), 164–179.

Næsset, E., 2009. Effects of different sensors, flying altitudes, and pulse repetition frequencies on forest canopy metrics and biophysical stand properties derived from small-footprint airborne laser data. Remote Sens. Environ. 113 (1), 148–159.

Næsset, E., 2014. Area-based inventory in Norway–from Innovation to an Operational Reality. Forestry Applications of Airborne Laser Scanning Springer, pp. 215–240.

Noordermeer, L., Bollandsås, O.M., Gobakken, T., Næsset, E., 2018. Direct and indirect site index determination for Norway spruce and Scots pine using bitemporal airborne laser scanner data. For. Ecol. Manage. 428, 104–114.

Noordermeer, L., Bollandsås, O.M., Ørka, H.O., Næsset, E., Gobakken, T., 2019a. Comparing the accuracies of forest attributes predicted from airborne laser scanning and digital aerial photogrammetry in operational forest inventories. Remote Sens. Environ. 226, 26–37.

Noordermeer, L., Økseter, R., Ørka, H.O., Gobakken, T., Næsset, E., Bollandsås, O.M., 2019b. Classifications of forest change by using bitemporal airborne laser scanner data. Remote Sens. 11 (18), 2145.

Packalén, P., Mehtätalo, L., Maltamo, M., 2011. ALS-based estimation of plot volume and site index in a eucalyptus plantation with a nonlinear mixed-effect model that accounts for the clone effect. Ann. For. Sci. 68 (6), 1085.

Persson, H.J., Fransson, J.E., 2016. Estimating site index from short-term TanDEM-X canopy height models. IEEE J. Sel. Top. Appl. Earth Obs. Remote Sens. 9 (8), 3598–3606.

Popescu, S.C., Wynne, R.H., Nelson, R.F., 2003. Measuring individual tree crown diameter with lidar and assessing its influence on estimating forest volume and biomass. Can. J. Remote Sens. 29 (5), 564–577.

Pretzsch, H., Grote, R., Reineking, B., Rötzer, T., Seifert, S., 2007. Models for forest ecosystem management: a European perspective. Ann. Bot. 101 (8), 1065–1087.

Ralston, C.W., 1964. Evaluation of forest site productivity. Int. Rev. For. Res. 1, 171–200.

Rennolls, K., 1978. "Top Height"; Its definition and estimation. Commonwealth For. Rev. 215–219.

Rönnholm, P., Hyyppä, J., Hyyppä, H., Haggrén, H., Yu, X., Kaartinen, H., 2004. Calibration of laser-derived tree height estimates by means of photogrammetric techniques. Scand. J. For. Res. 19 (6), 524–528.

Schliep, K., Hechenbichler, K., 2014. kknn: weighted k-nearest neighbors. R package. version 1.2-5. In.

Sharma, R.P., Brunner, A., Eid, T., Øyen, B.-H., 2011. Modelling dominant height growth from national forest inventory individual tree data with short time series and large age errors. For. Ecol. Manage. 262 (12), 2162–2175.

Skovsgaard, J.P., Vanclay, J.K., 2008. Forest site productivity: a review of the evolution of dendrometric concepts for even-aged stands. For.: Int. J. For. Res. 81 (1), 13–31.

Socha, J., Pierzchalski, M., Bałazy, R., Ciesielski, M., 2017. Modelling top height growth and site index using repeated laser scanning data. For. Ecol. Manage. 406, 307–317.

Solberg, S., Kvaalen, H., Puliti, S., 2019. Age-independent site index mapping with repeated single-tree airborne laser scanning. Scand. J. For. Res. (just-accepted) 1–31.

Stearns-Smith, S., 2002. Making sense of site index estimates in British Columbia: a quick look at the big picture. J. Ecosyst. Manage. 1 (2).

Tompalski, P., Coops, N.C., White, J.C., Wulder, M.A., Pickell, P.D., 2015. Estimating forest site productivity using airborne laser scanning data and Landsat time series. Can. J. Remote Sens. 41 (3), 232–245.

Tveite, B., 1977. Bonitetskurver for gran: Site-index curves for Norway spruce (Picea abies (L.) Karst). In: Norsk Inst. for Skogforskning.

Véga, C., St-Onge, B., 2009. Management mapping site index and age by linking a time series of canopy height models with growth curves. For. Ecol. Manage. 257 (3), 951–959.

Vestjord, 1967. Functions and tables for volume of standing trees. Norway spruce. Meddelelser fra det Norske Skogforsøksvesen, 22, 545-&.

Vestjordet, E., 1968. Merchantable volume of Norway spruce and Scots pine based on relative height and diameter at breast height or 2.5 m above stump level. Meddelelser fra det Norske Skogforsøksvesen 25, 411–459.

Wulder, M.A., Bater, C.W., Coops, N.C., Hilker, T., White, J.C., 2008. The role of LiDAR in sustainable forest management. For. Chronicle 84 (6), 807–826.

Yu, X., Hyyppä, J., Holopainen, M., Vastaranta, M.J.R.S., 2010. Comparison of area-based and individual tree-based methods for predicting plot-level forest attributes. Remote Sens. 2 (6), 1481–1495.

Yu, X., Hyyppä, J., Kukko, A., Maltamo, M., Kaartinen, H., 2006. Change detection techniques for canopy height growth measurements using airborne laser scanner data. Photogramm. Eng. Remote Sens. 72 (12), 1339–1348.

Paper IV

Economic utility of 3D remote sensing data for estimation of site index in forest management inventories: A comparison of airborne laser scanning, digital aerial photogrammetry and conventional practices

Lennart Noordermeer*, Terje Gobakken, Erik Næsset and Ole Martin Bollandsås

Faculty of Environmental Sciences and Natural Resource Management, Norwegian University of Life Sciences, NMBU, P.O. Box 5003, NO-1432 Ås, Norway

Abstract

One of the most crucial variables in forest planning is forest productivity, usually expressed as site index (SI). In forest management inventories, SI is commonly estimated with substantial error by a combination of aerial image interpretation, field assessment and information from previous inventories. Airborne laser scanning (ALS) and digital aerial photogrammetry (DAP) data can alternatively be used for SI estimation, however the economic utility of the inventory methods have not been compared. We compared seven methods of SI estimation in a cost-plus-loss analysis, by which we added the expected economic losses due to sub-optimal treatment decisions to the inventory costs. The methods were: direct estimation using models dependent on (i) bitemporal ALS data and (ii) ALS and subsequent DAP data, indirect estimation from canopy height trajectories estimated from (iii) bitemporal ALS data and (iv) ALS and subsequent DAP data, direct estimation using the age from the stand register and single-date canopy height estimated from (v) ALS and (vi) DAP, and manual interpretation from (vii) aerial imagery supported by field assessment and information from previous inventories. Methods i and ii gave the most reliable SI estimates and the lowest total inventory costs and are therefore recommended from an economic perspective.

*Corresponding author.
E-mail: lennart.noordermeer@nmbu.no

1. Introduction

Forest inventories aim at providing accurate information on forest resources and play a crucial role in forest planning (Bettinger et al., 2016). The choice of inventory design and intensity, however, and thus the level of investment in forest inventory data, poses a fundamental dilemma for forest planners. On the one hand, increased investment will likely increase the value of inventory data as a basis for decision-making. On the other hand, the costs of collecting additional data should not exceed the benefits. A trade-off therefore emerges between the cost of data collection and the value of the collected data in monetary terms (Kangas, 2010).

Cost-plus-loss analyses provide a means to compare the utility of different inventory methods in long-term forest planning (Burkhart et al., 1978; Hamilton, 1978). In cost-plus-loss analyses, the expected losses from sub-optimal decisions caused by erroneous inventory data are considered in addition to the inventory cost. Such losses can be quantified as losses in net present value (NPV) by using forest scenario models, i.e., decision support systems that simulate forest development over time based on given input variables, assumptions and constraints. Forest scenario models have proven highly beneficial for economic optimization of forest planning, because silvicultural treatment schedules can be generated using known errors calculated for given inventory methods, which can be compared to a reference treatment schedule generated without error. The resulting losses in NPV due to sub-optimal treatment decisions can then be quantified, and the preferred inventory method can be identified as the one that minimizes the total inventory cost (Holmström et al., 2003; Mäkinen et al., 2012).

In a study assessing the use of uncertain inventory data in a cost-plus-loss analysis, Eid (2000) found that errors in forest productivity had great impact on the NPV of forest stands. Forest productivity is most commonly represented by site index (SI), expressed as the expected dominant height (Hdom) at a given index age for a given species. In Norway, an index age of 40 years is used, and SI is estimated from empirical Hdom development curves using Hdom and age as input variables. Errors in SI may lead to sub-optimal decisions regarding the timing of final harvest and regeneration method, and potentially to financial losses for the forest owner.

SI of a stand can be determined from the observed age and height of a site tree that is representative of the stand in question. However, in Norwegian commercial forest management inventories, SI is commonly estimated at stand-level by means of manual interpretation of aerial images. Interpreters assess the growing conditions by considering the vegetation

structure, species composition and topography, and the assessment is often supported by relatively few and scattered field assessments and estimates from previous inventories. SI is challenging to determine without field work, and even in the field, age determination by tree coring is prone to errors (Niklasson, 2002; Villalba & Veblen, 1997) and some additional error should be expected for tree height measurements (Vasilescu, 2013). Furthermore, the selection of site trees can be challenging in uneven-aged stands and when retention trees are present (Kvaalen et al., 2015). Nevertheless, such conventional methods for SI estimation are common in Norwegian forest management inventories covering areas in the range of 50-1000 km^2. Apart from being time- and resource-consuming and therefore expensive, these methods are known to lead to large uncertainty (Gisnås, 1982; Næsset, 1994) and, potentially, sub-optimal treatment decisions (Eid, 2000; Eid & Moum, 1999) and thus increased total inventory costs.

Remotely sensed data are playing an increasingly important role in forest inventory (White et al., 2016). Airborne laser scanning (ALS) has found widespread application in forest inventories, because it provides accurate and continuous three-dimensional (3D) point cloud data on forest canopy structure over large forest areas (Maltamo et al., 2014). More recently, digital aerial photogrammetry (DAP) has emerged as an alternative for 3D point data extraction, as 3D data can be generated by stereo-matching of overlapping aerial images at considerably smaller costs (White et al., 2013). Although the accuracy of ALS-assisted estimates of forest attributes has been found to be better compared to those of DAP (Vastaranta et al., 2013), the economic utility of DAP data as a basis for decision making can be considered similar due to the cost advantages of DAP (Kangas et al., 2018). However, the use of DAP for forest inventory application requires a digital terrain model from a previous ALS acquisition for normalization of the DAP point cloud (Nurminen et al., 2013). DAP data are therefore particularly useful as a low-cost means to update existing ALS-assisted management inventories (Ali-Sisto & Packalen, 2016; Goodbody et al., 2019), for example by taking advantage of aerial imagery acquired for the purpose of orthophoto generation.

An increasing availability of multi-temporal 3D point cloud data has triggered great interest in the data's applications in forest inventory, including the estimation of SI. Previous studies have shown that SI can reliably be estimated from multi-temporal 3D data, either directly by using predictive models dependent on bitemporal canopy height metrics (Bollandsås et al., 2019; Noordermeer et al., 2018) or indirectly from estimated Hdom growth trajectories over time (Hollaus et al., 2015; Persson et al., 2016; Solberg et al., 2019; Véga & St-Onge, 2009). As an alternative, Holopainen et al. (2010) and Packalén et al. (2011) used canopy height estimates

derived from single-date ALS data and age obtained from a stand register to estimate forest productivity. Although the mentioned studies showed promising results in terms of accuracy, no research effort has been made to compare the economic value of different ALS- and DAP-based methods with conventional practices. In this study, we link errors in SI estimates obtained using seven inventory methods to consequential sub-optimal treatment decisions. By doing so, we quantify the total cost of each method by adding the potential economic losses due to the use of erroneous inventory data to the inventory costs.

Our objective was to compare the value of seven inventory methods for stand-level SI estimation in long-term forest planning. The methods were: direct estimation using models dependent on (i) bitemporal ALS data and (ii) ALS and subsequent DAP data, indirect estimation from canopy height trajectories estimated from (iii) bitemporal ALS data and (iv) ALS and subsequent DAP data, direct estimation using the age from the stand register and single-date canopy height estimated from (v) ALS and (vi) DAP, and manual interpretation from (vii) aerial imagery supported by field assessment and information from previous inventories.

2. Materials and Methods

2.1 Inventory area

We used data collected as part of a repeated commercial forest management inventory implemented in the municipality of Krødsherad in Norway. The area comprises approximately 50 km^2 of boreal forest, characterized by Norway spruce (*Picea abies* (L.) Karst.) growing mainly on high productivity sites, and Scots pine (*Pinus sylvestris* L.) on low productivity sites and sporadic stands of birch (*Betula pendula* Roth and *B. pubescens* Ehrh). The forest area is primarily managed for timber production. However, it provides a range of ecosystem functions including biodiversity maintenance, water regulation and recreation.

Fig. 1 Map showing the location of the study area in Krødsherad municipality.

During the initial inventory in 2001 (time T1), each stand was surveyed by a combination of field work and photo-interpretation to determine the dominant tree species, SI, and forest development class. Estimates of other forest attributes such as Hdom, basal area and stem number were obtained from ALS data. In 2001, the use of ALS data for forest management inventory was still in its experimental phase, and the Krødsherad inventory is considered a proof-of-concept study (Næsset, 2004, 2014). The inventory was repeated in 2016 (time T2) by which new aerial imagery, ground reference data and ALS data were acquired.

2.2 First field campaign

At T1, 116 circular sample plots of 233 m^2 were distributed systematically throughout the inventory area by means of a stratified systematic sampling design, for details see Næsset (2004). The stratification was based on three variables determined spatially continuously across the landscape (population) at stand-level: dominant tree species, SI and development class. All living trees with diameter at breast height (DBH) >10 cm were callipered within sample plots and tree species were recorded. Approximately 10 sample trees were selected using a relascope and their heights were measured using a Vertex™ hypsometer.

In addition to the sample plots, 57 validation plots were distributed over subjectively selected stands, with the aim of covering a wide variation in forest conditions with regard to dominant tree species, SI and development stage. Validation plots were designed to form squares of 61 × 61 m (Fig. 2) with areas of 3721 m^2, however after establishment in the field, the polygons deviated from this design both in shape and size due to challenging terrain (area range: 3377-4085 m^2). All living trees with DBH >10 cm were callipered, tree species were recorded, and approximately 20 sample trees were selected for height measurement.

Coordinates of sample plot centers and validation plot corners were estimated using a dual-frequency Javad receiver, observing pseudorange and carrier phase of both GPS and GLONASS satellites. Positioning data were collected over a period of 15-30 minutes for each sample plot center and 20-80 minutes for the validation plot corners. After data collection, all positions were marked with wooden sticks. All coordinates were corrected against reference data obtained with a Javad Legacy which served as a base station.
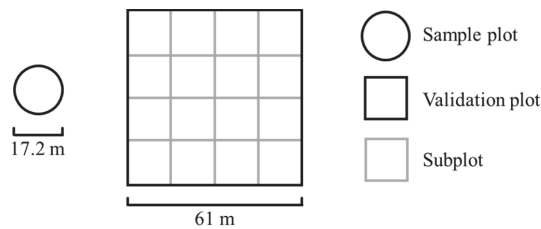

Fig. 2. Plot design.

2.3 Second field campaign

All plots were revisited during the summers of 2016 and 2017, whereby a Sony Xperia Z3 mobile phone GPS was first used to navigate to the plot locations. A total of 77 wooden sticks were found indicating the exact locations, and for the remaining locations, a Topcon Hiper SR was used in real-time kinematic mode to navigate to the planimetric coordinates estimated at T1. On those sample plots that had not been subject to final harvest, field measurements were performed using the same procedures as during the first field campaign. Additionally, two site trees were selected within each sample plot for which the height was measured and the age at breast height determined by coring. The site trees were the largest trees according to DBH of the dominant species within the plot, however retention trees were not selected.

The validation plots were re-measured using the same field procedures as during the first field campaign, however instead of registering the data to the entire validation plot, the plot was divided into 16 subplots of approximately 233 m^2 (Fig. 2) using cords with even spacing along the plot borders. The tree measurements were then performed separately for each subplot. In addition, age and height measurements were collected from one site tree within each subplot, selected using the criteria as described above. At T2, coordinates of sample plot centers and validation plot corners were estimated using a Topcon Legacy E+. After completing the field work, the obtained coordinates were corrected using reference data from the Norwegian Mapping Authority's base stations ensuring sub-meter positional accuracy.

2.4 Field data computation

The dominant species (according to basal area) was determined for each plot because Norwegian SI models are specific to either Norway spruce or Scots pine. We predicted the SI of site trees using empirical models (Sharma et al., 2011) with age and height as predictors, and computed SI for sample plots as the mean SI predicted for individual site trees. Because tree heights had only been measured for sample trees, we predicted the "base volume" of each callipered tree from the measured DBH and the height predicted with DBH-height models (Fitje & Vestjordet, 1977; Vestjordet, 1968) . We then predicted the "true volume" of sample trees using both measured DBH and height, and estimated the volume of each tree based on the ratio between "true" and "base" volumes. Finally, we obtained heights of all trees by inverting single-tree volume functions (Braastad, 1966; Brantseg, 1967; Vestjordet, 1967) to predict height instead of volume. We computed Hdom at the first and second points in time (Hdom$_{T1}$, Hdom$_{T2}$, respectively) as the mean height of those trees that corresponded to the 100 largest trees per hectare according to DBH. Further, we corrected the obtained Hdom estimates to match the date of ALS- and aerial image acquisition using a sigmoid growth model following Sharma et al. (2011). We computed the number of stems and basal area scaled to per-hectare units. Boxplots showing the distribution of the obtained ground reference values are displayed in Fig. 3.
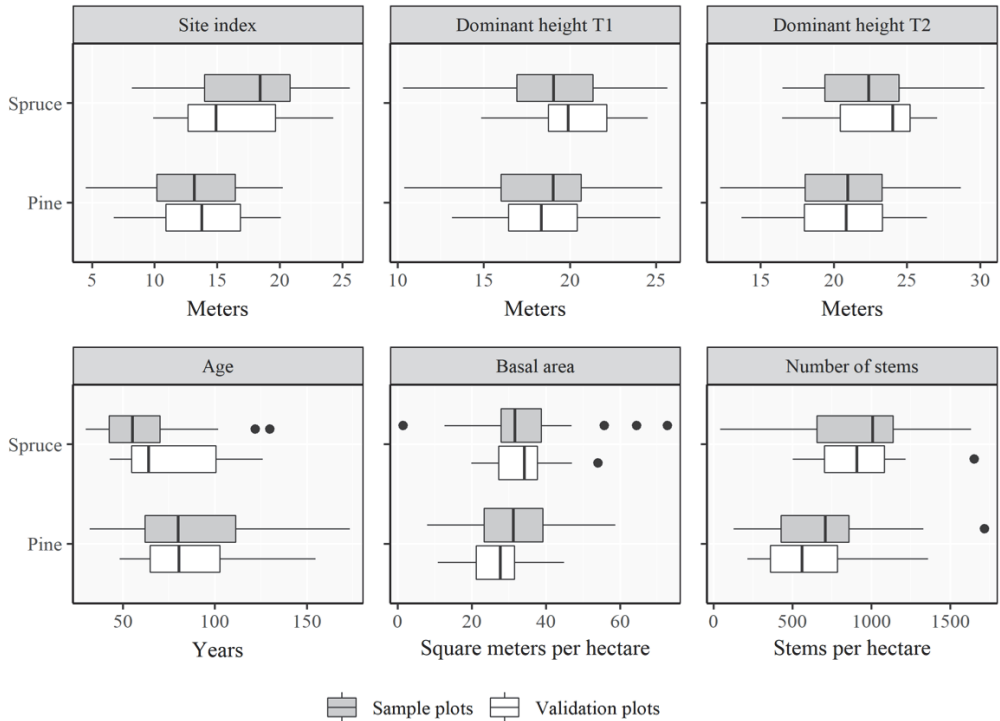
Fig. 3. Boxplots showing the distribution of ground reference values. We computed all forest attributes for the second point in time (T2) and additionally we computed dominant height for the first point in time (T1).

2.5 Airborne laser scanner data

ALS data were acquired at T1 with an Optech ALTM 1210 laser scanner, capable of recording both first and last echoes. The average flying altitude was 650 m above ground level and the average speed of flight was 75 m s^{-1}, the pulse repetition frequency was 10 kHz, and the average echo density was 0.9 m^{-2}. At T2, ALS data were acquired using a Riegl LMS Q-1560 laser scanner capable of recording up to seven echoes per pulse. The average flying altitude was 1280 m, the average flying speed was 69 m s^{-1}, the pulse repetition was 534 kHz and the average echo density was 11.8 m^{-2}. Both ALS surveys were carried out under leaf-on conditions.

2.6 Aerial photogrammetry

Black-and white panchromatic aerial images were acquired at T1 using a Wild RC30 aerial camera system, equipped with a 15/4 UAG-S lens with a focal length of 153.3 mm. Five lines were flown over the inventory area at an average altitude of about 3100 m, and 5-13 images were taken for each flight line. A Wild B8 stereo plotter was used for manual stereoscopic delineation of stand boundaries and interpretation of dominant tree species, SI and age for each

stand. The photogrammetric work was performed by trained interpreters who first spent two days in the inventory area for the purpose of calibrating their assessment with the local forest conditions.

At T2, red, green and blue (RGB) digital aerial images were acquired for the purpose of orthophoto generation for an area much larger than the inventory area, with a total of 75 flight lines and 8500 images. A Vexcel UltraCam Eagle camera and a Linos Vexcel HR Digaron lens with a focal length of 100.5 mm were used, the average flight altitude was 5300 m and the images had around 20% side- and 80% forward overlap. Trained photo interpreters updated the existing inventory maps in terms of stand boundaries, tree species, development class and SI. Furthermore, we generated 3D point clouds by stereo-matching the aerial images in SURE Aerial (nFrames, 2014; Rothermel et al., 2012) using default settings, for details see Noordermeer et al. (2019a). The obtained DAP point cloud had an average density of 37 points per m^2.

2.7 Point cloud processing

Both ALS point clouds were processed by the vendors, who classified points as ground or vegetation, and generated digital terrain models as triangular irregular networks from the points classified as ground. The ALS point clouds were normalized by subtracting the terrain height from all vegetation points to compute their heights relative to the ground. Because DAP data only characterize the height of objects that are visible on the imagery, typically the structure of the upper part of the canopy (White et al., 2013), we used the terrain model obtained from the ALS data from T2 to normalize the DAP point cloud.

From the two ALS point clouds and the DAP point cloud, we computed point cloud metrics for each sample plot and subplot of the validation plots characterizing the vertical distribution of points, using the lasR package (Ørka, 2012) in R. We only considered points with a height above the ground >2m, and for the ALS datasets, we only used first and single echoes for computing the point cloud metrics because we considered those to most accurately reflect Hdom and Hdom increment. The point cloud metrics comprised the height at the 90th percentile at the two points in time (T1H90, T2H90, respectively) and the mean point height (T1Hmean, T2Hmean, respectively). The ALS and DAP point cloud metrics were designated ".ALS" and ".DAP", respectively. Differential point cloud metrics were computed as the differences between metrics computed for T2 and the corresponding metrics computed for T1 and were designated "Δ" (ΔH90, ΔHmean).

2.8 Site index estimation

We distinguished between seven methods of SI estimation. For the first two methods, we predicted SI for subplots by the area-based approach (Næsset, 2002), using (i) bitemporal ALS data and (ii) ALS data and subsequent DAP data as described in the following. First, we regressed SI against bitemporal point cloud metrics. For each regression model, we selected a maximum of two point cloud metrics which minimized the residual standard error. We computed the variance inflation factor (VIF) for each predictor, and omitted candidate models for which the computed VIF exceeded 5 which is a common cut-off in multiple linear regression when avoiding multicollinearity (Sheather, 2009). We then applied the regression models for predicting SI for validation subplots.

For methods iii and iv, we applied the indirect method as proposed by Noordermeer et al. (2018) and derived the SI from Hdom trajectories estimated from (iii) bitemporal ALS data and (iv) ALS data and subsequent DAP data. We regressed Hdom at both points in time separately against metrics from the respective point clouds, using the regression procedures as explained above. For each validation plot, we then calculated the age needed to reach $Hdom_{T1}$ for all discrete values of SI ranging from 5 to 30, using empirical SI models (Sharma et al., 2011) which relate age, Hdom and SI. We then projected the height to T2 using the same empirical models, given each value of SI and the calculated age added to the length of the observation period. We then obtained the SI by interpolating between the two SI curves which corresponded most closely to the actual $Hdom_{T2}$.

For methods v and vi, we used the estimated $Hdom_{T2}$ and the age obtained from the stand register as input variables in the empirical SI models. For method vii, representing conventional practices, we obtained the SI for each validation plot from the stand register. Because SI should reflect the growth potential of a given site, the growth of dominant trees should not have sustained any major disruptions when determining SI (Stearns-Smith, 2002). Data were only available for the two points in time without any intermediate information on the height development of dominant trees, so we omitted those sample plots for which ground reference values of Hdom had decreased since the initial inventory. In the validation dataset, we correspondingly omitted subplots for which predicted values of Hdom had decreased. Finally, we estimated the SI and $Hdom_{T2}$ at validation plot-level as the mean of SI and $Hdom_{T2}$ predictions made for the remaining subplots.

We assessed the accuracy of the SI estimates made for validation plots by computing the root mean squared error (RMSE) and the mean differences (MD) between ground reference and ALS and DAP-assisted estimates. Furthermore, we computed the RMSE and MD relative to the ground reference mean values (RMSE%, MD%).

2.9 Inventory costs

The cost components of the inventory methods are given in Table 1. The cost estimates of photo interpretation and field plot data were provided by the forest owner's cooperative that implemented the inventory, and apply specifically to the inventory on which this study is based. The costs of aerial imagery, ALS and DAP data were provided by the vendor, and reflect the data costs when collected for areas of a size similar to the current inventory.

For all inventory methods considered in this study, aerial imagery is needed for stand delineation. The methods also share the same photo-interpretation procedures, the only difference being that all methods except conventional practices do not require the interpretation of SI, which will typically consume about a quarter of the time dedicated to photo-interpretation according to the forest owner's cooperative. Field data are required for all inventory alternatives, however we distinguished between the additional cost of obtaining ground reference data on SI. The cost estimate for ALS data acquisition included all the necessary data processing, and the cost of DAP data processing included image processing and point cloud generation. We assumed all data from T1 to be free of cost. It should be noted that ALS data acquisition costs for forest inventory have varied substantially in recent years due to various regionally and nationally coordinated acquisition campaigns with shared costs among stakeholders. From 2016 ALS data have been provided free of charge for forest inventory purposes due to a national campaign funded by the government to provide a new, detailed digital terrain model for the country. The ALS costs applied in this study represent an upper bound for such costs.

Table 1. Inventory costs.

Inventory method	Aerial imagery[a], 0.20 € ha-1	Photo interpretation[b], 3.00 € ha-1	Photo interpretation- site index, 1.00 € ha-1	Field plot inventory, 1.20 € ha-1	Ground reference site index, 0.06 € ha-1	ALS data[c], 1.00 € ha-1	DAP data processing[d], 0.10 € ha-1	Total cost (€ ha-1)
Direct method, bitemporal ALS	●	●		●	●	●		5.46
Direct method, ALS and subsequent DAP	●	●		●	●		●	4.56
Indirect method, bitemporal ALS	●	●		●		●		5.40
Indirect method, ALS and subsequent DAP	●	●		●			●	4.50
Single-date ALS	●	●		●		●		5.40
Single-date DAP	●	●		●			●	4.50
Conventional practices	●	●	●	●	●			5.46

[a] acquisition and orthophoto generation. [b] stand delineation and classification. [c] acquisition and processing, [d] image matching and point cloud generation.

2.10 Cost-plus-loss comparison

We used the forest scenario model GAYA (Hoen & Eid, 1990; Hoen & Gobakken, 1997) to quantify the expected losses due to sub-optimal treatment scheduling. GAYA projects forest attributes over a specified planning horizon and optimizes treatment schedules given a set of input variables describing the initial state of the forest (SI, age, Hdom, basal area, stem number), and assumptions regarding silvicultural practices (planting, natural regeneration, final harvest). The economically optimal timing of final harvest is solved following Faustmann (1849). DBH increment is projected using models constructed by Blingsmo (1984), Hdom increment is projected using Hdom development curves (Eriksson et al., 1997; Sharma et al., 2011) and mortality is projected using models constructed by Braastad (1982). Harvest revenues are estimated from gross price models (Blingsmo & Veidahl, 1992) and harvesting costs from a tariff agreed upon by Norwegian employers' and employees' organizations. The

output comprises a treatment schedule for each validation plot, i.e., the sequence of silvicultural treatments which optimizes the economic value of the forest over the specified planning horizon, and the corresponding cash flow in NPV.

Using an annual real discount rate of 3%, we generated treatment schedules for 20 periods of five years, i.e. a planning horizon of 100 years. For each period, we allowed two silvicultural treatments, namely clear cutting followed by planting on spruce-dominated plots, and clear cutting followed by natural regeneration on both spruce- and pine-dominated plots. We assumed treatments to be applied in the middle of the period. In cases where natural regeneration occurred, we assumed regeneration lags to vary from 5 years for high productivity sites (SI>26) to 20 years for low productivity sites (SI<6). We generated optimal treatment schedules for the validation plots using ground reference values of SI which we assumed to be free of error, and calculated the corresponding NPVs. Then, we generated sub-optimal treatment schedules using erroneous SI estimates obtained by each of the seven inventory methods, and calculated the corresponding NPVs. We calculated the losses as the difference between the NPVs of the optimal treatment schedules and the NPVs of the sub-optimal treatment schedules. Finally, we estimated the resulting mean NPV losses for each inventory method as:

$$\overline{\text{NPV}}_{\text{loss}} = \frac{1}{n} \sum_{i=1}^{n} (\text{NPV}_{\text{ref } i} - \text{NPV}_{\text{error } i})$$

Where $\text{NPV}_{\text{ref } i}$ is the calculated NPV (€ ha^{-1}) of using the reference SI of validation plot i and $\text{NPV}_{\text{error } i}$ is the calculated NPV for validation plot i when sub-optimal treatment schedules are used. Finally, we calculated the total costs of each inventory method by adding the mean NPV losses to the inventory cost:

$$\text{Total cost} = \text{inventory cost} + \overline{\text{NPV}}_{\text{loss}}$$

3. Results

3.1 Modelling and accuracy assessment

The selected ALS and DAP metrics and fit statistics (R^2) of the regression models are shown in Table 2. In general, models for predicting Hdom in pine-dominated forests displayed a better fit than those for spruce-dominated forest. For all Hdom models, only a single metric was selected whereas two metrics were selected for SI models.

Table 2. Fitted linear regression models and fit statistics.

Response variable[a]	Explanatory variables[b]	R^2
Spruce-dominated forest		
$Hdom_{T1}$	T1H90.ALS	0.83
$Hdom_{T2}$	T2H90.ALS	0.79
$Hdom_{T2}$	T2H90.DAP	0.78
SI	T1Hmean.ALS + T2Hmean.ALS	0.81
SI	T1Hmean.ALS + ΔH90.DAP	0.75
Pine-dominated forest		
$Hdom_{T1}$	T1Hmean.ALS	0.87
$Hdom_{T2}$	T2H90.ALS	0.89
$Hdom_{T2}$	T2Hmean.DAP	0.90
SI	T2H90.ALS + ΔH90.ALS	0.81
SI	T2Hmean.DAP + ΔH90.DAP	0.79

[a] $Hdom_{T1}$ and $Hdom_{T2}$ = dominant height (m) at the first point in time (T1)

and the second point in time (T2), respectively, SI = site index.

[b] T1H90.ALS and T2H90.ALS = 90th height percentile (m) at T1 and T2, respectively. T2H90.DAP = 90th height percentile (m) at T2 derived from DAP data. T1Hmean.ALS and T2Hmean.ALS = mean laser echo height (m) at T1 and T2, respectively. ΔH90.DAP and ΔH90.ALS differences in 90th height percentiles (m) derived from DAP and ALS data, respectively.

Fig. 4 shows ground reference values of $Hdom_{T2}$ plotted against corresponding estimates from ALS and DAP data, as well as the mean age obtained from site trees plotted against the age obtained from the stand register. DAP-assisted estimates of Hdom were slightly more accurate than ALS-assisted estimates. Even though the registered stand age represents the mean breast height age weighted by basal area, i.e., not necessarily equal to the age of site trees, many of the plot-level values coincided relatively well. For validation plot no. 290 however, the mean age obtained from site trees was 65 and the age obtained from the stand register was 135 (Fig, 4).
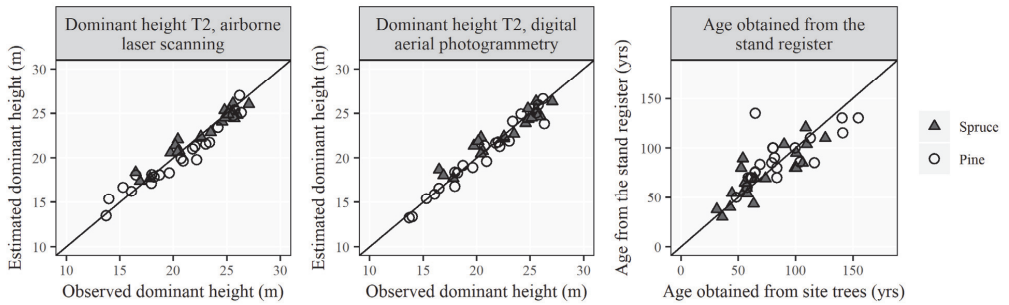
Fig. 4. Ground reference values of dominant height at the second point in time (T2) plotted against corresponding estimates from airborne laser scanning and digital aerial photogrammetry data, and age obtained from site trees plotted against age obtained from the stand register.

The direct method provided the most reliable SI estimates (Table 3). Errors in SI estimates were largest for indirect methods, and systematic errors for spruce-dominated validation plots were notable (Fig. 6). The use of Hdom estimates from single-date ALS or DAP data in combination with age obtained from the stand register seemed to provide reliable direct estimates in pine-dominated forest, however the estimated SI for the abovementioned validation plot no. 290 was considerably smaller than the observed SI (Fig. 5). Correspondingly, the SI estimate for this plot obtained by conventional practices had the largest error.

Table 3. Site index estimation errors.

Inventory method	Description	RMSE (m)	MD (m)	RMSE%	MD%
i	Direct method, bitemporal ALS	1.49	0.02	9.79	0.13
ii	Direct method, ALS and subsequent DAP	1.53	-0.11	10.04	-0.71
iii	Indirect method, bitemporal ALS	2.46	1.54	16.11	10.12
iv	Indirect method, ALS and subsequent DAP	2.66	1.10	17.49	7.21
v	Single-date ALS	2.11	0.65	13.91	4.29
vi	Single-date DAP	2.11	0.51	13.88	3.36
vii	Conventional practices	2.38	0.50	15.67	3.30

Fig. 5. Pine-dominated validation plot no. 290 (shown in red) for which the mean age obtained from site trees was 65 years whereas the age obtained from the stand register was 135 years. The white line represents the stand border.
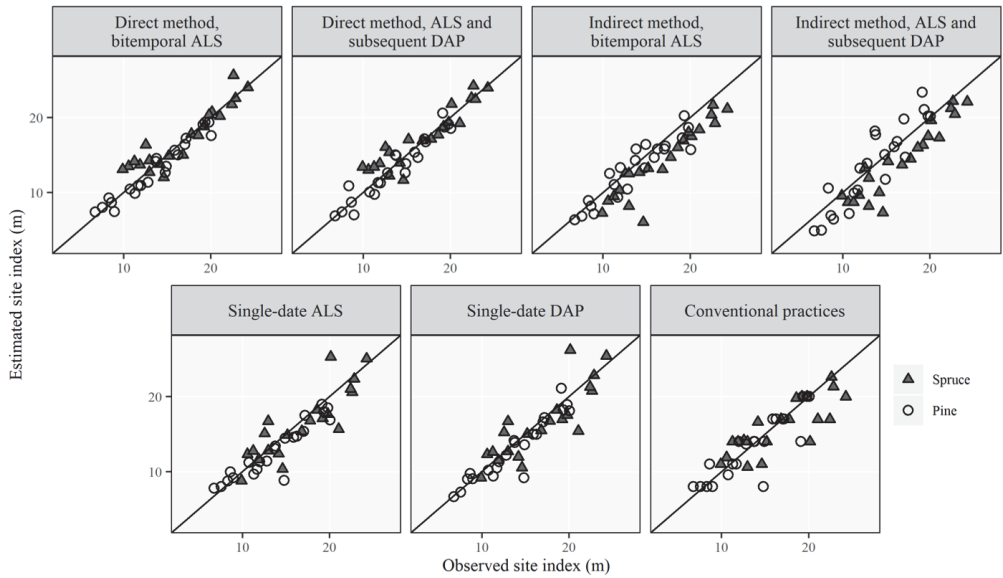

Fig. 6. Ground reference values of site index plotted against corresponding estimates obtained by the inventory methods.

3.2 Cost-plus-loss comparison

The calculated mean NPV losses and total inventory costs are shown in Table 4. Losses were smallest for direct estimation of SI with ALS and subsequent DAP data, and greatest for indirect estimation from bitemporal ALS data. The total inventory costs differed substantially among the inventory methods, where direct methods provided substantially smaller total costs. Fig. 7 shows that NPV losses were largely limited to approximately 100 € ha^{-1}, however the potential losses had a tendency to increase with larger values of SI.

Table 4. Inventory costs, mean net present value losses ($\overline{\mathrm{NPV}}_{\mathrm{loss}}$) and total costs.

Inventory method	Description	Inventory cost (€ ha^{-1})	$\overline{\mathrm{NPV}}_{\mathrm{loss}}$ (€ ha^{-1})	Total cost (€ ha^{-1})
i	Direct method, bitemporal ALS	5.46	27.94	33.40
ii	Direct method, ALS and subsequent DAP	4.56	25.30	29.80
iii	Indirect method, bitemporal ALS	5.40	75.30	80.70
iv	Indirect method, ALS and subsequent DAP	4.50	51.84	56.34
v	Single-date ALS	5.40	59.88	65.28
vi	Single-date DAP	4.50	56.70	61.20
vii	Conventional practices	5.46	58.20	63.66

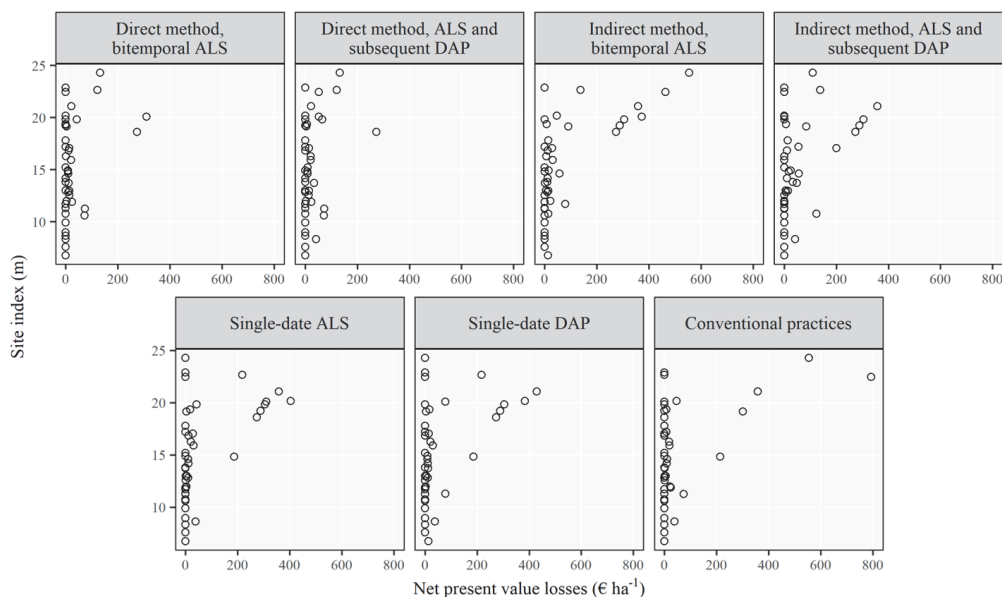
Fig. 7. Net present value losses plotted against ground reference values of site index. Each circle represents a validation plot.

4. Discussion

Data obtained from ALS and DAP provide a means to estimate SI as an alternative to conventional methods. We compared seven inventory methods for SI estimation by both assessing the accuracy of the obtained estimates and by linking the errors to consequential sub-optimal treatment decisions in long term forest planning. We found that the choice of method had great impact on both the accuracy and the economic value of the produced SI estimates.

4.1 Site index estimation

Two of the advantages of estimating SI following an area-based approach are that 1) SI can be estimated as a continuous variable, and 2) at sub-stand level, increasing the utility of the data (Eid & Økseter, 1999). Partly due to these advantages, direct methods based on bitemporal 3D data provided more reliable estimates of SI than conventional practices. The accuracy of SI estimates obtained by the direct method based on bitemporal ALS data were of similar magnitude as those earlier reported (Bollandsås et al., 2019; Persson et al., 2016). As an alternative, we tested the use of DAP data as a low-cost means to update a previous ALS-based inventory. Our results showed that ALS and subsequent DAP data provided accurate estimates of SI, which may be expected because DAP data are known to accurately characterize the top of the canopy, and thus the height of dominant trees (White et al., 2018). Thus, our results are particularly relevant from a cost-saving perspective, as point clouds can be generated cheaply from aerial imagery to update existing ALS inventories as a by-product of image acquisitions aimed at orthophoto production (Ginzler & Hobi, 2015).

We found indirect estimation of SI to be the least reliable inventory method, mainly due to the systematic errors obtained for spruce-dominated validation plots. By estimating the SI from Hdom growth trajectories over the specified observation period, the SI was underestimated for almost all spruce-dominated validation plots. This may be explained by the fact that the SI obtained by the direct and indirect methods were two different measures. The models used for direct estimation were fitted with values of SI based on the height development of site trees from the moment breast height was reached to the moment of measurement. Values obtained using the indirect method, on the other hand, were based on the height development of dominant trees during the observation period of 15 years. For consistency however, we based ground-reference values of SI on age-height relationships of site trees for all seven methods. Such age-height relationships are most commonly used in Norwegian forest management

inventories, and the resulting SI estimate is more robust against temporary fluctuations in growing conditions.

The use of single-date ALS and DAP data in combination with age obtained from the stand register provided a practical alternative, because such a method only requires canopy height information from a single point in time and age from the stand register which in most commercial inventories is available. Using the same approach, Packalén et al. (2011) obtained very good results with a RMSE% of 3 in eucalyptus monocultures in Bahia State, Brazil. In the mentioned study however, the stands were noticeably more homogenous; trees had been planted in rows with a fixed stem density, and the exact years of planting were known. Although even-aged plantations are common in Norway, in which case the date of planting is usually registered, a large portion of the production forests are uneven-aged, at least to some extent, making this approach less feasible. In addition, the age obtained from the stand register typically reflects the mean age at breast height weighted by basal area, and will likely differ from the age of site trees in stands with an uneven age structure. From interpretation of the aerial imagery, we noticed that several validation plots showed substantial variations in tree crown sizes, possibly due to an uneven age distribution (Fig. 5), and perhaps due to the presence of retention trees. In such cases where the forest structure appeared to be heterogenous, the use of bitemporal point cloud data provided more reliable estimates of SI. Thus, direct estimation of SI from Hdom estimates in combination with age obtained from the stand register may be a suitable approach primarily when applied to even-aged stands of which the age is known with high certainty.

In the current study, we omitted subplots for which the predicted Hdom had decreased between inventories as a means to exclude plots where Hdom had been disrupted. In other studies, disturbance classifications have been based on changes in other forest structural attributes (Næsset et al., 2013; Noordermeer et al., 2019b). However, increasing Hdom and other forest structural attributes will not guarantee undisrupted Hdom growth, which is a prerequisite for reliable SI estimation (Stearns-Smith, 2002). Alternatively, disturbances could be registered for each plot during field work and used for fitting a classifier, however such data were not available in the current study. Nevertheless, identifying forest areas in which Hdom growth has been disturbed is challenging whichever method of SI estimation is used, especially when based on bitemporal forest inventory data with long time intervals.

4.2 Cost-plus-loss comparison

The inventory costs were similar among the seven methods, partly because we assumed data from T1 to be free of cost. However, the losses due to errors in SI differed substantially. This result is in contrast to findings from Haara et al. (2019), but in accordance with findings from Eid (2000). In GAYA, the DBH and Hdom increment models used for projecting future stand development rely on SI as a predictor, which explains the great impact such errors have on the NPV when timing of the final harvest is considered. When SI is underestimated for example, as was the case for many validation plots when indirect methods were applied, the timing of final harvest will likely be delayed past the optimum, resulting in NPV losses. Furthermore, in accordance with results reported by Haara et al. (2019), we found that potential losses tended to increase with SI (Fig. 7), highlighting the importance of reliable estimates of SI on highly productive sites. Accuracies differed substantially among the seven inventory methods and the total inventory costs ranged from 29.80 to 80.70 € ha^{-1}, suggesting that costs can be reduced greatly by adopting suitable methods of SI estimation.

The use of long-term forest scenario models for economic optimization of forest planning entails a number of general simplifications and potential shortcomings that should be addressed. First, our analysis was limited to long-term forest planning without taking the value of information for tactical and operational decisions made at a short-term into account. Second, we assumed timber prices, the interest rate and harvesting costs to remain constant, when in fact they are likely to fluctuate over time. Third, we assumed ground reference values of SI, Hdom, basal area and number of stems to be free of errors, and in the erroneous datasets we used ground reference values for all attributes except for SI. Measurement errors will likely have affected the values of plot-level attributes, and additional uncertainty may arise from using empirical SI models. Furthermore, the isolation of SI as the single variable assumed to be affected by errors is a simplification in the sense that errors would in fact have occurred for all attributes, which may further impact the calculated NPV.

More specific limitations to this study included the assumption that maximizing the NPV was the only aim in the planning process, whereas environmental and recreational considerations may affect treatment decisions as well. Also, for simplicity, we limited our analysis to decisions regarding the timing and form of final felling and method of regeneration, omitting decision related to the timing and intensity of potential thinnings as we considered these to be less relevant for assessing the value of SI estimates. We assumed estimates of SI obtained from the

stand register to be valid for the validation plots, which in fact covered only parts of the stands. The design of the validation plots was selected to cover the variability of a typical stand, and to provide full census ground reference data, i.e., spatially continuous field data with which sampling errors are avoided. However, minor discrepancies between stand- and validation plot-level SI estimates may have occurred.

5. Conclusions

Our results indicate that for SI estimation, the choice of method has great impact on both the accuracy and the economic value of the produced estimates. Direct methods of SI estimation using bitemporal 3D data gave the best accuracy and the smallest total cost. DAP proved to be a suitable source of tree height data for SI estimation, which is a promising result from a cost-saving perspective, as DAP can be used as a low-cost means to replace ALS as a data source in repeated forest inventories. SI estimates from single-date ALS and DAP data in combination with age obtained from the stand register provided a practical alternative, suitable when applied to even-aged stands of which the age is known with high certainty. In summary, when repeating forest inventories based on remotely sensed 3D data, direct estimation of SI can be recommended as the preferred approach, at least from an economic planning perspective. Although such methods are restricted to forest areas in which Hdom growth has not been disrupted, they can be applied over large areas of forest automatically, with greater accuracy than conventional practices and at a smaller total cost.

Acknowledgements

References

Ali-Sisto, D., & Packalen, P. (2016). Forest change detection by using point clouds from dense image matching together with a LiDAR-derived terrain model. *IEEE Journal of Selected Topics in Applied Earth Observations and Remote Sensing, 10*(3), 1197-1206.

Bettinger, P., Boston, K., Siry, J. P., & Grebner, D. L. (2016). Forest management and planning.

Blingsmo, K. (1984). Diameter increment functions for stands of birch, Scots pine and Norway spruce. *Research Paper from Norwegian Forest Research Institute*.

Blingsmo, K. R., & Veidahl, A. (1992). *Functions for gross price of standing spruce and pine trees*: Norsk Institutt for Skogforskning.

Bollandsås, O. M., Ørka, H. O., Dalponte, M., Gobakken, T., & Næsset, E. (2019). Modelling Site Index in Forest Stands Using Airborne Hyperspectral Imagery and Bi-Temporal Laser Scanner Data. *Remote Sensing of Environment, 11*(9), 1020.

Braastad, H. (1966). Volume tables for birch. *Meddelelser fra det Norske Skogforsøksvesen, 21*, 23-78.

Braastad, H. (1982). Natural mortality in Picea abies stands. *Norwegian Forest Research Institute, Ås, Research Paper, 12*(82), 46.

Brantseg, A. (1967). Volume functions and tables for Scots pine South Norway. *Meddelelser fra det Norske Skogforsoksvesen, 22*, 695.

Burkhart, H. E., Stuck, R. D., Leuschner, W. A., & Reynolds, M. R. (1978). Allocating inventory resources for multiple-use planning. *Canadian journal of forest research, 8*(1), 100-110.

Eid, T. (2000). Use of uncertain inventory data in forestry scenario models and consequential incorrect harvest decisions. *Silva Fennica, 34*(2), 89-100.

Eid, T., & Moum, S. O. (1999). Bestandsuavhengig bonitering og nøyaktighet. *Rapport fra skogforskningen, 7*.

Eid, T., & Økseter, P. (1999). Bestandsuavhengig bonitering og konsekvenser. *Rapport fra skogforskningen, 8*.

Eriksson, H., Johansson, U., & Kiviste, A. (1997). A site-index model for pure and mixed stands of Betula pendula and Betula pubescens in Sweden. *Scandinavian journal of forest research, 12*(2), 149-156.

Faustmann, M. (1849). Berechnung des Werthes, welchen Waldboden, sowie noch nicht haubare Holzbestande fur die Waldwirthschaft besitzen [Calculation of the value which forest land and immature stands possess for forestry]. *Allgemeine Fotst-und Jagd-Zeitung, 25*, 441-455.

Fitje, A., & Vestjordet, E. (1977). Stand height curves and new tariff tables for Norway spruce. . *Meddelelser Fra Norsk Institutt for Skogforskning, 34*(2), 23–68.

Ginzler, C., & Hobi, M. L. (2015). Countrywide stereo-image matching for updating digital surface models in the framework of the Swiss National Forest Inventory. *Remote sensing letters, 7*(4), 4343-4370.

Gisnås, A. (1982). *Skogkartlegging ved fototyding i kartkonstruksjonsinstrument*: Norsk Institutt for skogforskning.

Goodbody, T. R., Coops, N. C., & White, J. C. (2019). Digital Aerial Photogrammetry for Updating Area-Based Forest Inventories: A Review of Opportunities, Challenges, and Future Directions. *Current Forestry Reports, 5*(2), 55-75.

Haara, A., Kangas, A., & Tuominen, S. (2019). Economic losses caused by tree species proportions and site type errors in forest management planning. *Silva Fennica, 53*(2), 10089.

Hamilton, D. (1978). Specifying precision in natural resource inventories. *PB US National Technical Information Service, USDA Forest Service, General Technical Report RM-55*, 276–281.

Hoen, H., & Eid, T. (1990). En modell for analyse av behandlingsstrategier for en skog ved bestandssimulering og lineær programmering (A model for analysis of treatment strategies for a forest applying standwise simulations and linear programming). *Department of Forest Sciences, Agricultural University of Norway, Report 9/90*, 35.

Hoen, H., & Gobakken, T. (1997). Brukermanual for bestandssimulatoren GAYA V1.20. *Department of Forest Sciences, Agricultural University of Norway, Internal Report, 59 pp*.

Hollaus, M., Eysn, L., Maier, B., & Pfeifer, N. (2015). Site index assessment based on multi-temporal ALS data. *Proceedings of SilviLaser 2015*.

Holmström, H., Kallur, H., & Ståhl, G. (2003). Cost-plus-loss analyses of forest inventory strategies based on kNN-assigned reference sample plot data. *Silva Fennica, 37*(3), 381-398.

Holopainen, M., Vastaranta, M., Haapanen, R., Yu, X., Hyyppä, J., Kaartinen, H., . . . Hyyppä, H. (2010). Site-type estimation using airborne laser scanning and stand register data. *The Photogrammetric Journal of Finland, 22*(1), 16-32.

Kangas, A., Gobakken, T., Puliti, S., Hauglin, M., & Næsset, E. (2018). Value of airborne laser scanning and digital aerial photogrammetry data in forest decision making. *Silva Fennica, 52*(1), 19.

Kangas, A. S. (2010). Value of forest information. *European Journal of Forest Research, 129*(5), 863-874.

Kvaalen, H., Solberg, S., & May, J. (2015). Aldersuavhengig bonitering med laserskanning av enkelttrær. *NIBIO REPORT, 1*(67), 31.

Mäkinen, A., Kangas, A., & Nurmi, M. (2012). Using cost-plus-loss analysis to define optimal forest inventory interval and forest inventory accuracy. *Silva Fennica, 46*(2), 211-226.

Maltamo, M., Næsset, E., & Vauhkonen, J. (2014). Forestry applications of airborne laser scanning. *Concepts and case studies. Managing Forest Ecosystems, 27*, p. 460.

Næsset, E. (1994). *Sammenlikning av ulike boniteringer av et skogområde*: Norsk institutt for skogforskning, Institutt for skogfag, NLH.

Næsset, E. (2002). Predicting forest stand characteristics with airborne scanning laser using a practical two-stage procedure and field data. *Remote Sensing of Environment, 80*(1), 88-99.

Næsset, E. (2004). Practical large-scale forest stand inventory using a small-footprint airborne scanning laser. *Scandinavian journal of forest research, 19*(2), 164-179.

Næsset, E. (2014). Area-based inventory in Norway–from innovation to an operational reality. In *Forestry applications of airborne laser scanning* (pp. 215-240): Springer.

Næsset, E., Bollandsås, O. M., Gobakken, T., Gregoire, T. G., & Ståhl, G. (2013). Model-assisted estimation of change in forest biomass over an 11 year period in a sample survey supported by airborne LiDAR: A case study with post-stratification to provide "activity data". *Remote Sensing of Environment, 128*, 299-314.

nFrames. (2014, 12/05/2014). SURE - Photogrammetric Surface Reconstruction from Imagery. Retrieved from ftp://ftp.ifp.uni-stuttgart.de/sure_public/SURE_Manual.pdf

Niklasson, M. (2002). A comparison of three age determination methods for suppressed Norway spruce: implications for age structure analysis. *Forest Ecology and Management, 161*(1-3), 279-288.

Noordermeer, L., Bollandsås, O. M., Gobakken, T., & Næsset, E. (2018). Direct and indirect site index determination for Norway spruce and Scots pine using bitemporal airborne laser scanner data. *Forest Ecology and Management, 428*, 104-114.

Noordermeer, L., Bollandsås, O. M., Ørka, H. O., Næsset, E., & Gobakken, T. (2019a). Comparing the accuracies of forest attributes predicted from airborne laser scanning and digital aerial photogrammetry in operational forest inventories. *Remote Sensing of Environment, 226*, 26-37.

Noordermeer, L., Økseter, R., Ørka, H. O., Gobakken, T., Næsset, E., & Bollandsås, O. M. (2019b). Classifications of Forest Change by Using Bitemporal Airborne Laser Scanner Data. *Remote Sensing of Environment, 11*(18), 2145.

Nurminen, K., Karjalainen, M., Yu, X., Hyyppä, J., & Honkavaara, E. (2013). Performance of dense digital surface models based on image matching in the estimation of plot-level forest variables. *ISPRS Journal of Photogrammetry, 83*, 104-115.

Ørka, H. O. (2012). *lasR package: Laser processing in R*. [Version 0.2].

Packalén, P., Mehtätalo, L., & Maltamo, M. (2011). ALS-based estimation of plot volume and site index in a eucalyptus plantation with a nonlinear mixed-effect model that accounts for the clone effect. *Annals of Forest Science, 68*(6), 1085.

Persson, H. J., Fransson, J. E., & Sensing, R. (2016). Estimating site index from short-term TanDEM-X canopy height models. *IEEE Journal of Selected Topics in Applied Earth Observations, 9*(8), 3598-3606.

Rothermel, M., Wenzel, K., Fritsch, D., & Haala, N. (2012). *SURE: Photogrammetric surface reconstruction from imagery*. Paper presented at the Proceedings LC3D Workshop, Berlin.

Sharma, R. P., Brunner, A., Eid, T., & Øyen, B.-H. (2011). Modelling dominant height growth from national forest inventory individual tree data with short time series and large age errors. *Forest Ecology and Management, 262*(12), 2162-2175.

Sheather, S. (2009). *A modern approach to regression with R*: Springer Science & Business Media.

Solberg, S., Kvaalen, H., & Puliti, S. (2019). Age-independent site index mapping with repeated single-tree airborne laser scanning. *Scandinavian journal of forest research, 34*(8), 763-770.

Stearns-Smith, S. (2002). Making sense of site index estimates in British Columbia: A quick look at the big picture. *Journal of Ecosystems and Management, 1*(2), 1-4.

Vasilescu, M. M. (2013). Standard error of tree height using Vertex III. *Bulletin of the Transilvania University of Brasov. Forestry, Wood Industry, Agricultural Food Engineering. Series II, 6*(2), 75.

Vastaranta, M., Wulder, M. A., White, J. C., Pekkarinen, A., Tuominen, S., Ginzler, C., . . . Hyyppä, H. (2013). Airborne laser scanning and digital stereo imagery measures of forest structure: comparative results and implications to forest mapping and inventory update. *Canadian Journal of Remote Sensing, 39*(5), 382-395.

Véga, C., & St-Onge, B. (2009). Mapping site index and age by linking a time series of canopy height models with growth curves. *Forest Ecology and Management, 257*(3), 951-959.

Vestjordet, E. (1967). Functions and tables for volume of standing trees. Norway spruce. *Meddelelser fra det Norske Skogforsoksvesen, 22*, 545.

Vestjordet, E. (1968). Merchantable volume of Norway spruce and Scots pine based on relative height and diameter at breast height or 2.5 m above stump level. *Meddelelser fra det Norske Skogforsøksvesen, 25*, 411-459.

Villalba, R., & Veblen, T. T. (1997). Improving estimates of total tree ages based on increment core samples. *Ecoscience, 4*(4), 534-542.

White, J. C., Coops, N. C., Wulder, M. A., Vastaranta, M., Hilker, T., & Tompalski, P. (2016). Remote sensing technologies for enhancing forest inventories: A review. *Canadian Journal of Remote Sensing, 42*(5), 619-641.

White, J. C., Tompalski, P., Coops, N. C., & Wulder, M. A. (2018). Comparison of airborne laser scanning and digital stereo imagery for characterizing forest canopy gaps in coastal temperate rainforests. *Remote Sensing of Environment, 208*, 1-14.

White, J. C., Wulder, M. A., Vastaranta, M., Coops, N. C., Pitt, D., & Woods, M. (2013). The utility of image-based point clouds for forest inventory: A comparison with airborne laser scanning. *Forests, 4*(3), 518-536.

Norwegian University
of Life Sciences